~~Top-down~~Tectonically- and ~~bottom-up controls on~~climatically-driven mountain-hopping erosion~~: insights~~ in Central Guatemala from detrital ^{10}Be and river profile analysis ~~in Central Guatemala~~

Gilles Y Brocard[1], Jane K Willenbring[2], Tristan Salles[3], Michael Cosca[4], Axel ~~Guttierez~~[5]Guttiérez-Orrego[5], Noé Cacao Chiquín[5], Sergio Morán-Ical[5], Christian Teyssier[6]

[1]Archéorient, University of Lyon 2, 69365 Lyon, France

[2] Department of Geological Sciences, Stanford University, Stanford, CA 94305, USA

[3]: School of Geosciences, University of Sydney, Camperdown, Australia

[4]: U.S. Geological Survey, Denver Federal Center, Denver, CO 80225, USA

[5]: Carrera de Geología, Universitad San Carlos de Guatemala, Centro Universitario del Noreste, 16001 Cobán, Guatemala.

[6]: Department of Earth Sciences, University of Minnesota, Minneapolis MN 55455, USA

Correspondence to: Gilles Brocard (gilles.brocard@mom.fr)

Abstract. The rise of a mountain range affects ~~the~~moisture circulation ~~of water around it, in the form of moisture and precipitation~~ in the atmosphere~~, as well as~~ and water ~~routing~~runoff across the land surface~~. These alterations~~, modifying the distribution of precipitation and ~~overland flow over surrounding landmasses ultimately affect hillslope~~ the shape of drainage patterns. Water routing in turn affects erosion on hillslopes and ~~river~~ incision~~.~~ in river channels. The ~~emergence~~rise of a ~~new~~ mountain range ~~therefore affects~~ thereby alters the erosion of ~~older~~surrounding mountain ranges~~ located in close proximity. Here, we use field data from~~. We document here such influence in Central Guatemala, where two parallel, closely spaced mountain ranges formed during two consecutive pulses of single-stepped uplift, one from 12 to ~~show that the rise of a new~~7 Ma (Sierra de Chuacús-Sierra de las Minas), and the second one after 7 Ma (Altos de Cuchumatanes). We explore the climatic and tectonic processes by which the rise of the most recent range ~~decreased~~ drove the slowing of river incision ~~over an older range. We then explore the top-down and bottom-up processes whereby the new range may have controlled river incision over the old range. We investigate, in particular, how the rise of the new range affected precipitation and~~ and hillslope erosion over the ~~older range, and to which extent drainage dynamics, in response to the rise of the new range, affected river incision rates. We first use the~~ previously-uplifted range. ^{40}Ar-^{39}Ar dating of perched volcanic

deposits ~~to document~~documents the sequential rise and incision of the two mountain ranges. ~~We then use detrital~~Terrestrial cosmogenic ^{10}Be in river sediments ~~to show~~shows that hillslopes in the older range ~~erodes~~today erode more slowly than in the younger range (20-150 vs. 300 m~~/~~·My^{-1}), and that ~~such~~these differences ~~scales with differences in~~ mimic the current distribution of precipitation~~. In the meantime~~, the ~~drainage of~~ younger range intercepting the atmospheric moisture before it reaches the older range. River channel steepness and deformation of paleovalleys in the new range further show that the younger has risen faster than the older range up to today. We review how atmospheric moisture interception and river long-profile adjustment to the rise of the new range contribute to the decrease in erosion rates over the old range. We then explore how the topography of the older range has evolved in response to the decrease in erosion rates. The old range ~~responded to the rise of the new range through widespread drainage reorganization, and the steepening of river profiles, thereby contributing~~undergoes topographic decay, owing to the stalling of ~~incision in the older range. The study of river profiles further show that, *As a result, the older range has been passively uplifted, and entered a phase of a slow topographic decay: pediments have formed along* ~~river incision around its base~~, ~~*while ancient headward*~~. Aridification makes such decay very slow, and dominated by backwearing, rather than downwearing, marked by the stacking of slowly-migrating erosion waves ~~*of erosion, located farther up*~~ along the mountain flanks, ~~*have almost stopped*~~ migrating. ~~Aridification and cessation of river incision together explain the slowing down of erosion over the older~~and by the formation of pediments around its base. The morphology of the old range is therefore transitioning from that of a front range~~. They represent top-down and bottom-up processes whereby the younger range controls erosion over the older one. These controls are regarded as instrumental in the nucleation and enlargement of orogenic plateaus forming above continental accretionary wedges.~~ to that of a dry interior range.

1. Introduction

The relief of mountain ranges affects the circulation of ~~water as~~ moisture in the atmosphere~~,~~ and ~~along river networks as~~of precipitated water across the land surface~~ runoff. The influx of atmospheric moisture is intercepted in the form of precipitation, and returned through stream discharge. The intensity of surface runoff and the rate of river incision control the rate of hillslope erosion. The characteristic length of atmospheric circulation cells and of drainage networks is generally larger than the size of the mountains, such that the effects of a mountain on erosion are felt widely beyond the footprint of the mountain. The most common consequence of atmospheric moisture interception is the concentration of rainfall~~. Moisture precipitates on the windward side of ~~a range, and the development of an extensive~~ mountains and rain ~~shadow that extends beyond its~~shadows are cast over their lee-side, and beyond on downwind reliefs (e.g.Meijers et al., 2018; Galewsky, 2009).

~~Once precipitated, water~~Overland flow generates hillslope erosion and ~~eroded sediments generate a return flux that affects~~ river ~~drainage in many ways. These effects~~incision. River drainages are ~~felt not only~~dynamic systems that transmit downstream ~~of a rising mountain range, but also~~ disturbances that affect their headwaters, and also transmit upstream~~,~~ ~~because~~ disturbances affecting their downstream ~~changes affect the evolution of upstream~~ reaches, in particular the adjustment of river profiles to the rise of mountain ranges (Humphrey and Heller, 1995; Whittaker and Boulton, 2012)~~, and, therefore, ultimately affect the hillslopes connected to the upstream reaches~~. Signals are then transmitted from the rivers to the toe of valley slopes, and then uphill along valley slopes (Harvey, 2002; Mudd and Furbish, 2007). ~~A mountain ranges therefore exerts~~ Through this combination of top-down ~~controls (e.g. (~~precipitation~~, vegetation cover, weathering, surface~~ and runoff~~, landsliding),~~) and bottom-up ~~controls~~ (upstream-migrating signals ~~of erosion along stream networks) on erosive~~) processes ~~operating over surrounding areas.~~, the rise of a mountain affects the erosion of surrounding reliefs.

The growth of contractional orogens commonly involves outward, sequential propagation of contraction. Moisture, on the other hand, is often advected from the foreland toward the orogen interior. Precipitated water is then commonly returned to the foreland along river networks that flow from the interior to the foreland. In such setting, the in-sequence rise of frontal ranges, at the margins of orogens, will therefore frequently occur both upwind and downstream of ~~an~~ pre-existing ~~mountain occurs typically during the growth and widening of an orogenic accretionary wedge~~reliefs (Garcia-Castellanos, 2007). ~~Through a combination of enhanced tectonic uplift across river courses, and of aridification, the rise of the new mountain can trigger the rerouting, and sometimes the full disintegration of river networks draining preexisting ranges. These processes are regarded as some of the most potent mechanism of formation of orogenic plateaus~~The rise of a new frontal range therefore leads to the aridification of previously uplifted ones. In the meantime, the new frontal range rises across the course of rivers that flow from the interior to the foreland. It will impart the steepening of rivers transverse to the range (Leland et al., 1998), thereby promoting a transient decreases in river incision rates farther upstream (Champel et al., 2002). It may spark the reorganization of the range-transverse river network (Jackson et al., 2002; van der Beek et al., 2002). In some cases, topography and tectonic structure will adapt fast enough to re-establish a new equilibrium relief, equilibrium climate, and equilibrium tectonic structure (Willett and Brandon, 2002; Whipple and Meade, 2006). In other cases, the slowing down of the landscape response, upstream and downwind or a rising range, as a result of aridification, will lead to the disintegration of river drainages, following by the topographic decay of the interior ranges, an evolution conducive to the nucleation and growth of orogenic plateaus (Sobel et al., 2003; Garcia-Castellanos, 2007). These two evolutionary pathways have been explored at the scale of entire orogens, but they are less frequently documented at the scale of individual mountain ranges, where the hallmark of these evolutions interferes with more local signals resulting from spatial variations in bedrock erodibility, topographic inheritances, or stochastic processes such as landslides.

~~Here we document the erosional and topographic hallmark of these processes in Guatemala, across the narrow Central American land bridge. Elongate ranges have risen since Middle Miocene times along the North American Caribbean~~

plate boundary. The first range to rise is also the closest to the plate boundary. Deep valleys were incised through the range until the late Miocene We document here the effects of the rise of a recent mountain range (the 170 km-long Altos de Cuchumatanes, or AC range) on the evolution of an older range (the 220 km-long Sierra de Chuacús-Sierra de las Minas, or SC-SM range) in Guatemala (Fig.1). Sharp topographic, climatic, and tectonic gradients affect this relatively small (350 x 100 km) area, allowing us to conduct detailed investigation of the interactions between the two ranges. The SC-SM range grew first; its flanks were deeply eroded in late Miocene time (Brocard et al., 2011). InThe AC range started to grow at the end of the late Miocene, however, uplift broadened, propagating farther away from the plate boundary.next to the SC-SM range. The rise of a new mountain range across the path of rivers that drained the preexisting range led to their rapid tectonic defeat, spurring a pulse of AC range sparked widespread drainage rearrangement, and in front of the aridification of the defeatedSC-SM, characterized by numerous river valleyscaptures (Brocard et al., 2011). Drainage rearrangement consisted in a series of riverThese captures, affecting a deeply dissected landscape. Contrary to expectations, river captureshowever, did not causegenerate upstream-migrating waves of accelerated erosion. Instead, river incision almost completely stalled upstream of the capture sites (Brocard et al., 2011). In this paper we seek to identify the top-down and bottom-up controls on erosion that arrested river incision in the first uplifted range, upstream of the capture sites. To achieve this, we investigate the geomorphic evolution of the first uplifted range, and contrast this evolution with the evolution of the younger range. We investigated in particular the spatial distribution of hillslope erosion rates in these ranges, provided by detrital terrestrial ^{10}Be concentrations and the characteristics of the long profile of the rivers that drain these ranges today.We investigate here the processes that arrested river incision, and retrieve from the characteristics of their river long-profiles some insights on how arrested incision affected the evolution of these ranges.

New ^{40}Ar/^{39}Ar ages on volcanic rocks are first providedhelp us to better constraintighten the uplift chronology of river incision and surface uplift in the studied ranges. TheSC-SM range. Detrital terrestrial ^{10}Be concentration of river sediments is then compared to the present-day distribution of precipitation to assess the importance of topographically-controlled rainfall on hillslope erosion. River rates provide a snapshot of current spatial variations of erosion rates across the study area. Profile linearization is implemented to study the complex long-profiles are then used to assess of the response of rivers to tectonic uplift,that drain these two ranges. River knickpoints are then carefully classified in order to extract river knickpoints that inform long-term landscape dynamics and the response time of river incision to tectonic and climatic changes. These data arethe sequential uplift of the two ranges. We then discuss successively the contribution of topographically-controlled climate and of river profile adjustment to the observed decrease in incision rates in the SC range during the rise of the AC range. We then useddiscuss how both processes contribute to the overall decrease in erosion over the SC range, and to assess the influence of river incision on hillslope erosion.the slowing down of migrating knickpoints. We finally present some topographic characteristics that appear as direct consequences of the slowing down of erosion over the older range.

2. Origin and evolution of the mountain ranges of Central Guatemala

2.1. Tectonics and orogenesis

Left-lateral motion along the North American-Caribbean plate boundary has generatedproduced elongate ranges parallel to the plate boundary in Central Guatemala (Fig.11a). We investigatedinvestigate here the growth and erosion of two of these ranges, namely (Fig.1b). Rocks in the Sierra de las Minas (SC-SM) Sierra de Chuacús (SC), and Altos de Cuchumatanes (AC) Sierra de Chamá. These rangesrange display a deeply penetrative, sub-vertical tectonic grainfabric, imparted by 70 My of left-lateral wrenching along the Caribbean-North American plate boundary (Ratschbacher et al., 2009; Ortega-Gutierrez et al., 2004; Ortega-Obregón et al., 2008). Since Eocene times, left-lateral motion between the Caribbean and North American plates has been mostly accommodated mostly by the Motagua fault, and, to a lesser extent, by the Polochic fault. (Fig.2b). The Motagua fault is, with its >1,100 km of total cumulative displacementoffset, the active subaerial fault with the largest cumulative offset on Earth. The Polochic fault has a total offset 125± ± 5 km (Burkart, 1978). It seems to branchThe Polochic fault probably branches out of the Motagua fault offshore, somewhere in the Caribbean Sea in the east,(Fig.1a), before running on land at an average distance of 50 km from the Motagua fault. Strain along the plate boundary is strongly partitioned: these two faults display between almost pure left-lateral shear, whileslip on the Motagua and Polochic faults and boundary-normal plate motion is accommodated by dip-slip on faults that are parallel to the Polochic and Motagua faults (Authemayou et al., 2011b; Brocard et al., 2012).

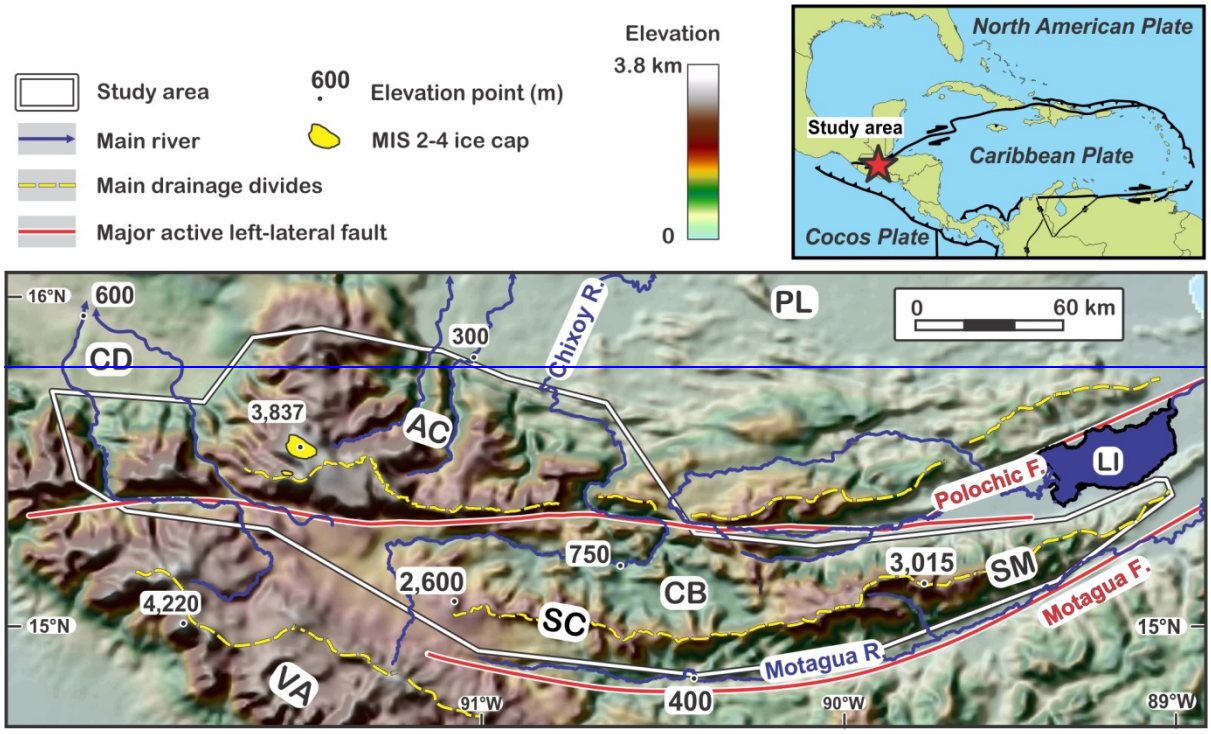
Study area
600
Elevation point (m)
Main river
MIS 2-4 ice cap
Main drainage divides
Major active left-lateral fault
Elevation
3.8 km
0
North American Plate
Study area
Caribbean Plate
Cocos Plate
16°N
15°N
600
300
CD
3,837
AC
Chixoy R.
PL
0
60 km
Polochic F.
LI
750
2,600
CB
3,015
SM
Motagua F.
4,220
SC
Motagua R.
VA
400
91°W
90°W
89°W

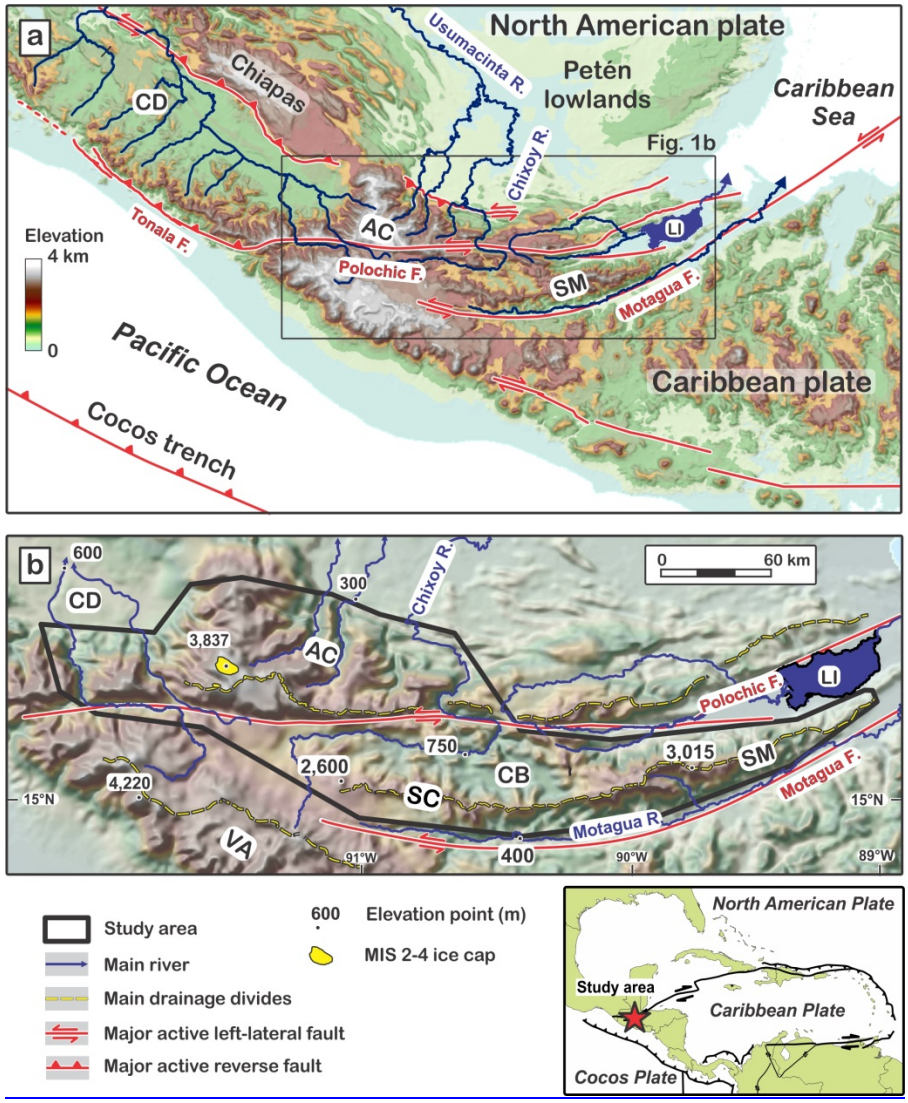

Figure 1. Shaded topography of the study area, ~~with indication~~showing the tectonic setting of ~~its main~~ Central Guatemala in general (a), and of the studied range specifically (b).Topographic features~~.~~
~~Topographic features~~: CB: Chixóy River basin, CD: Central Depression of Chiapas, AC: Altos de Cuchumatanes ~~Highs,~~(AC range), LI: Lake Izabal, ~~PL: Petén lowlands,~~ SC: Sierra de Chuacús~~,~~ (SC range), SM: Sierra de las Minas~~,~~ (SM range), VA: Central American Volcanic Arc. MIS: $\delta^{18}O$ Marine Isotopic Stage

Today, ~~the topography of the region~~Central Guatemala is ~~very pronounced, display~~ straddled by 3-4 km-high ranges ~~separated by valley as lows~~that separate deep valleys with floors stand at elevations as low as 0.2-0.~~6~~8 km ~~in elevation~~ (Fig.~~1).~~1b). In Middle Miocene times, however, the topography of ~~the region~~Central Guatemala was much more subdued ~~back in Middle Miocene time,~~. Remnants of that past topography (referred to as ~~evidenced~~ the ~~preservation, on most~~Maya surface (Brocard et al., 2011)) still cap numerous mountaintops~~, of remnants of a once extensive, low relief Middle Miocene surface (Maya surface,~~ across the study area (Fig.2). ~~The Middle Miocene surface bevels~~They are separated by regions where the Maya surface has been deeply incised (Fig.3). The low Miocene relief formed from the topographic decay of Eocene folds (Authemayou et al., 2011b; Brocard et al., 2011). ~~Surface~~It grades to the east and north into lowlands, near the Caribbean Sea, indicating that it formed near sea level. Its uplift started after the Middle Miocene, ~~originally~~then affecting both ~~sides of~~ the ~~Motagua fault~~southern (Simon-Labric et al., 2013), and northern side of the Motagua fault, as far north as the Polochic fault (Brocard et al., 2011)~~. Uplift may have been triggered by slab break off, affecting the Central American subduction zone (Rogers et al., 2002).~~. Uplift led the rise of the SC-SM range during the late Miocene. Valleys up to 1,000 m deep were ~~then~~ incised within ~~the~~its northern flank ~~of the SC range,~~ between 12 ~~and~~to 7 Ma (Brocard et al., 2011). ~~Basalt flows were emplaced along the southern base of the SC range between 6.1and 3.1 Ma (Tobisch, 1986). They indicate that 1,000-1,500 m of incision occurred along Motagua valley while the northern side of the SC range was being incised (Fig.3).~~

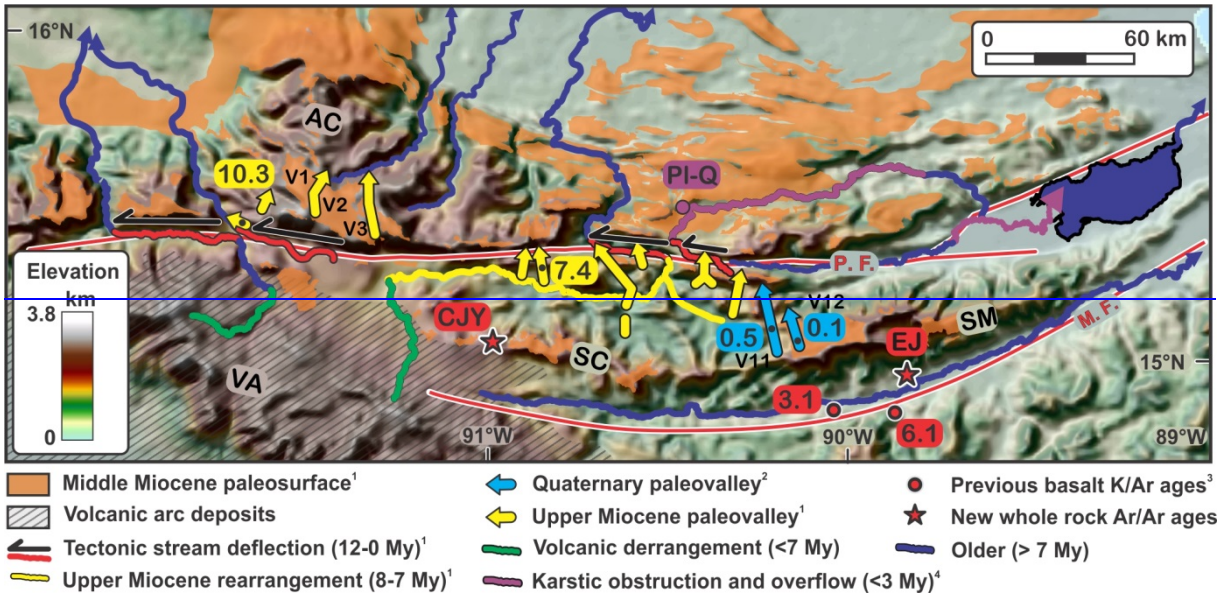

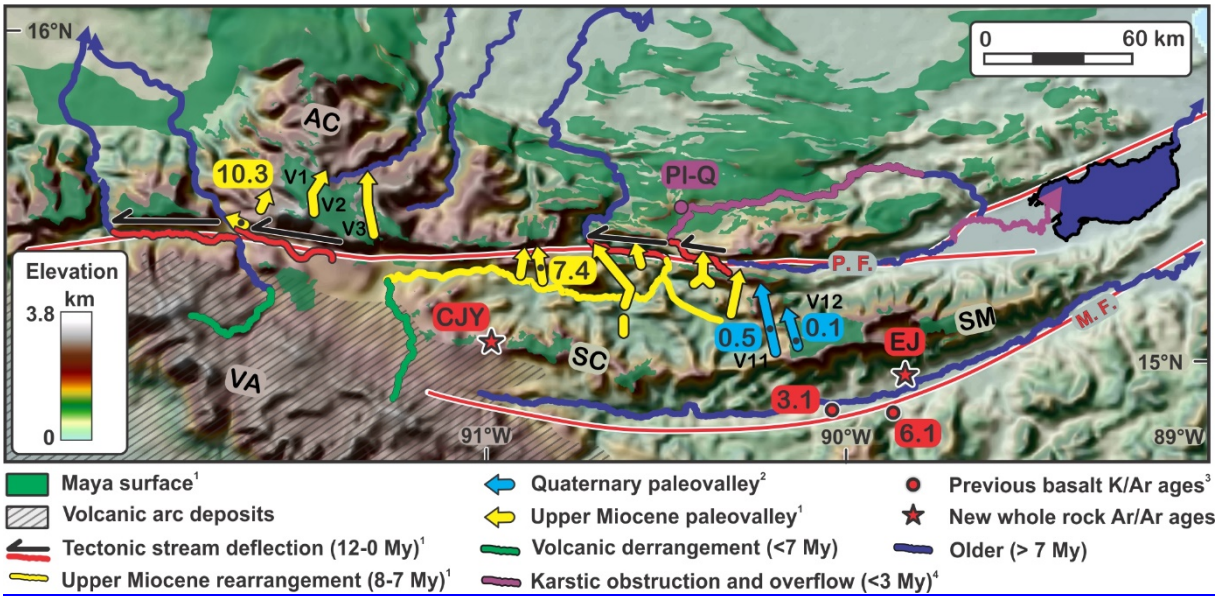

Figure 2. Age of geomorphic markers and drainage lines. Ages of Miocene valleys and Quaternary paleovalleys (V1-V12) provided in My. Data source: 1: (Brocard et al., 2011), 2: (Brocard et al., 2012), 3: (Tobisch, 1986), 4: Plio-Quaternary lacustrine deposits (Brocard et al., 2015a). Newly dated lavas: CJY: Chujuyúb, EJ: El Jute. Range names: AC: Altos de Cuchumatanes, SC: Sierra de Chuacús, SM: Sierra de las Minas, VA: volcanic arc. Faults: MF: Motagua, PF: Polochic. Background: shaded GTOPO 30 DEM.

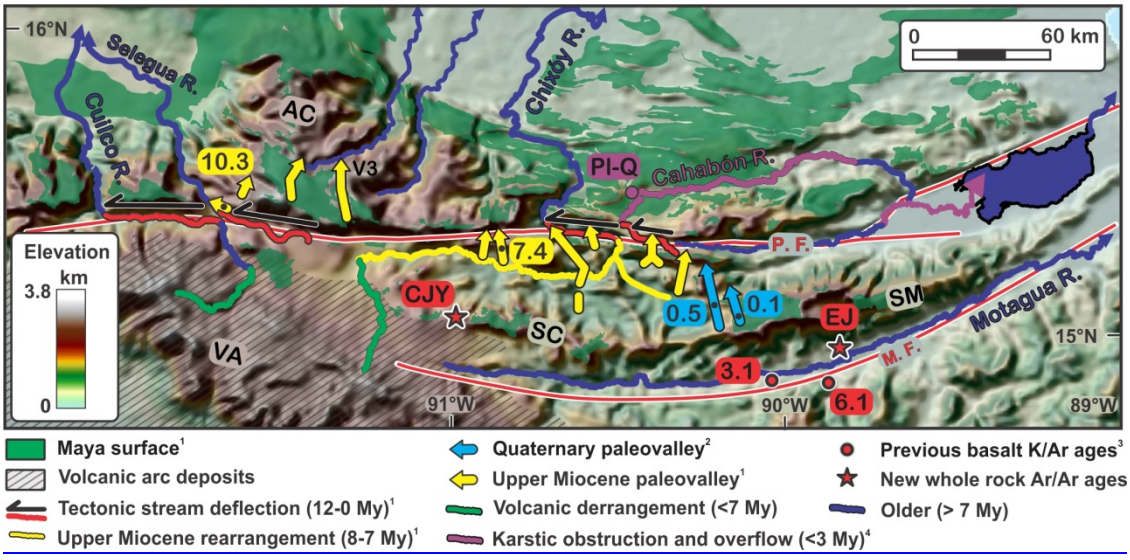

Figure 3. Incision below the Middle Miocene Maya surface, based on the elevation of surface remnants (upland relict surface). Incision contour line spacing: 1km.

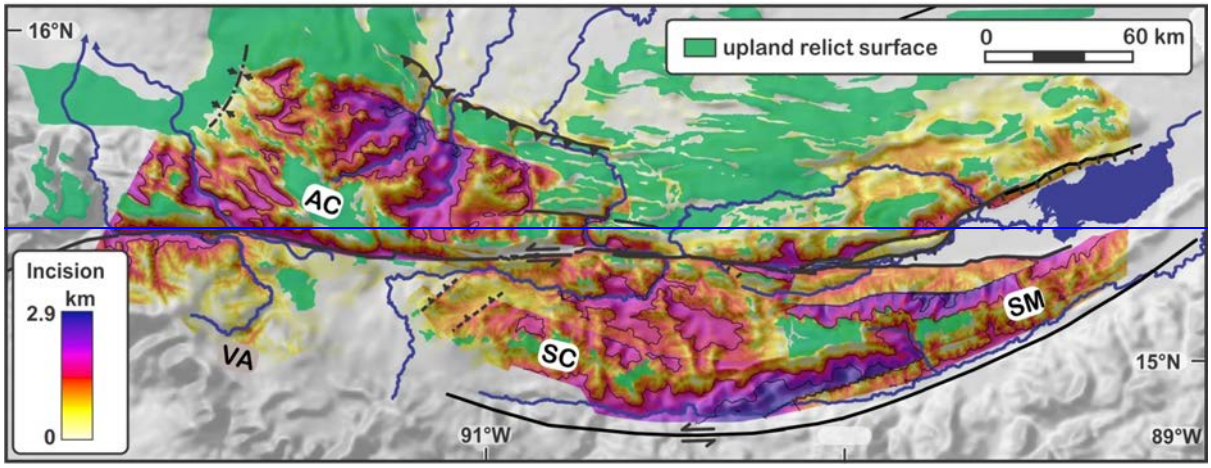

Figure 3. Incision below the Middle Miocene Maya surface, based on the elevation of surface remnants (upland relict surface). Incision contour line spacing: 1km. Yellow dashed lines: range drainage divides .AC: Altos de Cuchumatanes, SC: Sierra de Chuacús, SM: Sierra de las Minas, VA: volcanic arc.

The pattern of uplift changed in the Late Miocene, Uplift propagated north of the Polochic fault, when contraction (Authemayou et al., 2011a) triggered the rise of the AC range (Brocard et al., 2011). The AC range would have started rising in the west ~12 My ago, progressing 150 km eastward during the following 5 MyLate Miocene (Brocard et al., 2011). The AC range developed acrossIt was marked by the rise of the AC range in response to contraction in the North American plate (Authemayou et al., 2011a). The rise of the AC range drove widespread reorganization of the course of several riversriver network that drainedrains the northern flank of the SC-SM range. In reaction, the drainage reorganized. Most of these rivers were defeated, leaving (Fig. 2). Numerous river valleys were then abandoned valleys in the AC range (Fig. 2). The rivers united upstream of the AC range, gathering into a few streams thatand were able to maintain their course across the rising structure. Deformation of the abandoned valleysleft stranded on the rising AC range. Their deformation indicates that the AC range has risen >1-2 km relative to the SC range duringover the past 7 My (Brocard et al., 2011). The AC range today accommodates shortening within the hanging wall of the transpressional Ixcán fault to the north (Guzmán-Speziale, 2010)(Fig. 4), and kink folding to the NW (Authemayou et al., 2011b). Surface uplift is probably fueled by this contraction, combined with erosional unloading affecting the deeply dissected flanks of the range (Fig. 3).Earthquake focal mechanisms further indicate that the tectonic structures bordering the AC range to the north still accommodates shortening today (Guzmán-Speziale, 2010; Authemayou et al., 2011b). A 20 x 30 km ice cap spread over the summit plateau of the AC range (Fig. 1) during the last glaciation (Anderson et al., 1973; Lachniet and Vazquez-Selem, 2005). However, unlike other

neotropical mountains (Lachniet and Vazquez-Selem, 2005), the AC range does not host remnants of earlier, more extensive ice caps. Their absence implies that ice caps formed during earlier glaciations were smaller despite climatic conditions everywhere else conducive to more extensive ice covers. The AC range therefore appears to rise fast enough to expose increasing areas to snow accumulation from one glacial cycle to the next.

Contraction prevails in the west While contraction has defined the evolution of the western part of the study area, and extension prevails in the east, due totranstension has prevailed further east since at least the Late Miocene. Such dominance of transtension in the east results chiefly from an eastward increase in the divergence angle between fault orientation andthe strike of the plate boundary and the direction of plate motion (Rogers and Mann, 2007). Transtension initiated the openingled to development of the Lake Izabal basin along the Polochic fault during the Middle Miocene (Carballo-Hernandez et al., 1988). Transtension has continued up to today, leading to the burial of the Maya surface under (Fig.1a) into which ~5 km of terrigenous sediments (Bartole et al., 2019). Transtension at the eastern end of the Motagua fault has, likewise, generated anhave accumulated since the Middle Miocene (Carballo-Hernandez et al., 1988; Bartole et al., 2019). Transtension also led the growth of another ≥1.4 km-deep, elongate (125x15 km) fault basin more than 1.4 km deep sedimentary basin at the eastern termination of the subaerial trace of the Motagua fault, next to the Caribbean Sea (Carballo-Hernandez et al., 1988). Starting in the Pliocene, . Transtension spread farther west, disruptingfurther to the west during the Pliocene, generating still-active normal faults that disrupt the northern flank of the SM range and the western end of the SC range (Authemayou et al., 2011b; Brocard et al., 2012). It continues today at slow slip rates north of the Sierra de las Minas (Brocard et al., 2012), and along the Polochic fault (Authemayou et al., 2012).

Slip on the Motagua fault is purely left lateral today, but vertical displacements generated narrow sedimentary basins along the fault in the past (Ratschbacher et al., 2009). During Eocene times (Newcomb, 1975) an elongate transform basin formed north of the fault; it was filled by the fluvial Subinal Formation which has an exposed thickness ≥1,500 m (Hirschman, 1962). The Subinal Fm. was fed by streams draining the northern side of the basin, and by an axial drainage that prefigures the current Motagua River. However the axial drainage may have flowed westward, instead of eastwards, toward southern Mexico, were Motagua valley type rock assemblages are found (Abdullin et al., 2016). The Subinal formation is broken into tilted blocks separated by steep angle faults with strike-slip and dip-slip displacements (Muller, 1979; Johnson, 1984). To the north, it seems to lie

in tectonic contact against the SC-SM basement rocks, usually along high-angle reverse faults (Muller, 1979; Bosc, 1971a).

2.12. Drainage evolution during the rise of the Central Guatemala mountain ranges

The evolution of the drainage network in response to contractional and transtensional uplift has been studied in detail (Brocard et al., 2011; Brocard et al., 2012). The rivers analyzed here correspond to the most stable flow lines of this network. They are deeply entrenched in basement rocks of the SC-SM and AC ranges, and their courses have not drifted since the

~~early stages of mountain growth. At their downstream end, they join river reaches that have experienced dramatic changes since~~ **since the Middle Miocene** ~~times (Fig. 2). These changes are the following: fisrt, the rivers that cross the Polochic fault have been deflected by left-lateral slip along the fault, developing tectonic deflections up to 40 km long~~

The rivers that drain the northern flank of the SC range represent the headwaters of a network that, farther downstream, experienced widespread reorganization during the late Miocene (Fig.2). Reorganization led to the formation of range-parallel rivers between the SC-SM and the AC ranges that collect the rivers that drain the northern flank of the SC-SM range and funnel them into the Chixóy River, one of the few rivers (together with the Cahabón, Chixóy, Selegua, and Cuilco Rivers, Fig.2), that still crosses the AC range. These rivers that cross the AC range also cross the trace of left-lateral Polochic fault, before entering the AC range. The Polochic fault has deflected and lengthened the course of the rivers that cross its trace (Fig.2) since the late Miocene (Brocard et al., 2011)~~. Second, the uplift of the AC range defeated range transverse rivers, promoting drainage reversal along defeated transverse valleys, and the formation of range parallel streams, such as the Chixóy River (Brocard et al., 2011). Third, transtensional faulting along the northern flank of the SM range has sparked a second pulse of drainage reorganization in Quaternary time, consisting of river captures and avulsions, at the benefits of the Polochic and Chixóy river catchments, and at the expense of the Cahabón River catchment (Brocard et al., 2012). Fourth, the growth of the Central American Volcanic arc further deranged river networks located in the west of the study area. The drainage of the arc is recent and often changing, especially after the many large, caldera-forming eruptions that have reshaped the topography of the arc since the Pliocene (Rose et al., 1999). Fifth, over the karstic highlands, north of the Polochic fault, rapid changes in river courses occur following the opening and closure of subterranean karstic pathways, since at least the Pliocene~~. Transtensional faulting along the northern flank of the SM range has initiated a second and still ongoing pulse of drainage reorganization during the Quaternary (Fig.2) (Brocard et al., 2012).

Large volcanoclastic aprons have piled up along the NE flank of the Central American Volcanic arc since the Pliocene. They have buried the western end of the SC range, deranging its river network. This complex area is therefore excluded from the present study. Likewise, the karstic highlands of Central Guatemala, especially those located north of the Polochic fault are also excluded from the analysis, their dynamics is mostly under the influence of the higher-frequency opening and closure of subterranean karstic pathways (Brocard et al., 2015a; Brocard et al., 2016a). ~~All these drainage rearrangements have affected the base levels of the rivers targeted in this study.~~

2.3. ~~Evolution~~Current pattern of ~~precipitations~~precipitation

~~Present day mean annual precipitation varies sharply across the study area (Fig. 4). Moisture from the Pacific and Atlantic oceans generates orographic precipitation along moisture facing slopes, while rain shadows develop over inland facing~~

~~slopes. As a result, and despite its narrowness (260 km in Central Guatemala), the Central American land bridge hosts a central dry corridor, surrounded by mountain ranges that experience marked asymmetric rainfall. The AC range receives as much as 4-6 m.yr^{-1} of precipitation on its northern flank due to the ingress of Caribbean moisture~~Moisture tracking from the Pacific Ocean and from the Caribbean Sea is intercepted by the slopes that face the western and eastern coasts of Guatemala, as well as the Petén lowlands in the north (Fig. 4). The AC range receives 4-6 m.yr^{-1} of mean annual precipitation along its northern flank in the Zona Reina (Thattai et al., 2003). In the west, the Central American Volcanic Arc intercepts moisture rising from the Pacific Ocean. In the east, moisture from the ~~SM range funnels~~ Caribbean ~~moisture~~ Sea is channeled along the Lake Izabal basin~~, with more precipitation taking place along its~~ and then rises up the northern ~~side, with intense~~flank of the SM range. Fog interception represents a substantial part of the annual precipitation above 2,000 m in the SM range (Holder, 2004). ~~The SM uplands are therefore mantled by thick soils, with frequent mass-wasting (Bucknam et al., 2001; Ramos Scharrón et al., 2012). By contrast, the SC range, surrounded on all sides by other topographic barriers, is much drier. Semi-arid conditions are reached on the floor of surrounding valleys~~The volcanic arc, the SM range, and the AC range cast rain shadows over the Corridor Seco (Machorro, 2014)~~.~~

~~The 7.4 My-old fossil forest of Sicaché (Fig. 2), located in an upper Miocene paleovalley on the southern side of the AC range, included pine trees and fern trees, growing over thick soils, suggesting mean annual precipitation ranging between 950 and 1,300 mm.yr^{-1}. This in an area now dominated by xerophytic vegetation~~, and in particular over the SC range, which receives little precipitation. Semi-arid climate is reached on the floor of the valleys that surround the SC range. ~~(Brocard et al., 2011). The fossil forest indicate a deeper penetration of the Caribbean moisture in the past, before the abandonment and uplift of the valleys that crossed the AC range.~~

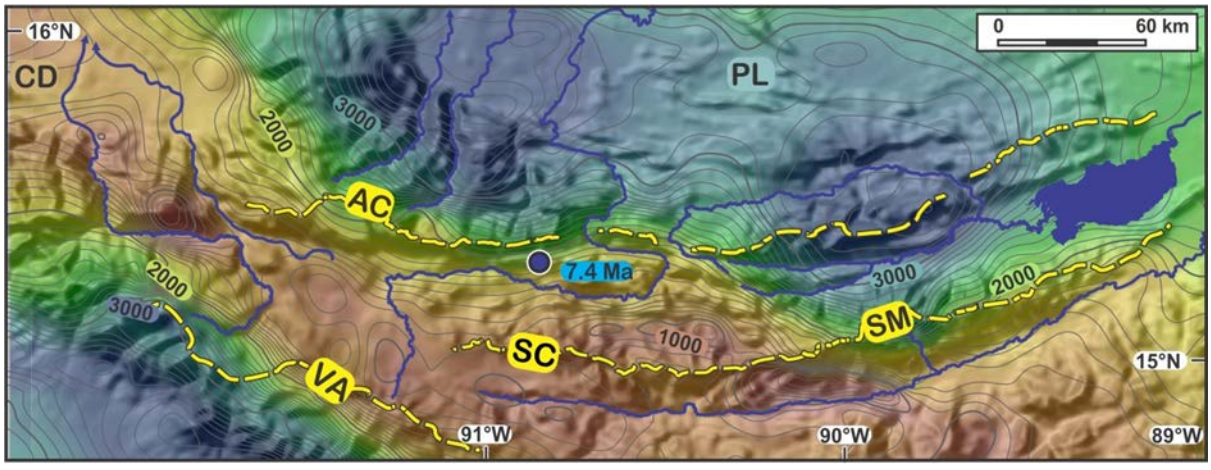

Figure 4. Mean annual precipitation across the study (MARN, 2017) from dry (red) to wet (blue). Isohyet spacing: 100 mm, draped over the shadowed GTOPO 30 DEM. Yellow dashed lines: range drainage divides. Blue dot: location of the fossil forest of Sicaché, buried below a 7.4 My-old ignimbrite (Brocard et al., 2011). CD: Central Depression of Chiapas, AC: Altos de Cuchumatanes, PL: Petén lowlands, SC: Sierra de Chuacús, SM: Sierra de las Minas, VA: volcanic arc.

2.4. Bedrock lithology

~~Bedrock erodibility exerts a strong control on the response time of river incision to rock uplift (Yanites et al., 2013; Brocard and Van der Beek, 2006; Finnegan et al., 2005; Duvall et al., 2004). The distribution of~~ Rock belts in Central Guatemala ~~tends~~tend to follow the strike of mountain ranges (Fig. 5). Late Cretaceous schists and gneisses of the Chuacús Fm. form the core of the SC-SM range. They are flanked ~~to the south and to the north~~ by the late Cretaceous migmatites of the San Agustin Fm., and by the marbles and amphibolites of the Jones Fm. In the north, this metamorphic core ~~lies to~~is tectonically juxtaposed across the ~~north in faulted contact against~~Baja Verapaz shear zone to the basement of North America, ~~composed of low grade metamorphic rocks of pre Permian age (Santa Rosa Fm.) derived from Ordovician Carboniferous sedimentary rocks~~ which mostly covered by a Permian megasequence of terrigenous sediments and carbonates (Sacapulas, Tactic-Esperanza, and Chochal Fms.(Anderson et al., 1973)). These units are intruded by Ordovician (e.g. Rabinal), Triassic, and Jurassic (e.g. Matanzas) granites. ~~They underlie the floor of the Chixóy River Basin, between the SC and AC ranges. They also crop out in the core of the AC range. These basement rocks are overlain by a Permian megasequence of conglomerates, shales, marls, and limestones (Sacapulas, Tactic Esperanza, and Chochal Fms. respectively (Anderson et al., 1973)), that mostly exposed in the AC range, and, to a lesser extent, in the eastern part of the SM range.~~

A megasequence of continental terrigenous sediments (the Todos Santos Fm.), Cretaceous carbonates, and Cretaceous evaporites (Cobán Fm., Campur Fm.) covers much of the AC range (Fig. 5). Ultramafic rocks obducted over the carbonates in Late Cretaceous (Campanian) time are preserved within weakly metamorphic synformal klippes (Baja Verapaz, Santa Cruz, and Juan de Paz ophiolites). Higher grade serpentine mélanges crop out along the Motagua valley (Flores et al., 2013).

~~A megasequence of continental Jurassic red beds (Todos Santos Fm.), Cretaceous carbonates and Cretaceous evaporites (Cobán Fm., Campur Fm.) is exposed over much of the AC range (Fig. 5). The strong development of karstic processes in its carbonate rocks generates complex and rapidly shifting water routing (Brocard et al., 2015a), making the erosional response of the drainage more difficult to study. For these reasons these areas are excluded from the study. Ultramafic rocks were obducted over the carbonates in Campanian time. They are preserved within weakly metamorphic synformal klippes (Baja Verapaz, Santa Cruz, and Juan de Paz). Higher grade serpentine mélanges crop out along the Motagua valley (Flores et al., 2013).~~

The southern base of the SC-SM range is incised into sediments deposited in elongate transtensional basins that formed along the Motagua fault (Ratschbacher et al., 2009). During Eocene times (Newcomb, 1975) one such basin was filled by the red beds of the Subinal Formation (Fig.5), which has an exposed thickness of ≥1,500 m (Hirschman, 1962). Its sediments were provided by the current basement of the SC-SM range, and by the more mature fluvial sediments of an axial

river that prefigures the current Motagua River (Guttiérrez, 2008). It now lies in tectonic contact against the SC-SM basement rocks, usually along high-angle reverse faults (Muller, 1979; Bosc, 1971a).

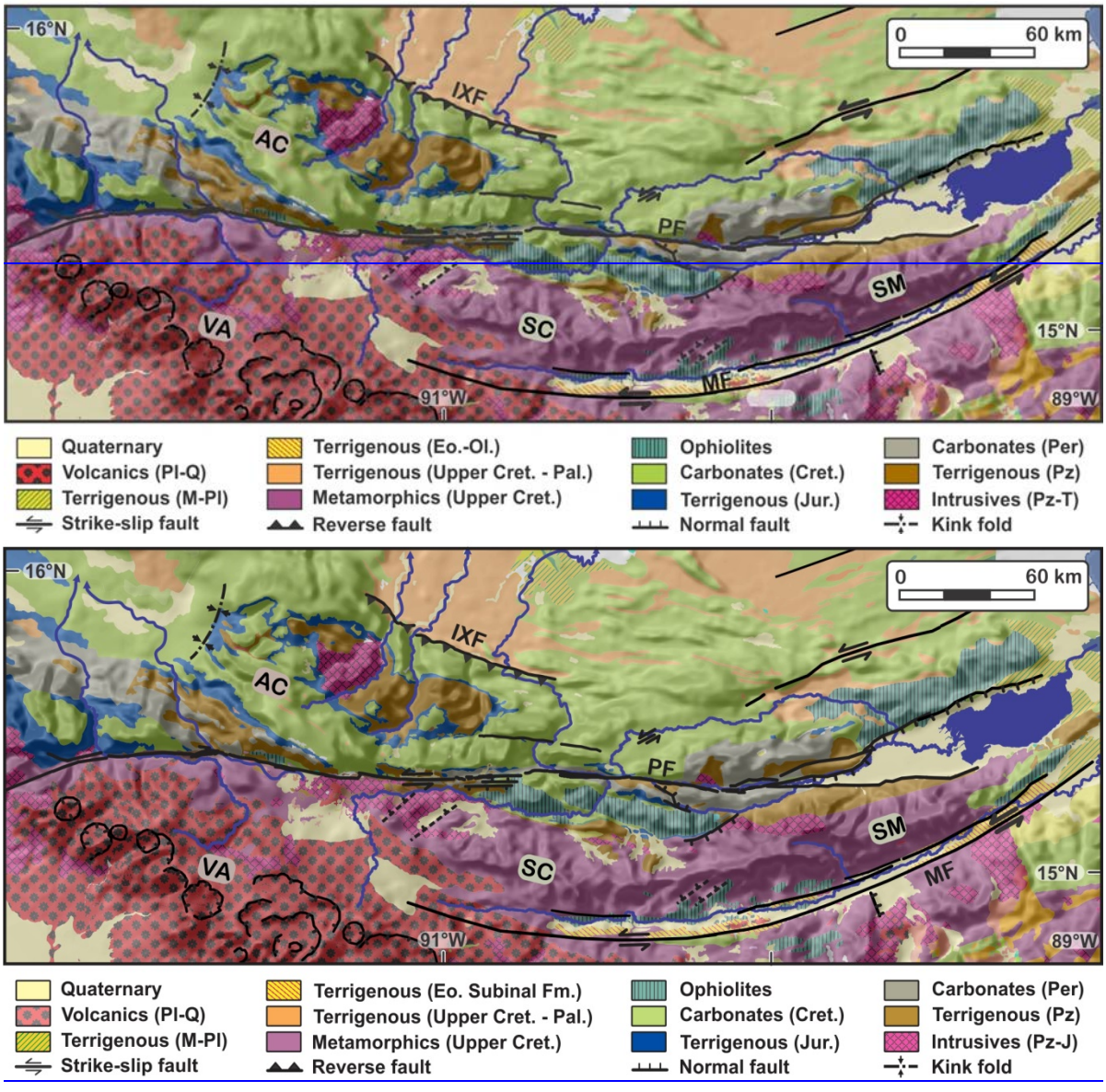

Figure 5. Geology and structure of Central Guatemala (Instituto Geográfico Nacional de Guatemala; Instituto Hondureño de Geología y Minas; Instituto Nacional de estadística y geografía de México), draped over the GTOPO 30 DEM. ~~Faults:~~AC: Altos de Cuchumatanes, IXF: Ixcán fault, MF: Motagua fault, PF: Polochic fault, SC: Sierra de Chuacús, SM: Sierra de las Minas, VA: volcanic arc.

3. Methods

3.1. ^{40}Ar-^{39}Ar radiometric dating of volcanic rocks

The age of the low-relief Maya surface has been constrained previously using bracketing age markers (Brocard et al., 2011). ~~The age of the low relief Maya surface was previously constrained by bracketing marker ages. To improve the dating of the surface, we dated a clast of basaltic andesite embedded within a lahar deposit that rests on the Maya surface, at the western end of the Sierra de Chuacús (Fig. 2). The age of incision of the Motagua valley has been previously constrained using alkaline basalts exposed along the floor of the Motagua valley (Tobisch, 1986). To refine the chronology of incision of the Motagua valley, we dated a basalt flow located 500 m above the Motagua River near El Jute (Bosc, 1971b), in the foothills of the Sierra de las Minas (Fig. 6). Two ^{40}Ar/^{39}Ar whole rock ages on the basalt of El Jute and one whole rock age on the basaltic andesite of Chujuyúb were obtained at the U.S. Geological Survey (USGS) in Denver, CO, USA (Appendix A).~~

~~**3.2. Terrestrial ^{10}Be erosion rates**~~

To improve the dating of the Maya surface we dated andesite boulders embedded in a lahar deposit that rests on the Maya surface, at the western termination of the SC-range near the locality of Chujuyúb (Fig. 2). To establish the chronology of incision of the Motagua valley, we used previously dated alkaline basalts located on the floor of the Motagua valley (Tobisch, 1986), and dated a basalt flow located 500 m above the Motagua River in the foothills of the Sierra de las Minas, near the town of El Jute (Bosc, 1971b) (Fig. 6). Two ^{40}Ar/^{39}Ar whole-rock ages were retrieved from the basalt of El Jute, and one whole-rock age was obtained on the basaltic andesite of Chujuyúb by the U.S. Geological Survey (USGS) in Denver, CO, USA (see Supplement 1).

3.2. Terrestrial ^{10}Be erosion rates

We measured the concentration of ^{10}Be in quartz ~~hosted in ridgeline~~grains extracted from soils and river sediments ~~provides.~~ We used their ^{10}Be concentration to calculate hillslope erosion rates, integrated over the past 10^3-10^4 years (~~Appendix B~~see Supplement 2). The ~~soils~~soil and ~~rocks~~rock samples were collected along ridgelines ~~located~~ in the SM range. They provide ~~site specific~~ erosion rates restricted to the site of sampling (Table S2-1, Fig. S2-3c). ~~They~~ Three of these samples consist of ~~crushed and amalgamated~~ quartzose vein fragments ~~hosted in~~exhumed from weathered orthogneiss ~~(3~~, while the two remaining samples~~), and of single blocks of~~ come from a highly weathered pegmatite ~~from~~that crops out on the monadnock of Cerro las Palomas, ~~a monadnock located on~~in the Montaña El Imposible (~~2 samples~~Fig. S2-3b).

The majority of the ~~dataset~~samples, however, consist of ~~^{10}Be concentration measured in~~ riverborne quartz~~,~~ collected in the bed of 30 rivers ~~that drain~~in the SM, SC, and AC ranges (Fig. 6, Table S2-2, Fig. S2-3).~~.~~ They provide catchment-averaged ~~estimates of soil~~ hillslope erosion ~~rate~~rates (Brown et al., 1995). ~~In mountainous regions, the amount of ^{10}Be produced during the downhill transport of quartz grains and their subsequent transport along rivers is usually small compared to the amount of ^{10}Be produced during the final exhumation of quartz grains through the topmost 2-3 m of soils and rock below the ground surface. The concentration of ^{10}Be is therefore expected to directly reflect hillslope erosion.~~

~~Quartz grains were~~The quartz was extracted from the sand grain-size fraction (250-500 µm) of ~~30 rivers (Fig.~~ the river sediments.~~6, Table S2-2, Fig. S2-3). Many of the sampled rivers drain similar quartz-bearing formations (such as, in particular, the extensive Chuacús Fm. in the SC-SM range, and the extensive Santa Rosa Fm. in the SC and the AC ranges).~~ ^{10}Be production increases ~~sharply~~rapidly with elevation. ~~Therefore~~As a result, systematic altitudinal variations in ~~quartz~~the concentration ~~can affect~~of quartz of the source rocks may distort the calculation of erosion rates~~, if homogeneity is assumed. The distribution of quartz-feeding formations in the sampled catchment does not vary consistently with elevation except in the Altos de Cuchumatanes (Fig. S2-3A), where~~. Such layout in encountered in AC range (Fig. S2-3a), in which a sensitivity analysis ~~was conducted: we weighted the ^{10}Be production according to back of the envelope estimates of the relative quartz concentration of the formation outcropping in each catchment. We found the resulting~~to this effect ~~to remain marginal, however (<5%, Table S2-2). Quartz enrichment from the fresh rock to the topsoil is commonly important~~was conducted. The ^{10}Be production was weighted according to estimates of the quartz concentration in the source rocks. Weathering is intense in tropical mountains, promoting the concentration of quartz in the soils, ~~where weathering is intense. It leads to~~and an underestimation of erosion rates that increases with increasing weathering intensity. An assessment of ~~its potential amplitude~~the effect of quartz enrichment was therefore conducted~~,~~ (Table S2-2), using quartz enrichment values ~~measured in topical~~ from mountain tropical soils ~~from~~of Puerto Rico (Ferrier et al., 2010).

The sampling was further designed such as to document erosion rates within nested catchments (Fig. 6. Fig. S2-3a,b), in order to capture ~~systematic~~ along-stream variations in erosion rates, such as those produced by ~~waves of enhanced stream incision along the drainage network~~headward-migrating knickpoints ~~(Willenbring et al., 2013).~~

~~Samples were prepared at the ^{10}Be extraction lab of the Department of Geology and Geophysics at the University of Minnesota, and~~(Willenbring et al., 2013b; Brocard et al., 2015b). The samples were prepared at the ^{10}Be extraction laboratory of the Department of Geology and Geophysics at the University of Minnesota, as well as at the PennCIL lab of the Earth and Environmental Sciences department at the University of Pennsylvania (~~Appendix B~~see Supplement 2).

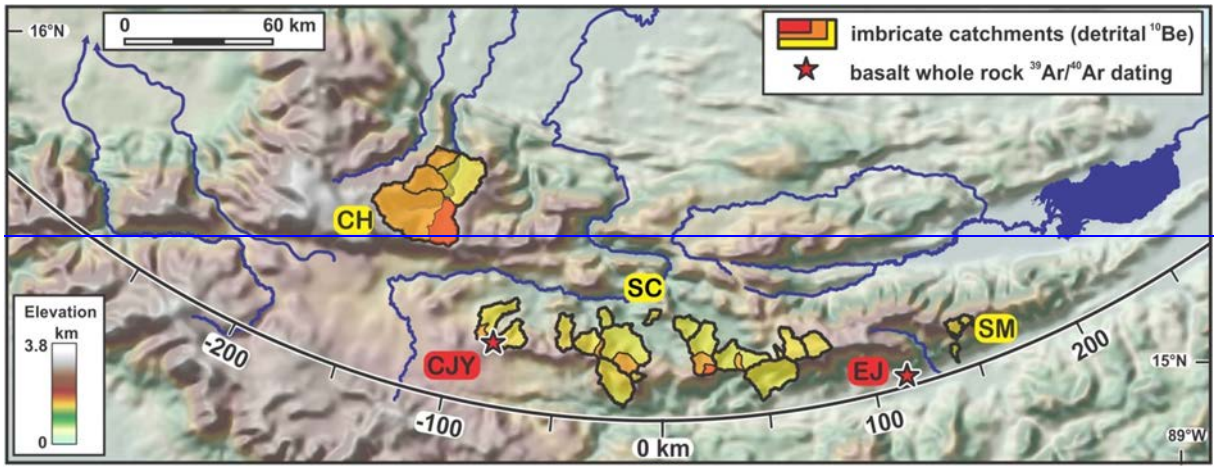

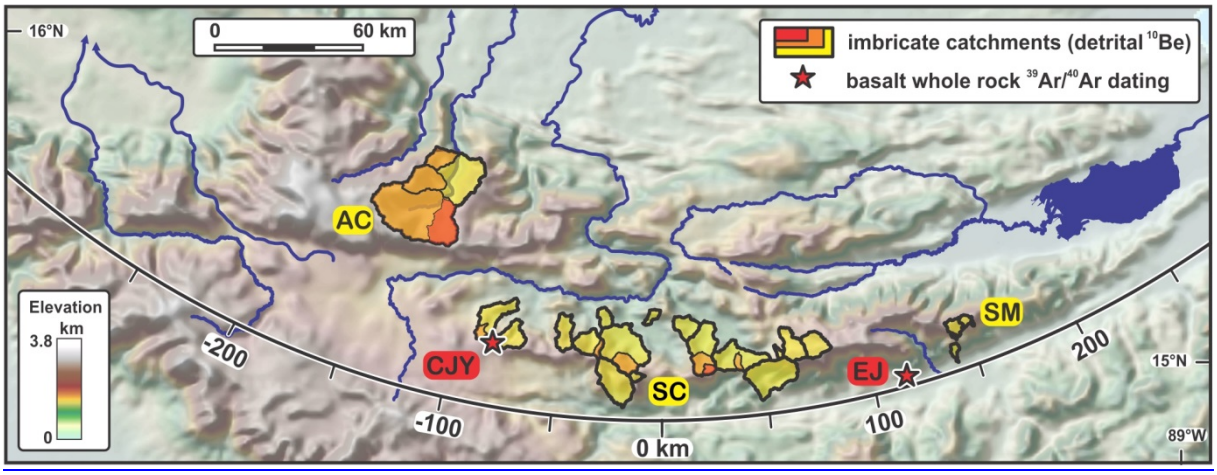

Figure 6. Catchments sampled for the ^{10}Be analysis (AC: Altos de Cuchumatanes, SC: Sierra de Chuacús, SM: Sierra de las Minas), and ^{40}Ar/^{39}Ar dating (CJY: Chujuyúb, EJ: El Jute). Enlarged maps of the catchments and their lithologies are provided in Fig. S2-1). The arcuate line represents the axis used for plate boundary-parallel projections of Figs. 10 and 12.

3.3. Calculation of an erosion index

To test the influence of hillslope steepness and precipitation on ^{10}Be-derived erosion rates, we calculated a normalized erosion index (Montgomery and Stolar, 2006; Finnegan et al., 2008). The erosion index assumes that hillslope erosion is driven by surface runoff along hillslopes, during rainfall events. over the study area, and averaged it over the extent of the sampled catchments. In its simplest form, the erosion index (EI) correlates the entrainment of particles by surface runoff may therefore correlate withto hillslope steepness and annual rainfall. The erosion index is calculated asWe used a power function of these two parameters. Here, itformulation in which this entrainment is assumed to be proportional to shear stress: Eq. (1):

$$EI = Q^{1/3} \cdot S^{2/3} \quad (1)$$

where Q is discharge (in m^3/s^{-1}) and S the along-slope gradient (m/m). Other choices of exponent values can be made depending of assumptions on the entrainment of soil particles (such as proportional to stream power per unit length or unit area). To assess the sensitivity of the results to the choice of the exponent, we also implemented a more basic version of the erosion index, in which the index scales linearly with discharge and slope.$^{-1}$). Slope was extracted from the national Guatemalan IGN DEM at 20 ma resolution of 20 m, and discharge was calculated using the mean annual precipitations

~~of~~provided in the MARN (2017) report. Rainfall values were corrected for evapotranspiration, using a map of vegetation from the ~~(MARN, 2017), and evapotranspiration values representing 10-82% of the total rainfall, depending on the type of vegetation, derived~~MARN (2017) report, and evapotranspiration values from the Puerto Rico GAP project (Gould et al., 2008)~~.~~, which amount to 10-82% of the total rainfall, for the different types of vegetation reported in the MARN report. EI values were normalized to the highest obtained ~~erosion index~~EI value within the study area.

3.~~-~~4. River profile segmentation

~~To study the response of stream incision to uplift, particularly in the form of upstream migrating waves of accelerated or decelerated incision,~~

We extracted the long-profiles of 220 rivers ~~draining~~located in the AC, SC, and SM ranges~~ from~~, using the Guatemala national 20 m-resolution DEM~~,~~ released by the National Geographic Institute of Guatemala. ~~Karstic processes~~The beds of these rivers were observed on stereoscopic couples of aerial photographs provided by the National Geographic Institute of Guatemala (see next section for details). These observations allowed us to sieve out rivers along the expression of longer-term river dynamics is hidden by shorter-term adjustments to karstic disturbances, debris flows, and deep-seated landslides ~~dominate the evolution of many small streams, which were therefore excluded from the dataset.~~. A subset of the 110 rivers that ~~better~~best capture ~~the evolution of the overall landscape~~long-term trends was used in the final analysis (Fig.7).

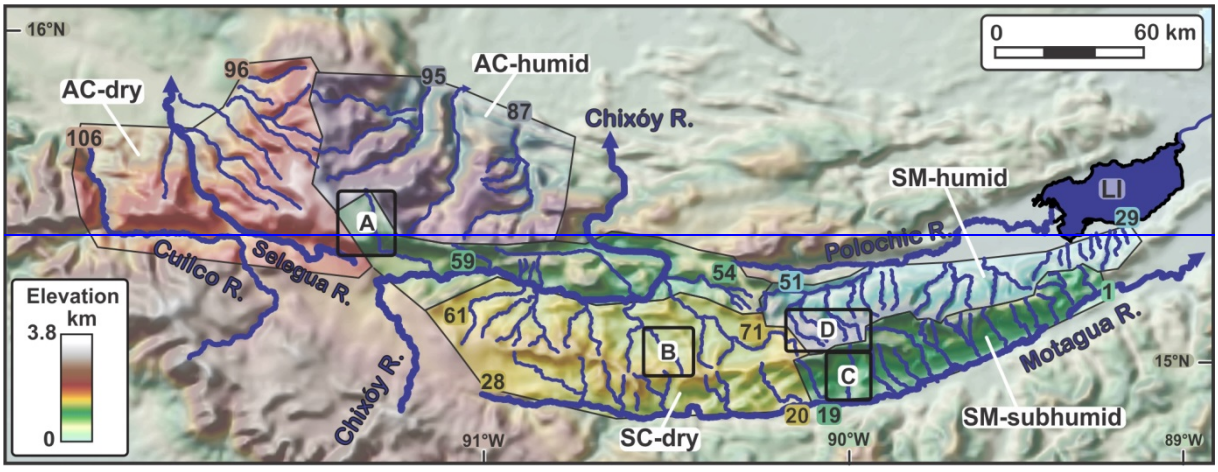

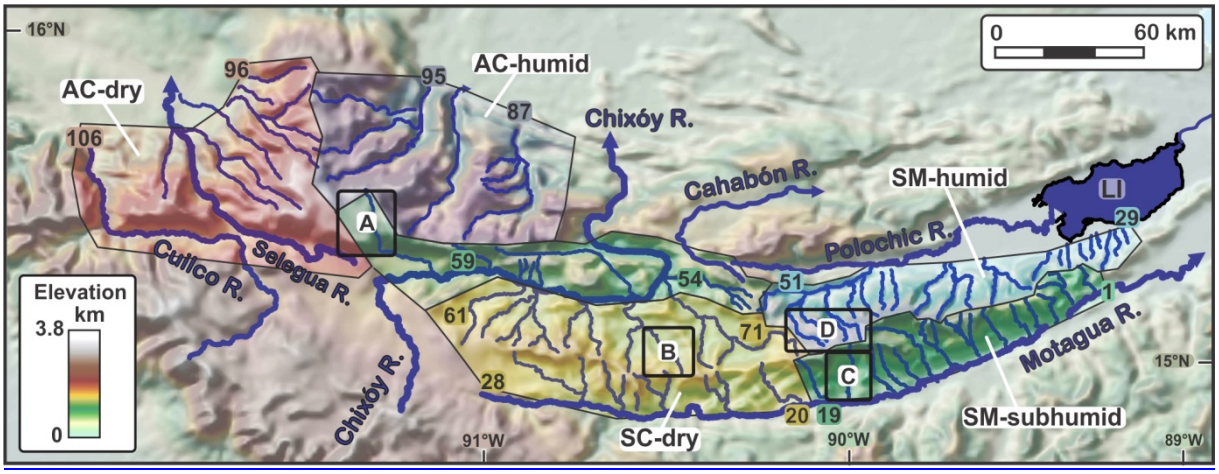

435 Figure 7. Distribution and grouping of the streams used in the river long-profile analysis, and their grouping by geographic areas. AC: Altos de Cuchumatanes, LI: Lake Izabal, PF: Polochic fault, SC: Sierra de Chuacús, SM: Sierra de las Minas. Numbers ~~refer~~(1-106) correspond to the numbers ascribed to the rivers, as listed in table S4-1. The corresponding river profiles are presented on Figs S4-2 to S4-7, and on Fig. ~~12a,b. Location and extent~~12. Boxes A-D: footprints of the maps displayed on Fig. 8.

440 ~~River gradients decrease steadily in the downstream direction due to the increase in river discharge. Convex and concave up breaks in slope generate irregularities in this overall trend. Convex up breaks are referred to as river knickpoints. All breaks in slope observed here, whether convex or concave up, are referred to as knickpoints. Knickpoints most commonly manifest adaptations of river gradient to along stream changes in rock uplift rate, bedrock erodibility, sediment flux, and sediment grain size. We refer to such knickpoints as steady knickpoints, because their location only changes very slowly, tracking~~
445 ~~spatio-temporal changes in the distribution of rock types, rock uplift, or sediment fluxes and grain size. By contrast, step changes in base level generate knickpoints located at the front of waves of accelerated or decelerated incision which migrate in the upstream direction. Such knickpoints are here after referred to as migrating knickpoints, as they usually migrate along stream much quicker than steady knickpoints. The identification of knickpoints and their classification as steady or migrating commonly resorts to a linearization of river profiles that filters out the downstream increase in stream discharge. Among the~~
450 ~~most commonly used linearization methods one finds the projection of river profiles in DS plots, in which river profiles are represented in a log (downstream distance) vs. local river gradient space (Goldrick and Bishop, 1995), and in AS plots, in which river profiles are projected in a log (local drainage area) vs. log (local slope) space (Howard, 1994). Large step increases in discharge at stream junctions makes linearization results difficult to interpret in AS plot, combined with the noise commonly observed in slope data, which makes it difficult to separate steady and migrating knickpoints. This is~~
455 ~~reinforced at places where changes in slope spread over lengths close to the spacing of stream junctions. For this reason, the integral method (Perron and Royden, 2013) has gained popularity. Elevation is plotted (on chi plots or χ plots) as a function of chi (or χ), which is an upstream integral of incremental upstream distance, divided by a normalized local drainage area: Eq. (2):~~

~~(2)~~

460

To identify knickpoints along the river profiles, we resort to a linearization method that filters out the downstream increase in stream discharge. We chose the integral method (Perron and Royden, 2013), in which elevation is plotted (on chi-plots or χ-plots) as a function of chi (or χ), which is an upstream integral of incremental upstream distance, divided by a normalized local drainage area: Eq. (2):

$$\chi = \int_{xo}^{x} \frac{Ao}{A(x')}^{\frac{m}{n}} dx' \quad (2)$$

where *A* and *x* are the drainage area ~~and upstream distance, respectively; Ao and xo a reference drainage area and a reference upstream distance taken at the same point, respectively, m and n two exponents encapsulating the influence of drainage area and local slope on river incision rate, respectively. One of the caveats of this linearization is that it requires foreknowledge of ratio the ratio m/n (intrinsic concavity, or θ).~~(in m^2) and upstream distance (in m), respectively; *Ao* (in m^2) a reference drainage area and *xo* a reference upstream distance taken at the same point, *m* and *n* two exponents that encapsulate the influence of drainage area and of local slope on river incision rate, respectively. This method overcomes a lot of the scatter that plague earlier linearization methods(Whipple and Tucker, 2002; Goldrick and Bishop, 1995). One of its caveats, however, is that it requires a foreknowledge of the intrinsic concavity, or θ, defined as m/n. The value of θ can be determined by incrementally fitting river profiles to a straight line (Mudd et al., 2014). Such approach ~~requires relatively simple~~is convenient on river profiles~~,~~ made up of a small number of successive segments. Many rivers in the study area, however, have highly segmented profiles~~.~~ (see section 4.3), preventing convergence toward a single value. Besides, the value of θ may ~~also~~ change along-stream~~,~~ as a result of changes in climate (Murphy et al., 2016)~~, of~~ or changes in the dominant erosive processes operating on the streambed (Brocard and Van der Beek, 2006)~~, of~~ such as the alternation of detachment-limited (Howard, 1994) and transport-limited river incision (Whipple and Tucker, 2002), ~~and of~~or such as the alternation of sediment-starved and overfed reaches (Sklar and Dietrich, 2006). Therefore, instead of fitting θ to each river profile, we ~~therefore~~ applied a common normalizing concavity θ_n value of 0.5 to all river profiles, after assessing best fit values on a subset of streams (~~Appendix C~~see Supplement 3). This initial screening showed that most concavity values range between 0.4 and 0.6, as predicted by theoretical studies (Perron and Royden, 2013; Whipple, 2004)~~. Most outliers have higher concavities. Profiles with θ > 0.7 probably incorporate diffuse downstream changes in dynamics, such as, for example, transitions from boulder-armored reaches to gravel-cobble bars reaches~~, supporting the choice of a concavity of 0.5.

3.5. Classification of stream segments

The morphology of the streambeds was examined along ~~the~~each linearized ~~segments was determined~~segment using stereoscopic black-and-white 0.5-m resolution aerial photographs ~~shot~~taken in 2001 provided by the Guatemala National

Institute of Geography (~~Appendix D). These~~see Supplement 4). Observations were punctually ground-proofed ~~in the~~during field ~~(Figs. S4-2 to S4-7).~~work campaigns stretching over 6 years. River beds were ~~classified~~grouped into ~~the following categories,~~types according to the bed component that dominantly ~~controls~~determines river gradient along each segment, namely: bedrock, bedrock and gravel bars, gravel bars over bedrock strath, gravel bars over thick alluvial fill, colluvium, large immobile boulders, boulders and gravel bars, boulders and bedrock (Table S4-1). ~~Incision is~~Classification failed in many headwater channels because their bed is masked by overhanging riparian vegetation. The classification roughly reflects differences in the factors that determine stream incision. River incision is indeed likely detachment-limited along bedload-dominated reaches, and transport-limited along gravel- and cobble-dominated reaches ~~resting~~, lying over bedrock straths (Tucker and Whipple, 2002; Brocard and Van der Beek, 2006). ~~Identification was left undetermined along many headwater channels, where streambeds are masked by overhanging riparian vegetation.~~Boulder-armoured reaches are chocked by slowly- to non-moving boulders that act more like bedrock than bedload, and are therefore detachment-limited. However, unlike other types of bedrock channels, these boulder channels do not reflect the erodibility of the underlying bedrock, but that of surrounding hillslopes, because the majority of the boulders originate from the valley sides. Changes in streambed type from one segment to the next assisted the classification of river knickpoints (see following section).

~~Changes in streambed type from one segment to the next reflect changes in incision rates, or in bedrock resistance. They therefore assist the identification of the origin of the knickpoints. Boulder-armoured reaches are dominated by slowly-moving to non-moving boulders that act as a bedrock substrate, rather as a bedload. They are often delivered by valley flanks to river channels and therefore reflect the geology of the hillslopes rather than that of the streambeds. Changes in streambed type are usually sharp along streams across knickpoints. The ranking of segments in discrete classes still somewhat artificially discretizes a rather continuous spectrum of observed streambed conditions when all rivers are analysed together.~~

3.6. Classification of river knickpoints

~~The knickpoints were classified into the following categories:~~

~~1. Lithogenic knickpoints produced by along stream variations in bedrock erodibility. Downstream increases in erodibility generate concave-up knickpoints, whereas downstream decreases in erodibility generate convex-up knickpoints.~~

~~2. Lithogenic knickpoints produced by sudden changes in the relative orientation between the strike of the streambed and the strike and dip/pitch of the dominant structural grain (bedding, tectonic cleavage, foliation, lineation). Erodibility is usually higher parallel to the structural grain. Convex knickpoints develop where stream courses veer from subparallel to crosswise to the structural grain. Conversely, concave knickpoints develop where streams become subparallel to the structural grain.~~

~~3. Equilibrium tectonic knickpoints, produced by along stream variations in rock uplift rate. They are convex-up if rock uplift and stream incision increase in the downstream direction, and concave-up otherwise.~~

~~4. Alluvial knickpoints, generated by downstream changes in grain size. Convex-up alluvial knickpoints result from an increase in bedload grain-size, usually where steep tributaries injects a coarse bedload into a trunk stream. Concave-up knickpoints result from a rapid decrease in grain size, usually through sorting at the boulder-gravel or gravel-sand transitions where bedload grain size distribution is strongly multimodal.~~

~~5. Concave-up transitions from detachment-limited to transport-limited river incision, usually at the apex of alluvial fans (Fig.~~ Convex-up breaks-in slope along river profiles are commonly referred to as river knickpoints. For convenience, we refer here to all breaks-in-slope, whether convex or concave, as knickpoints. Knickpoints were classified as lithogenic, alluvial, tectonic, migrating and miscellaneous (see supplement 4). Miscellaneous knickpoints represent adaptations or river profiles to local, stochastic disturbances (such as landslides and epigenies), and are usually short-lived. Most knickpoints in the study area are adaptations of river gradients to along-stream variations in rock uplift rate, bedrock erodibility, sediment flux, or sediment grain size. These knickpoints can be regarded as steady, inasmuch as their location only changes very slowly along the river profiles, tracking spatial changes in the distribution of rock types, rock uplift, sediment fluxes and bedload grain size. By contrast, knickpoints that spearhead step-increases or step-decreases in river incision rates migrate in the upstream direction along river profiles in the form of waves of accelerated (Rosenbloom and Anderson, 1994; Merritts et al., 1994) or decelerated incision~~8c), and pediments (Fig. 8b). Such transitions nucleate at major discontinuities (fault, lithological boundary), and then migrate upstream by backfilling, or by pedimentation. They can be viewed as a concave-up version of the following category~~ (Howard, 1997). They are hereafter referred to as migrating knickpoints, for they usually migrate faster than the knickpoints previously described. Concave-up migrating knickpoints commonly mark the transition from detachment-limited to transport-limited river incision (Whipple and Tucker, 2002) are usually found at the apex of alluvial fans (Fig. 8c), and pediments (Fig. 8b).

~~6. Unstable, upstream migrating convex knickpoints, produced by an increase in base-level lowering rate (Rosenbloom and Anderson, 1994; Merritts et al., 1994). They are convex, separating upstream, slower incising reaches, from downstream, faster incising reaches. Their location is, in principle, independent from lithological boundaries, and controlled by the laws of knickpoint propagation (see below). In some cases, they consist of two successive convexities: an upper convexity set into a soft shallow substrate (alluvium, saprolite), ahead of a second, usually steeper knickpoint, set into the underlying, harder substrate (Fig.~~

Theoretical geometric differences between migrating and steady knickpoints in linearized spaces~~ 8d). Such knickpoints propagate along many several branches of the drainage network, when produced by a common change in base-level. In the study area, however, some headward migrating knickpoint can be tied to more local causes, such as river captures and avulsions (Brocard et al., 2012). A few migrating knickpoints have also formed on resistant rock, upstream of more erodible substrates. Their formation then results from the entrenchment of a previously unsegmented stream into two different lithologies. They are labelled as superimposition transient knickpoints.~~

~~7. Miscellaneous knickpoints produced by a variety of other local causes. In the study area, deep-seated landslides entering river beds have obstructed the rivers and triggered sedimentary back-filling upstream. Steeper profiles are formed across the landslides, where incision rapidly erodes the obstruction itself, or the opposite valley flanks by epigeny. Paroxysmal eruptions along the Central American Volcanic Arc have occasionally caused widespread infilling the valleys of Central Guatemala by volcanoclastic flows. The most recent event of this kind occurred 84 ky ago, during the formation of the Atitlán caldera (Rose et al., 1987), when 100-200 m of primary and reworked pumice filled many valleys (Brocard and Morán, 2014; Tobisch, 1986). Rivers have long re-incised the fills down to their pre-eruption levels, but one long-lasting effect of this disturbance was the re-incision of some river courses by epigeny away from former valley axes, in the valley flanks, generating knickpoints.~~

~~Steady knickpoints correspond to categories 1–4, while migrating knickpoints correspond to categories 5-6. River profile analysis~~ have been used to discriminate unstable, migrating knickpoints from stable, equilibrium knickpoints (Goldrick and Bishop, 1995; Perron and Royden, 2013; Whipple and Tucker, 2002). In χ-space, upstream migrating knickpoints which celerity is controlled by the stream power law, ~~propagating~~ and that propagate along ~~the~~ various branches of a single drainage~~, and that propagate~~ through a homogenous substrate ~~experiencing~~affected by homogeneous rock uplift, should all share the same elevation and the same χ value (Royden and Taylor Perron, 2013). In the real world, however, variations in bedrock erodibility, climate, and rock uplift often scatter these values, challenging interpretations based on these sole geometric properties, in particular in areas where environmental heterogeneities generate steady knickpoints ~~with height~~which heights and wavelengths are similar to that of ~~the~~ migrating knickpoints interspersed among them.

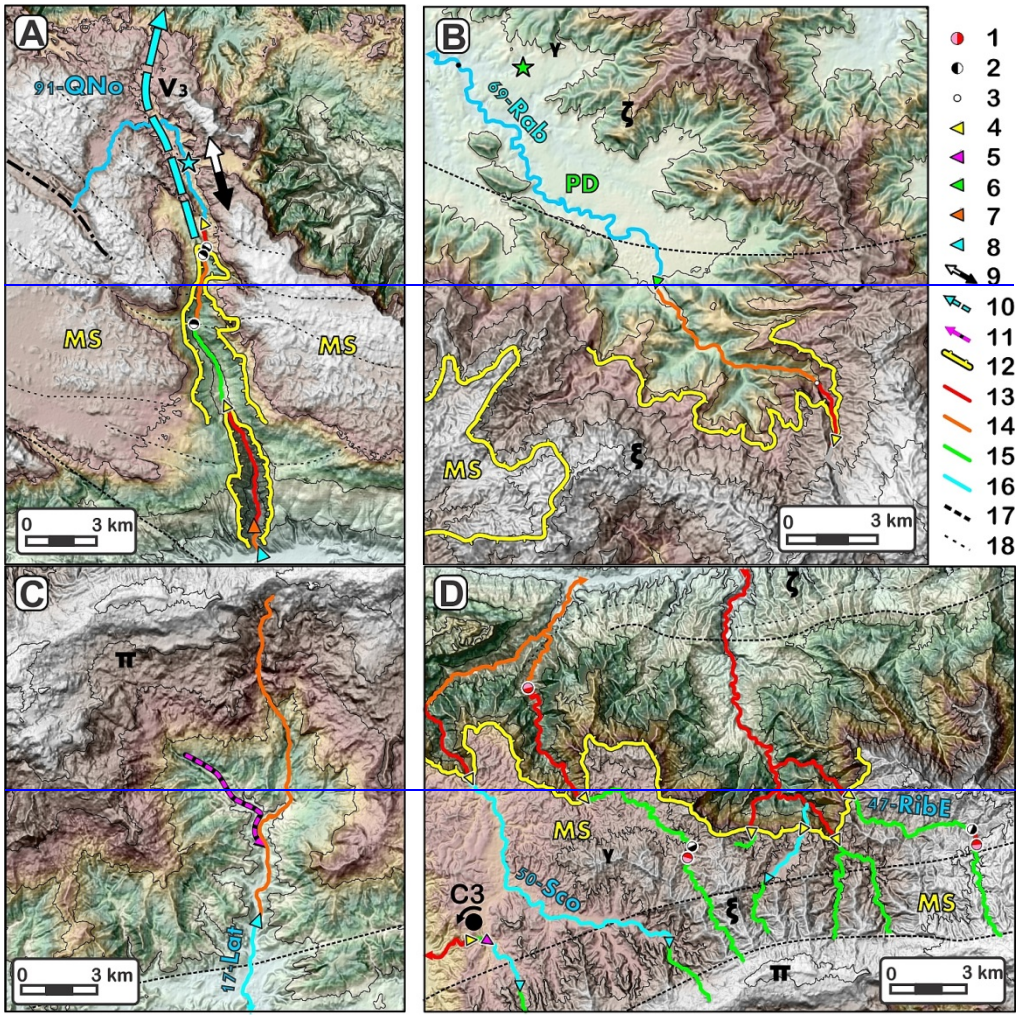

Figure 8. Examples of some knickpoint types in their geomorphic setting. Shaded and sloped 20-m resolution ALOS DEM © JAXA. Location of maps on Fig. 7. (a) paleovalley V3 of Quilén Novillo Chancol (AC Range), showing the paleovalley shallowly incised in the Maya surface (MS), and its rejuvenation, following drainage reversal, by two nested waves of headward-migrating erosion, the lower one clearly related to the uplift and steepening of the southern flank of the AC range with respect to the SC range farther south. (b): stepped topography in the SC range, with headward migrating knickpoints dismantling the Maya surface, an intermediate wave of dissection, and a pediment (PD) forming at the base of the range, (c): diffusive erosion in serpentinite mélange, catchment of Río Hato (SM Range), (d): dissection of the Maya surface along the northern flank of the SM Range. Blue star: gravel of the QN Chancol paleovalley (Brocard et al., 2011). Green star: outcrop of pedimented granite.

Lithology: ζ: schist and slate, ξ: gneiss, Y: granite, π: serpentinite mélange. Knickpoints: 1: lithogenic, 2: structural, 3: undetermined, 4: headward-migrating, 5: headward-migrating in soft substrate, 6: pediment apex, 7: boulder fan apex, 8: gravelly fan apex, 9: drainage reversal, 10: paleovalley, 11: large debris flow deposit, 12: front of erosion; river bed environment: 13: bedrock, 14: boulder, 15: gravel

~~over bedrock, 16: gravel, 17: lithological boundary, 18: bedding trace. C3: 200 ky-old~~

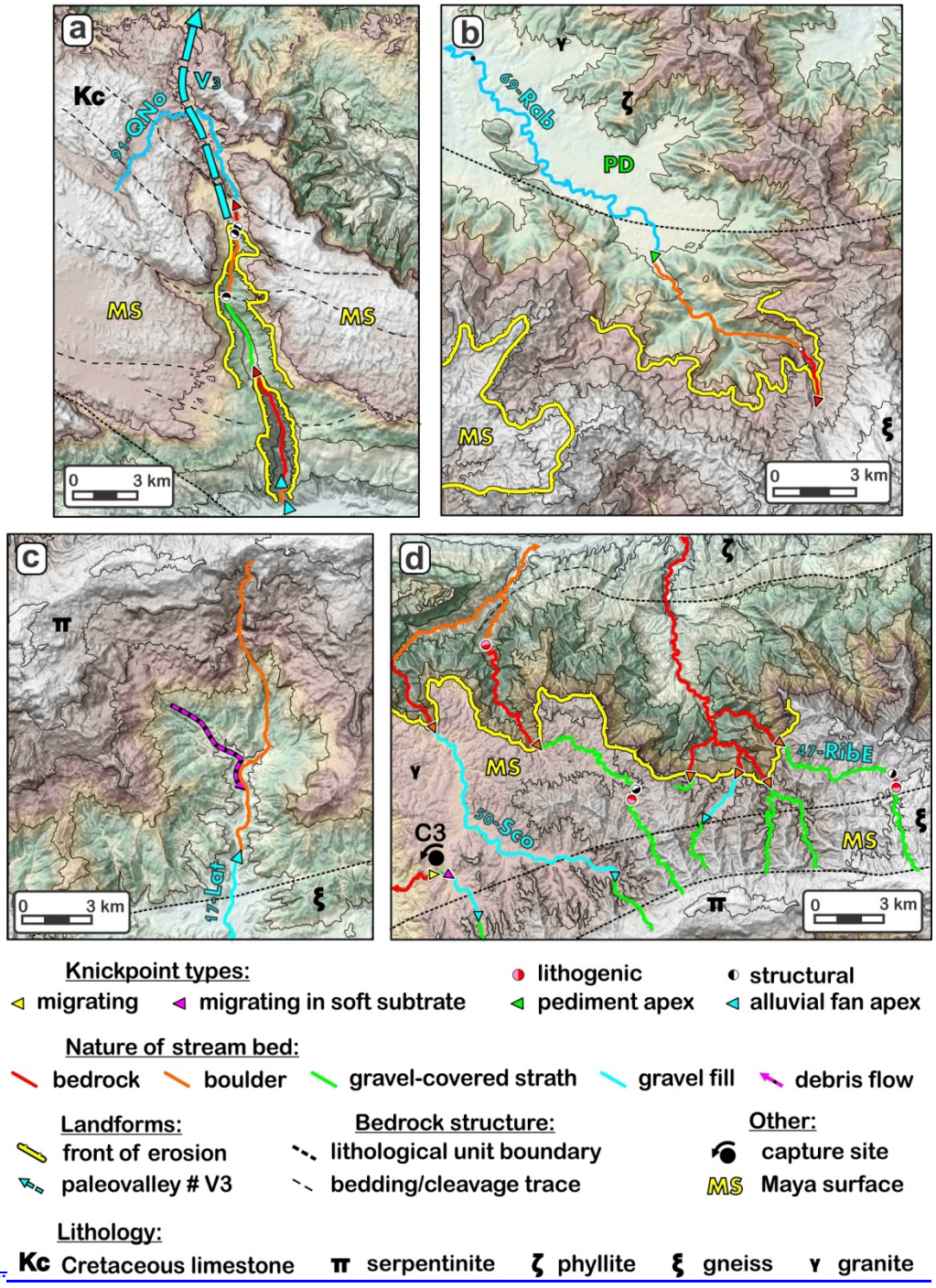

~~avulsion.~~

Figure 8. Examples of some knickpoint types in their geomorphic setting. Shaded and sloped 20 m resolution ALOS DEM © JAXA. Location of maps on Fig. 7. (a) valley of the Quilén Novillo-Chancol river (91-QNo, AC Range), showing paleovalley V3 (fig.2) shallowly incised into the Maya surface (Brocard et al., 2011), and two imbricated waves of erosion migrating up the reversed (southward-directed) drainage of the valley. (b) typical stepped topography of the SC range, in the valley of the Rabinal river (69-Rab), showing three, imbricate, upstream-migrating erosive signals distributed along the mountain slope. The upper one is a wave of erosion that dissects the Maya surface, half-way down the mountain flank one finds a second wave of increased erosion, while the basal and final wave is composed of pediment (PD) apexs that spearhead the upstream growth of pediments. (c) Diffusive erosion in serpentinite mélanges, in the catchment of Río Hato (17-Lat, SM Range). (d) dissection of the Maya surface by prominent migrating knickpoints along the northern flank of the SM Range, from the Ribaco to the Chilasco Rivers (47-Rib to 50Sco). C3: 200 ky-old avulsion site (Brocard et al., 2012).

Under such circumstances, additional discriminating elements must be used. ~~One consists of checking~~As a first screening, we checked whether the observed knickpoints coincide with marked variations in bedrock erodibility ~~or~~, rock uplift rates, or local anomalies, in which case they ~~are likely to be steady, or if, conversely, knickpoints left geomorphic evidence of their migration, or tend to cluster with elevation in which case they are likely to be migrating.~~were regarded as steady. To assess the effect of lithological variations we used the 1:50,000 and 1:250,000 geological quadrangles of Guatemala, and topical geologic maps from published papers (e.g. (Brocard et al., 2011; Bosc, 1971a) ~~to assess the effect of lithologic changes on knickpoint location.~~. The stereoscopic black-and white 0.5-m aerial photographs of the Guatemala National Institute of Geography were used to refine the location of lithological contacts, and to assess the effects of bedrock fabric, fault damage zones, active faults, deep-seated landslides, and large debris flows on the ~~distribution of profile irregularities. We used our foreknowledge of migrating knickpoints produced by Quaternary drainage rearrangement (Brocard et al., 2012), and by active tectonics~~location of the knickpoints. We used our foreknowledge of the active tectonics of the area (Authemayou et al., 2011a; Authemayou et al., 2012; Brocard et al., 2012) ~~to assist the determination of the origin of other knickpoints. Convexities with no obvious local origin were then regarded as potential headward migrating knickpoints. The method presents the following limitations: first, local influences can be missed as a result of the imprecision of geologic mapping, especially in the least accessible parts of the SM and AC ranges.~~ and of Quaternary drainage reorganization (Brocard et al., 2012) to assist the identification of tectonic knickpoints and of some migrating knickpoints. The remaining knickpoints were then considered as potentially migrating. We then looked for supporting evidence, such as geomorphic markers of knickpoint migration, in particular break-in-slopes running along valley flanks, tied to specific knickpoints (Fig. 8a,b) after verifying that such break-in-slopes were not the result of lithological variations along the valley sides. Changes in erosion~~Second, large intraformational changes in facies can generate variations in bedrock resistance as sharp as, or even sharper than erodibility differences between mapped geological units. These two effects may lead to the interpretation of stable~~

~~knickpoints as upstream migrating. Conversely, some headward migrating knickpoints may be pinned to lithological contacts (Crosby and Whipple, 2006) and filtered out by the analysis. Classification as headward migrating knickpoint is locally assisted by the presence of break in slopes running along valley flanks and tied to a river knickpoints (Fig. 8a,b). They can represent the propagation of the erosive signal upslope, once it has been ensured that such break in slopes do not result from lithological variations along the valley sides (which is common in the AC range). Changes in incision~~ rates along hillslopes produced by the passage of a migrating knickpoint can also be marked by changes in drainage density, which reflect changes in saprolite thickness (Brocard et al., 2015b). In a few cases the passage of migrating knickpoints ~~is~~was marked by ~~the presence of~~ abandoned river terraces and hanging pediments.

The method above has some limitations: first, local variations in bedrock erodibility maybe not be systematically detected, as a result of the imprecision of geologic mapping, especially in the least accessible parts of the SM and AC ranges. Second, large intraformational changes in facies can generate variations in bedrock resistance as sharp as, or even sharper than erodibility differences between mapped geological units. These two effects may lead to the interpretation of stable knickpoints as migrating knickpoints. Conversely, some migrating knickpoints may be pinned to lithological contacts (Crosby and Whipple, 2006), and filtered out by the analysis. Nonetheless, we consider that, given the large number of analysed knickpoints, the analysis captures the most import aspects of the evolution of the landscape within the study area.

4. Results

4.1. ~~Chronology of base levels lowering~~ Rock uplift and stream incision chronology from $^{40}Ar/^{39}Ar$ dating

The Maya surface ~~is thought to have~~(Fig. 2,3) likely formed close to sea level, because it can be ~~tracked almost uninterrupted from~~ traced to the coast of the Caribbean Sea ~~to the Pacific Ocean.~~(Brocard et al., 2011). It was once covered by extensive fluvial deposits, especially south of the Motagua fault, where ~~the~~these fluvial deposits are ~~covered by~~preserved below extensive ignimbrites (Williams and McBirney, 1969). The lahar ~~sampled near~~deposit of Chujuyúb ~~belongs to a sequence of volcanoclastic rocks produced by the Central American volcanic arc and deposited~~ rests directly onto a thick saprolite that blankets the Maya surface. Lahar emplacement predates the incision of a ~~450m~~450 m-deep valley. The lahar yielded a plateau age of 12.54 ± 0.04 ~~My~~Ma (Fig. S1-1, Table S1-2). It indicates that incision at ~~Chujuyúb~~ this site started after 12 ~~My~~Ma. This is consistent with the previously proposed 12 ~~My old~~Ma entrenchment of the Cuilco River valley into the Maya surface~~,~~ (Fig.7), 70 km to the NW of Chujuyúb (Brocard et al., 2011)~~;~~, as well as with ~~the~~a 10.3 ~~My old age of~~Ma ignimbrite emplaced in the shallowly-incised Colotenango valley ~~(Authemayou et al., 2012),~~(Fig.2), 35 km to the NNW~~; and~~ of Chujuyúb (Authemayou et al., 2012). It is also consistent with ~~the ~>~~a 7.4 ~~My incision of paleovalleys~~Ma ignimbrite deposited in a 1 km-deep paleovalley, incised into the Maya surface~~, located~~ (Fig.2), 10-30 km ~~farther~~ to the NE of

Chujuyúb (Brocard et al., 2011). ~~Considering~~ The depth ~~of entrenchment of~~ reached by the late Miocene ~~paleovalleys,~~valleys prior to their abandonment implies that incision ~~would have~~ proceeded at ≥140-280 m~~/My along the now abandoned Miocene valleys~~ ·My^{-1} from 12 to 7 Ma, assuming that the ~~initial~~ dissection of the Maya surface started ~~everywhere~~ at 12 ~~My~~Ma (a, Fig. 9). ~~Individual valley~~ Incision rates~~, averages~~ averaged over the length of ~~each paleovalley, range~~ the valleys between the SC and AC ranges, range from 145 ~~and~~to 205 m~~/~~·My^{-1} (b, Fig. 9). ~~These rates stand in sharp contrast with~~ Subsequent incision ~~by the Chixóy River and its tributaries which~~, from the base of the late Miocene valley fills, down to modern valley floors, only amounts to ~~not more than~~ a few tens of meters, at rates of <30 m~~/My, between the SC and AC ranges~~·My^{-1} (c, Fig. ~~9). The incision chronology of the northern flank of the Sierra de Chuacús consists of a single pulse of rapid incision from 12 to 7 My, and then by very slow incision ever since.~~ 9).

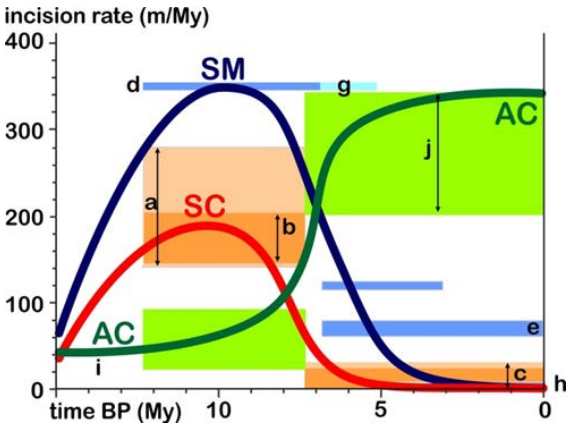

Figure 9. Evolution of incision rates in the studied ranges.
Shades of blue: Sierra de las Minas (SM). Shades of red: Sierra de Chuacús (SC). Shades of green: Altos de Cuchumatanes (AC). a-j: see main text.

The chronology of incision along the southern side of the SC range is documented by remnants of basalt flows scattered along the floor of the Motagua valley. These flows track from vents located south of the valley, in the Caribbean plate (Tobisch, 1986). The outcrop of El Jute represents the distal end of a lava flow which abutted the base of the SM range, backfilling the Huijo River valley with ≥ 70 m of basalt. The base of the flow lies >400 m above the Huijo River. Using the modern gradient of the transport-limited Huijo River as a proxy for its 6 My-old gradient, we find that the basalt flow crossed the Motagua River 360 m above the current elevation of the Motagua River. The basalt yields a plateau age of 6.88 ± 0.03 Ma, and a slightly less constrained total age of 6.46 ± 0.09 Ma (Fig. S1-1, Table S1-2). Assuming that incision of the Maya surface started 12 My ago, then the 2.6 km-deep Motagua valley would have been incised at ~350 m·My^{-1} between 12

and 7 Ma (d, Fig. 9). Incision would have continued until today at an average rate 79 ± 4 m·My^{-1}. If the basalt dam was removed rapidly however, then incision would have instead proceeded more slowly, at 59 ± 9 m·My^{-1}. The chronology of incision can be refined by incorporating the ages of the previously dated basalts (Tobisch, 1986). The closest occurrence, located 6 km upstream along the Motagua River, is the 6.1 Ma Cerro lo de China flow. The flow was actually emplaced 120 km farther west at current plate-boundary slip rates, because it lies on the southern side of the Motagua fault. Conversely, the 3.1 ± 0.7 Ma Cerro Onanopa was emplaced on the same side of the plate boundary, 16 km upstream of El Jute. Its high vesicularity implies an emplacement at, or near the ground surface, rather than as a sill, deep within the Subinal Fm., followed by exhumation. Its base lies <10 m above the Motagua River. Strath terraces of the Motagua River have been cut in its flanks (Tobisch, 1986), indicating that the flow underwent some minor burial and exhumation. The accordance in elevation between its basal contact and the Motagua River suggests that the Motagua River has oscillated tightly around its current vertical position over the past 3 My. Incision of the Motagua valley, from the elevation of the basalt of El Jute, down to the current valley floor, would thus have occurred between 6.1 and 3.1 Ma, at > 110 ± 40 m·My^{-1} (f, Fig. 9). If, after the emplacement of the basalt of El Jute, incision continued at the same ~350 m·My^{-1} rate as before (g, Fig. 9), then incision would have reached the current valley floor at ~5 Ma, no incision taking place afterwards (h, Fig. 9). ~~The evolution of the southern flank of the SC range could be more complex due to the presence of a narrow, elongate trough basin that formed between the range and the Motagua fault during Eocene time. The trough was filled with the continental red beds of the Subinal Formation. Reactivation of this fault basin in transtension since the Middle Miocene~~The evolution of incision during the rise of the SC-SM range therefore looks similar on either side of the range: it is dominated by a single step of rapid incision, at 140-350 m·My-1, between 12 and 7-5 Ma, followed by an almost complete cessation of incision along the main trunk streams (the Motagua and Chixóy Rivers), which act as base levels of the streams located in the SC range.

Note that large steeply-dipping faults bound the Eocene fill of the Motagua valley. Dip-slip on these faults could be responsible, in part or in whole, for the deepening of the Motagua valley, a possibility contemplated by Tobisch (1986). Various traits of the valley, however, rule out ~~a strong~~any substantial contribution of ~~tectonics to its deepening.~~these faults. First, fluvial sediments ~~transiting through the valley since the Eocene~~ have bypassed ~~it~~the Motagua valley since Eocene time, feeding a transtensional basin ~~farther east,~~ at the lowest ~~end~~eastern d of the Motagua valley~~, located beyond the study area.~~. Second, ~~there is no evidence of normal fault slip affecting~~ the alluvial fans that ~~intersect the bounding faults of the basin.~~have grown astride these faults show no evidence of faulting, nor any anomaly in their catchment/fan surface ratios (Tobisch, 1986). Third, the faults encountered along the base of the SC-SM range exhibit only ancient, ductile to ductile-brittle left-lateral deformation (Bosc, 1971a; Roper, 1978). ~~Last, the low relief surfaces that top the summits north and south of the Motagua fault lie at the same elevation (Simon Labric et al., 2013), implying that if trough reactivation had occurred, it would be perfectly balanced across bounding faults such that not net tectonic offset is observed from one side of the structure to the other.~~Last, the middle Miocene low-relief surfaces lie at about the same elevation north and south of the

Motagua fault (Simon-Labric et al., 2013). Extension on antithetic boundary faults would need to remain well-balanced, despite hundreds of kilometers of left-lateral displacement along the Motagua fault since the middle Miocene, to avoid the development of significant offsets of these surfaces. The deepening of the Motagua valley therefore appears to have been achieved by erosion, through the ~~preferential~~ removal of the erodible Eocene sediments ~~filling~~that filled the Eocene fault ~~corridor~~basin, giving the valley the appearance of a recently active graben.

~~Remnants of alkali basalt flows are scattered along the Motagua valley. The lithosphere on the north side of the valley has not been the source of any Cenozoic magmatism (Simon-Labric et al., 2013). By contrast, the lithosphere on the southern side of the valley is warm, and occupied by a Tertiary-Quaternary back-arc alkaline magmatic province (Walker et al., 2011). The lava flows found on the Motagua valley floor track were all delivered by vents located in the south (Tobisch, 1986). The outcrop of El Jute represents the distal end of a lava flow which, after crossing the Motagua valley, abutted the base of the SM range, backfilling the Huijo River valley with ≥ 70 m of basalt. The base of the flow lies >400 m above the axis of the Huijo River valley. Using the modern gradient of the Huijo River valley as a proxy for its 6 My old gradient, we find that the basalt flow crossed the Motagua River 360 m above the current elevation of the Motagua River. The basalt yields a plateau age of 6.88 ± 0.03 My, and a slightly less constrained total age of 6.46 ± 0.09 My (Fig.~~

The incision chronology of the AC range is constrained by transverse~~S1-1, Table S1-2). Assuming that the Maya surface started being incised 12 My ago, the 2.6 km deep Motagua valley would have been excavated at ~350 m/My from 12 to 7 My at El jute (d, Fig. 9). Incision would have since proceeded at 79 ± 4 m/My. If the basalt dam was removed rapidly, then incision would have proceeded more slowly, at 59 ± 9 m/My. This incision chronology can be refined by adding previously dated basalts (Tobisch, 1986). The closest dated occurrence is the 6.1 My old Cerro lo de China, located 6 km upstream, along the Motagua River. Cerro lo de China is located on the other side of the plate boundary, such that it was in fact emplaced 120 km farther up the Motagua valley 6.1 My ago. The 3.1 ±0.7 My old Cerro Onanopa lies 16 km upstream of El Jute, but on the same side of the plate boundary. Its high vesicularity suggests that it was emplaced at the ground surface, rather than as a shallow sill within the Subinal Fm. Its base lies <10 m above the Motagua River. Strath terraces have been cut by the Motagua River in its flanks (Tobisch, 1986), indicating that it underwent some burial and exhumation. The accordance in elevation between its basal contact and the Motagua River most likely indicates that the Motagua River has only oscillated tightly around its current vertical position over the past 3 My. The incision of the Motagua valley, from the elevation of the El Jute basalt down to that of the current valley floor would thus have occurred from 6.1 to 3.1 Ma, at > 110 ± 40 m/My (f, Fig. 9). If, after the emplacement of the El Jute basalt, incision continued unabated at ~350 m/My as before the emplacement of the basalt (g, Fig. 9), then the valley would have reached its current depth 5 My ago (h, Fig. 9).~~

~~The evolution of incision during the rise of the SC-SM range therefore looks similar on both sides of the range, and is, dominated by a single step of rapid incision at 140-350 m/My from 12 to 7.5 My ago, followed by an almost complete cessation of incision along the main trunk streams (Motagua and Chixóy River) that represent the base levels of the streams analyzed hereafter.~~

~~The late Miocene~~ paleovalleys ~~were deeply incised into the SM-SC range, but only~~ that are shallowly incised into the ~~AC range~~Maya surface (e.g. Fig. 8a; i, Fig. 9~~), indicating low rates~~). Uplift of ~~incision in~~ the AC range~~, while the SC-SM range were rapidly uplifted. Since then, however, dissection has incised valleys~~ since their abandonment has allowed the incision of 1,500~~ m to~~ 2,600 m deep valleys along the northern flank of the ~~AC range, implying a considerable increase in~~

~~incision rates as a result of the uplift of the AC range,~~range (Fig. 3) at 200-350 m~~/~~·My^{-1} (j, Fig. ~~9).~~9). River incision of the AC range therefore started and developed while river incision in the SC-SM rang was stalling.

4.2. ~~Distribution of~~Spatial variations in ^{10}Be-derived erosion rates

Catchment-~~wide~~averaged detrital ^{10}Be erosion rates range from 11 m~~.~~·My^{-1} ~~over~~within the catchments that drain the Maya surface ~~in~~on the SM range, up to 330 m~~.~~·My^{-1} along the wet and steep northern flank of the AC range (Fig. 10). Most ~~slow erosion rates~~ slowly-eroding catchments are ~~found in~~located within the SC range. Weighting ~~these~~erosion rates by the relative concentration of quartz in quartz-feeding lithologies ~~only~~ marginally affects ~~these erosion~~the calculated rates (by 3.4% on average in the SC range, 4.8% in the SM range, and < 7% in the AC range). Quartz enrichment ~~in~~corrections, on the ~~topsoil could~~other hand, increase erosion rates by up to 40% (Fig. 10, Table S2-2~~).~~), but the amplitude of this effect remains speculative, in the absence of field measurements. However, because quartz enrichment increases with weathering intensity, ~~such as it~~its effect is probably ~~less pronounced~~smaller in the AC range, where soils erode the fastest. Quartz enrichment ~~would~~corrections can be therefore ~~tend~~expected to reduce the contrast in erosion rates between the SC-SM range and the AC range~~, without suppressing it~~.

~~The nested catchment analysis (arrows, Fig. 10) reveals a marked downstream increase in erosion rate in the AC range (from CATA to CHEL to XAC). In the SC range, a downstream increase is expected in the headwaters, due to a decreasing contribution of slowly eroding low relief uplands with downstream distance (Willenbring et al., 2013). Farther downstream, however, a decrease is expected, when the rivers start crossing pediments located on the floor of the Chixóy River basin. The expected increase is observed (from PAS to PAE), but it is much less pronounced than in the AC range. The expected decrease is also observed (from XEU to CUB), but it is likewise quite subdued. In one case, the expected succession of increase and decrease is not observed (from SMS to SMM to SMI).~~

~~In the SM range, catchments are not nested but they still display increasing rates of erosion down the mountain flank, as the entrenchment in the Maya surface increases (COL to FRI to RAN), with one outlier (SLO). The magnitude of increase is intermediate between those observed in the SC and CA ranges.~~

In the AC range, erosion rates (arrows, Fig. 10) show a marked increase from the drier, and less steep highlands, to the wet and steep frontal slopes (from CATA to CHEL to XAC). The SM range displays a similar trend of increasing erosion down the mountain flank, as entrenchment in the Maya surface increases (from COL to FRI to RAN), with one outlier (SLO). The magnitude of increase is intermediate between that observed in the SC and CA ranges. In the SC range indeed, a downstream increase would be expected initially, in the downstream direction, from the drainage divide down the mountain flanks, from the decreasing contribution of slowly-eroding low-relief uplands with downstream distance (Willenbring et al., 2013b). It would be followed by a decrease in erosion rates as rivers start draining the pediments that floor the Chixóy River catchment. An increase in erosion rate, downstream of the paleosurface is observed (from PAS to PAE), but it is much less pronounced than in the AC range. The following decrease in erosion rate is also very subdued (from XEU to CUB). In one case (from SMS to SMM to SMI), no increase nor decrease is observed.

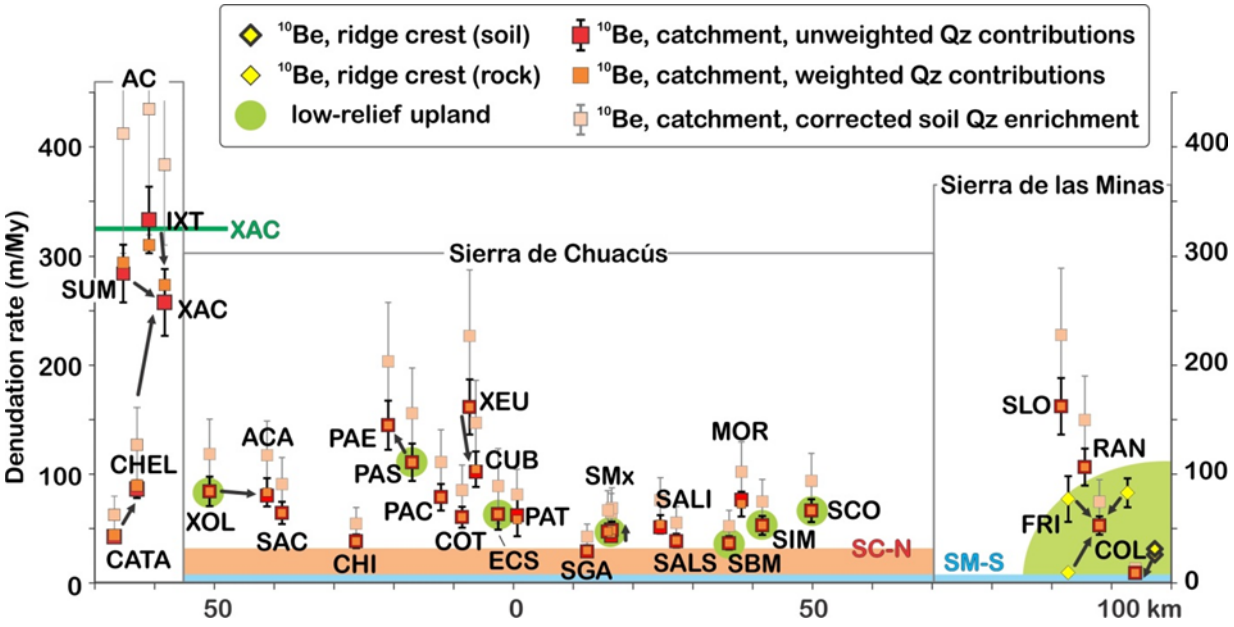

Figure 10. Variations in detrital ^{10}Be denudation rates along the strike of the plate boundary, from the AC range in the west, to the SM range in the east. Data are projected along the strike of the plate boundary, on an arc displayed on Fig. 6. Arrows shows feeding directions, from hillslope sites to nested catchments. Low relief uplands drain remnants of the Middle Miocene Maya surface. Denudation rates are compared to incision rates along the northern (salmon, SC-N) and southern (blue, SM-S) base of the SC-SM range, over the past 7 My. XAC: peak incision rates in the AC range along Río Xacbal, where incision below the Maya surface along the river course is maximum (Fig. 3).

4.3. Distribution of streambed types

~~The analysis~~9% of ~~streambeds was conducted along each straight segment obtained from~~ the ~~linearizing in χ space. Among the final 93~~ rivers ~~and 452 segments~~ retained in the analysis~~, 9% have no~~ do not host any knickpoint, 16% host one knickpoint, 51% host 2~~-~~ to 5 knickpoints, and 25% host 5-12 knickpoints (Fig. 11). ~~Among segments,~~This distribution highlights the high degree of segmentation of many rivers in the AC and SC-SM ranges, and the high concentration of knickpoints within these ranges. These knickpoints separate 452 river segments, of which 92% are well linearized, 6% are concave, and 2% are convex~~.~~, for an applied intrinsic concavity $\theta = 0.5$. The river segments were grouped by streambed types. Their distribution according to elevation along the studied ranges is displayed on Figure 12, and their distribution between north- and south-facing flanks is displayed on Figures S4-2 to S4-6.

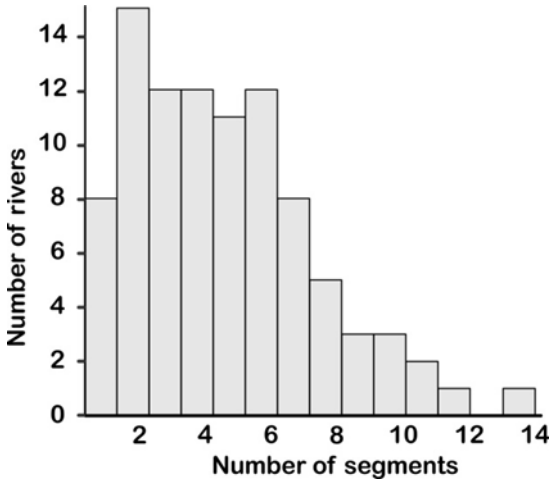

Figure 11. Distribution of rivers according to the number of segments identified in each river

The distribution of alluvial reaches ~~with elevation along the strike of~~is bimodal in the SC-SM ~~and AC ranges~~range (Fig. 12a1-b2~~) is bimodal, the majority of~~): alluvial reaches ~~being located~~tend to be found either at the base of the mountains ~~(along the Motagua valley, the Chixóy River basin, the basin of Lake Izabal, the Central Depression of Chiapas and the Petén lowlands),~~ or at high elevation, ~~on~~over the remnants of the Maya surface ~~and along rivers slightly entrenched into it~~ (e.g. Fig. ~~8a~~8 a,d). ~~The~~High-elevation alluvial reaches ~~located at high elevation carry a sandy to gravelly~~tend to transport a rather fine-grained bedload, composed of sand derived from the weathering of ~~underlying crystalline rocks. Gravel is~~micaschist, gneiss and granite, and of gravel derived from ~~weathering resistant~~ quartzose veins and silicified pegmatites (Brocard et al., 2012)~~.~~. Intermediate-elevation alluvial reaches ~~at intermediate elevations are less common. They form~~occur upstream of obstructions, most notably landslides ~~(notably~~ in the SM-SC range~~),~~, over extremely erodible fault damage zones, and within localized areas of tectonic subsidence (especially along the Polochic fault corridor, on the southern flank of the AC range~~), and over extremely erodible lithologies such as fault damage zones and fault gouge.~~).

~~-~~Boulder reaches are found mostly on crystalline rocks~~, boulder armoring is~~. They are then more ~~common in~~frequent on the wet ~~parts of the~~slopes SM range than on the dry ~~parts~~slopes of the SC range. In the SM range, many of these boulder-strewn reaches ~~result from the~~ have formed out of debris flows deposits, by winnowing of ~~the~~their matrix ~~of debris flows that invaded the streambeds.~~. The SM range is first range hit by Atlantic tropical depressions tracking from the Caribbean Sea. ~~High intensity rainfall events~~They frequently trigger ~~considerable and frequent landsliding~~numerous landslides along its wettest slopes (Ramos Scharrón et al., 2012; Bucknam et al., 2001). ~~The SM range may also be more susceptible to earthquake triggered landsliding that the SC range,~~ Because it soils are more ~~likely~~often close to ~~be~~ water-

~~saturated~~saturation, it is also affected by numerous landslides when ~~an earthquake occurs.~~earthquakes strike the range (Harp et al., 1981). Boulder armoring is also common in the SM range over the serpentinite mélanges that locally crop out up to high elevations along ~~the~~its southern flank ~~of the SM-SC range~~, owing to the ~~high erodibility of the matrix of the mélanges, and to the~~ presence of ~~large~~ knockers embedded within ~~it~~the mélanges (e.g. Fig. 8c). Boulder-strewn reaches ~~are also more frequent than bedrock reaches~~ in the AC range~~. There, rivers frequently flow~~ are observed over phyllites ~~of the Tactic Fm., but their beds are armored by~~ . There, the boulders ~~shed by hillslopes along which~~ are made of the most resistant beds of the ~~Tactic Fm. are exhumed. They are also commonly contributed by the overlying~~ Pennsylvanian phyllites, and of sandstone and limestone ~~of the Todos Santos and Cobán Fms~~blocks of overlying formations that have sled along the valley flanks.

Bedrock reaches are most commonly found downstream of convex migrating knickpoints, the distribution of which is present in the following section.

4.5. Distribution of ~~knickpoint types~~steady and migrating knickpoints

~~About 40% of~~Among the 350 identified knickpoints, 40% can be tied to variations in bedrock erodibility, ~~while~~6% to temporary obstructions, 8% ~~are related~~ to active tectonics, 21% to upstream-migrating waves of accelerated erosion, and 14% to upstream-migrating waves of decelerated incision. 11% are composite and ~~include~~result from some combination of the above.

Details about the significance of the distribution of steady knickpoints is provided in Suppl., as well as a systematic review of the origin of various identified clusters of migrating knickpoints. The origin of some migrating knickpoints can be tied to well-identified and well-dated river Quaternary diversions (e.g. S3-1 to S3-3, Fig. 12a2, (Brocard et al., 2012)). Most migrating knickpoints dot the margins of upland low-relief surface remnants (Fig. 12 a1 and a2; Fig. 8d). ~~—~~

~~Concave-up knickpoints fringe the southern base of the SM-SC range (Fig. 12 a1). They are located at the apex of broad, alluvial fans, upstream of the transition between resistant basement rocks and more erodible ophiolitic mélanges or Eocene red beds. They are also found along the northern base of the SM range, at the apex of the alluvial fans that grade to the fill of the Lake Izabal basin. Along the northern base of the SC range, concave-up knickpoints are located farther into the range, away from the range-parallel trunk steam (the Chixóy River), from which they are separated by broad, pedimented valley floors. These pediments are partially covered by pumice emplaced during the last paroxysmal eruption of the Atitlán caldera 84 ky ago. The pumice has long been dispersed from below the riverbeds, such that the rivers rest directly on the underlying buried pedimented surfaces. In the AC range, most concave-up knickpoints are located above the Ixcán reverse fault and mark the transition between the AC range and the Petén lowlands.~~

~~Lithogenic knickpoints produced by large changes in bedrock resistance or by changes in the orientation of the streams with respect to the fabric of the substrate are frequent halfway down the mountain flanks. Some are also produced by subtle changes in bedrock resistance farther up the mountain flanks, where crystalline rocks weather to sand and gravel, and where streambeds are not armoured by immobile boulders or large cobbles (e.g. Fig. 8c). The absence of boulder armouring makes such stream more sensitive to bedrock erodibility variations. Similar sensitivity is also found high up the AC range, where limestones and sandstones deliver little sediment to the streams. Another series of lithogenic knickpoints are found in the lowest reaches of streams draining the northern flank of the AC just before they join the Chixóy River, downstream of pedimented valley floors (Fig. 8b). A possible explanation is that the coarsest bedload is retained on the pediments, increasing their sensitivity to changes in bedrock erodibility farther downstream.~~

~~The majority of tectonic knickpoints are concentrated on the southern flank of the AC range along a few 100s of meters from the active trace of the Polochic fault, owing to the growth pressure ridges, and within 4 km of the fault owing to the opening of narrow transtensional corridors (Authemayou et al., 2012). No tectonic knickpoints are found along the southern flank of the releasing bend of Lake Izabal, suggesting that no large normal fault is present there. This is consistent with the sedimentary architecture of the basin (Bartole et al., 2019; Carballo-Hernandez et al., 1988) which indicates that most of the vertical throw over the lifetime of the bend has taken place along the northern side of the basin. Conversely, the overall downstream steepening of river profiles along the northern flank of the AC range over the hanging wall of the Ixcán transpressional fault probably reflects increasing rock uplift within 20 km of the fault. This steepening is commonly rather diffuse, but at places it is associated with a change in bedrock lithology, and expressed by a change in streambed type. Such knickpoints are therefore classified as composite, tectonic-lithogenic knickpoints (Fig. 12b2).~~

~~Among the population of headward-migrating knickpoints, a few are associated with well-identified and dated river diversions (~~They may have therefore initiated farther down their drainage networks, when the Maya surface started being incised, at ~12 Ma on the SM-SC range. Other clusters of migrating knickpoints are found halfway down the flanks of the ranges. The most conspicuous of these is restricted to the northern flank of the SC range, within the watershed of the Chixóy River. It hangs above a series of concave-up migrating knickpoints dotting the apexes of pediments, which extend is also restricted to the drainage of the Chixóy River. The significance of these concave-up knickpoints and their genetic relationship with the cluster of convex knickpoints located above them is discussed in section 5.3.2.

~~S3-1 to S3-3, Fig. 12a2) which occurred during the Quaternary along the Cahabón River (Brocard et al., 2012). Avulsions and river captures sparked the incision of canyons 500 to 1,000 m deep, spearheaded by prominent migrating knickpoints. Most headward-migrating knickpoints are located along the margins of upland low-relief surface remnants (Fig. 12 a1 and a2; Fig. 8d). The fact that they seem less common in the AC range stems from the fact that because large tracts of the low-relief areas are heavily karstified and lack an organized continuous water routing network, that would otherwise produce such knickpoints as it flows away from these low relief areas. A few clusters of headward-migrating knickpoints are found halfway down the flanks of the ranges. One such cluster affects the lower southern flank of the SC range. Its elevation coincides with that of tertiary ignimbrites (Fig. 12a1). Another cluster is found half-way down the northern flank of the SC range. It is observed in the Chixóy River catchment, but not along the northern flank of the SM range, in the Polochic-Panimaquito rivers catchment. A poorly defined cluster seems to exist along the southern flank of the AC range. There, headward-migrating knickpoints are locally well-expressed (e.g. Fig. 8a), but the ascription of some knickpoints to this cluster is probably obscured by the presence of many tectonic disruptions along the Polochic fault. Another cluster of headward-migrating knickpoints is present halfway down the northwest flank of the AC range, toward the central depression of Chiapas (Fig. 12). There, the horizontal bedding of the bedrock makes it difficult to separate headward-migrating knickpoints from lithogenic knickpoints, because they generate similar topographic landforms. Some of the knickpoints identified as lithogenic could be as-well headward-migrating knickpoints. This may lead to an underestimation of the number of headward-migrating knickpoints along the northern and northwestern flanks of the AC range.~~

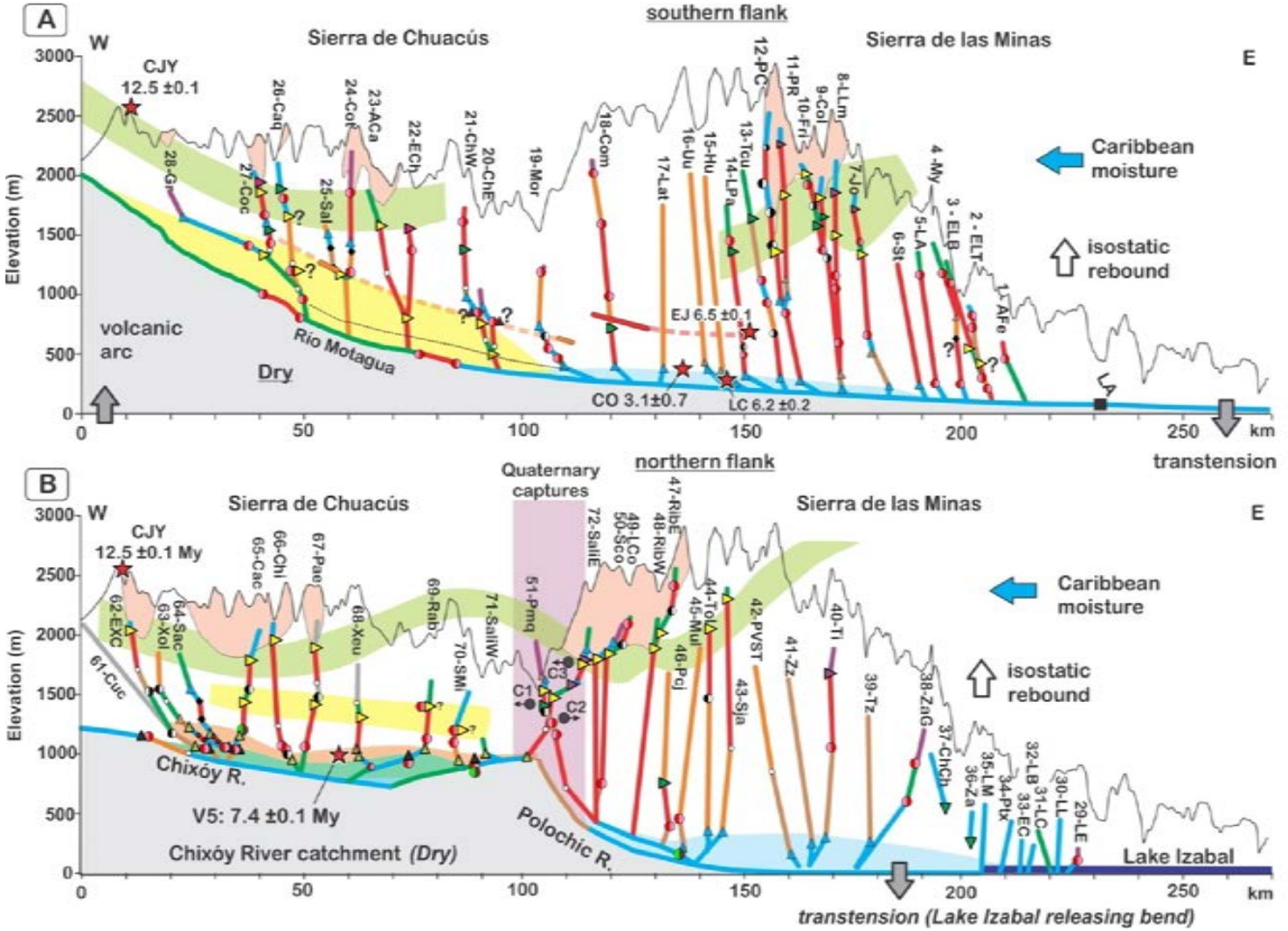

Figure 12. (a) and (b). Distribution of linearized stream segments and knickpoints along the SC-SM range.

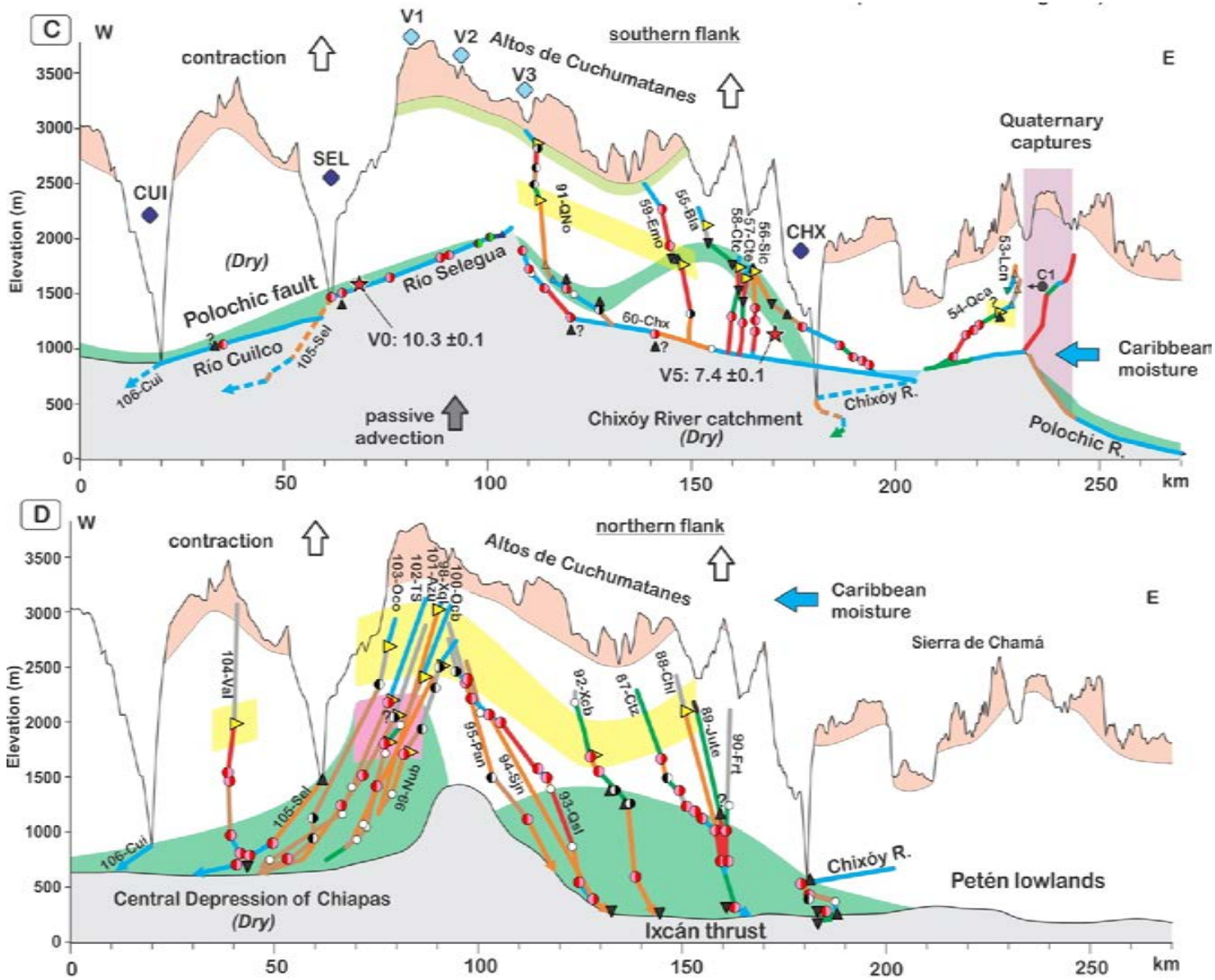

Figure 12.(c) and (d): distribution of linearized stream segments and knickpoints along the AC ranges.

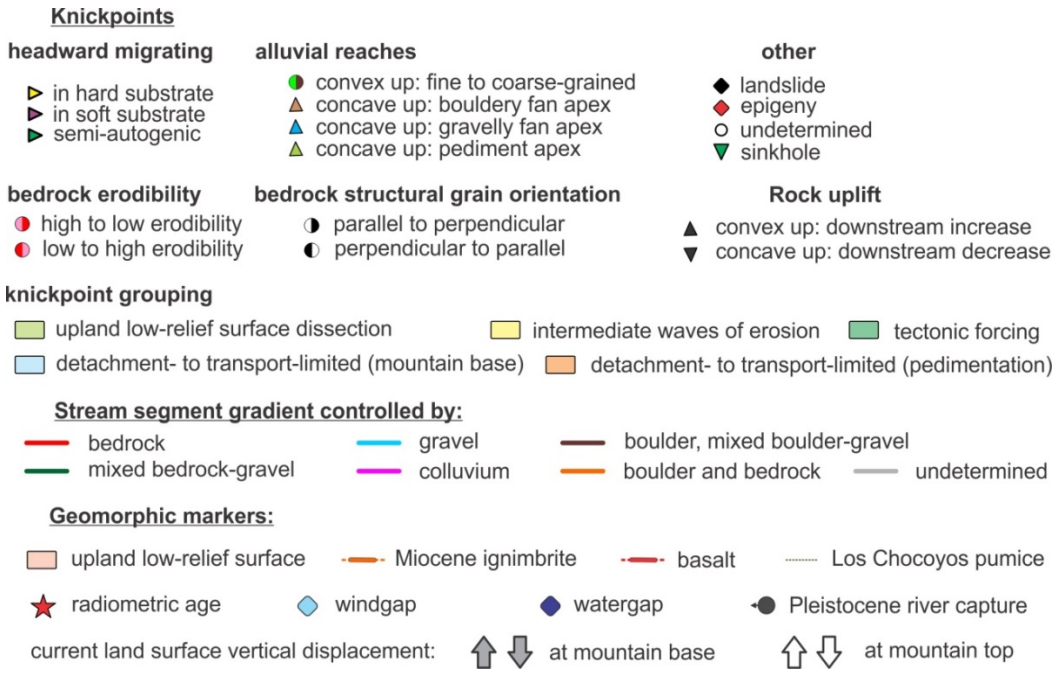

Figure 12. Distribution of linearized stream segments and knickpoints along the SC-SM and AC ranges. Mountain ranges are projected on the plate boundary, according to a small circle defined on Fig. 6. (a) and (b) southern and northern flanks of the SC-SM range, (c) and (d): southern and northern flanks of the AC range. Key to abbreviated stream names is provided in Table S4-1 and in the captions of figures S4-2 to S4-7. ~~Watergap~~Water gap names: CUI: Cuilco, SEL: Selegua, CHX: Chixóy. Paleovalley numbering from Brocard et al. (2011), river capture numbering from Brocard et al. (2012). LA: city of Los Amates.

5. Discussion

~~**5. Discussion**~~

The decline of river incision rates in the SC-SM range was coeval to the rise of incision rates in the AC range, suggesting that the rise of the AC range was instrumental in the decline of incision rates in the SC-SM range. The AC range may have affected incision rates range in two ways. First, by decreasing moisture delivery to the SC-SM range, it may have reduced hillslope erosion rates and the delivery of water and sediment to the streams, thereby decreasing river incision rates. Second, by forcing the drainage of the northern side of the SC range to adjust to a new rock uplift field, it promoted a decrease in river incision rates, upstream of the AC, among the rivers of the SC range that still cross the AC range. After reviewing the potential contributions of the

~~**5.1.** top-down and bottom-up **controls on hillslope ^{10}Be erosion rates**~~ processes, we analyse their effects on the present-day morphological evolution of the SC-SM range.

5.1. Effect of the rise of the AC range on climate-driven erosion

5.1.1. Climate and hillslope erosion

Silicate weathering has been found to be three times faster on the wet (1,800-3,000 mm·y^{1}, Fig.4) side of the SM range than along its drier (1,000-2,400-mm·y^{-1}) side (McAdams et al., 2015).

~~The decrease in erosion rates from the AC to the SC range, and from the SM to the SC range, matches the decrease in precipitation from north to south, and from east to west generated by the interception of moisture by the AC and SM ranges and by the development of rain shadows extending over the southern flank of the SM range and over the entire SC range. As a result, silicate weathering is three times faster along the windward side of the SM range than along its leeward side (McAdams et al., 2015). It is likely, therefore, that precipitation driven chemical and mechanical weathering play an important role in the present day distribution of erosion rates across Central Guatemala. This role is assessed using two calculations of the erosion index: one that assumes that erosion scales with local precipitations and hillslope gradient (as a proxy for soil moisture and chemical weathering), and another that assumes that erosion scales with shear stress during overland flow (as a proxy for mechanical weathering). At first glance, catchment averaged ^{10}Be detrital erosion rates scale with precipitation and slope (Fig. 13a,c). The relationship is linear in the AC range (r^2=@), which displays a six-fold increase in erosion rate, from 50 to 300 m/My, from the interior of the range to its front. This downstream increase results from the concentration of precipitation near the northern front of the range, but it may be combined with an increase in tectonic uplift rate on the hanging wall of the Ixcán fault. The correlation between the erosion index and hillslope erosion rate is also strong from one range to the next, but is weaker within the two other ranges. t is the weakest in the SC range, where erosion is the slowest (30-70m/My).~~

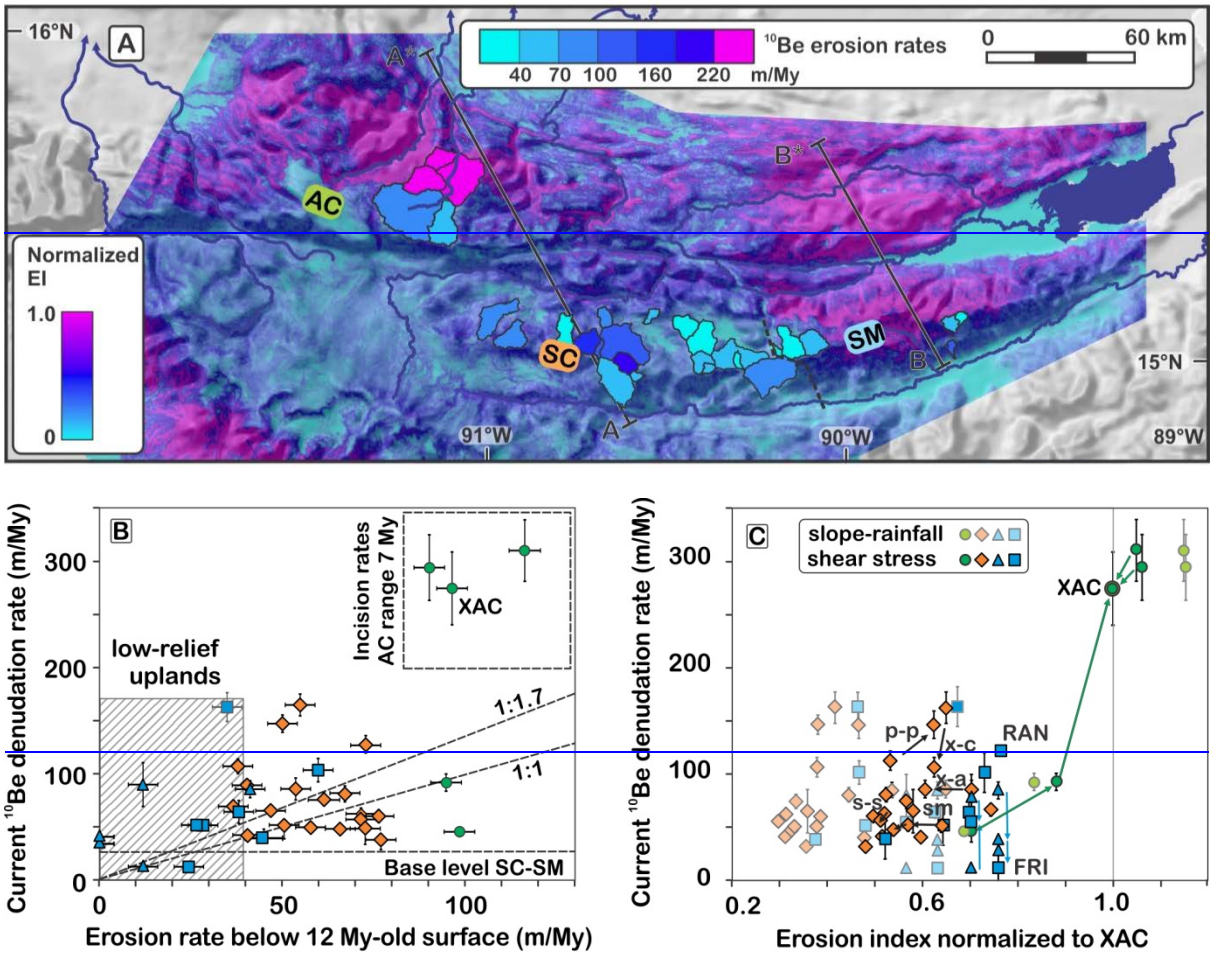

Using detrital cosmogenic ^{10}Be we find that the the wet (1,900-3,700 mm·y^{-1}) side of the the AC range erodes on average distinctively faster (with a 92 % probability, based on a Welch's t-test, with t = 2.246, p = 0.08) than the drier (900-1,300 mm·y^{-1}) SC range. Individual catchments document a sixfold increase in erosion (50 to 300 m·My^{-1}), from the SC range to the AC range (Fig.10, Fig. 13b,c). The spatial distribution of erosion rates predicted by the Erosion Index (Fig.13a), which combines the effects of slope and precipitation on erosion, is consistent with the spatial distribution of measured detrital ^{10}Be erosion rates. ^{10}Be-source slopes in the AC range receive three times more precipitation (MAP = 3.2 ± 0.7 m·y^{-1}) than their counterparts of the SC and SM ranges (MAP= 0.9 ± 0.4 and 1.2± 0.3 m·y^{-1}, respectively, Fig.13b). ^{10}Be-feeding slopes in the AC range are also 1.2 times steeper (26 ± 4°) than in the SC and SM ranges (22±3 and 22 ± 2°, respectively, Fig.13c). In the AC range, a linear relationship is observed between erosion rate and both precipitation (r^2= 0.83) and slope (r^2=0.95). This correlation is not as strong when all ranges are considered (r^2= 0.61 for precipitation and 0.52 for slope), and very weak

within the SC and SM range datasets (-0.1<r^2<0.4). The stronger correlation observed in the AC range reflects foremost the greater homogeneity in bedrock erodibility among the measured catchments. Slope gradient and MAP are good predictors of hillslope erosion rates at precipitation is > 2 m·y^{-1} (Fig. 13b), but a linear relationship predicts that erosion ceases for MAP <2 m·y^{-1} and slopes < 15°. It is probable that the curve flattens for MAP < 2 m·y^{-1} a trend observed elsewhere, for example for MAP < 2 m·y^{-1} on Kauai (Ferrier et al., 2013). Low erosion rates (< 50 m·My^{-1}) are observed in many catchments of the the SC and SM ranges that still all maintain average slopes ≥ 19 °(Fig.13c), when such low erosion rates are rather observed at slope values < 10° globally (Willenbring et al., 2013a).

For MAP < 2 m·y^{-1}, MAP is a poor predictor of erosion rates, likely because storminess and rainfall intensity increasingly become better predictors of hillslope erosion (Liang et al., 2019). The strong correlation between slope and erosion rates in the AC range suggests that slopes have not, on average, reached the critical threshold of slope stability (Clarke and Burbank, 2010). At low precipitation rates, within the SC range, slope steepness faintly captures some of the variations in erosion rates (r^2= 0.41). Comparison between nested individual catchments show that, in 4 out of 6 instances, decreases of increases in EI values are not echoed by significant changes in erosion rates.

It seems therefore that the most arid regions of the study area erode slowly to very slowly, despite maintaining steep slopes, and that slopes, like MAP, become poor predictor of the short-term (10^3-10^4y) hillslope erosion rates. The pattern of catchment-averaged ^{10}Be erosion rates points to a role of climate in the erosion of the ranges, in particular in the limitation of erosion on steep slopes. Fluctuations of climate, over millions of years, could therefore affect the long-term evolution of these ranges. This aspect is explored in the following section, in particular the role of mountain building on the climate of Central Guatemala.

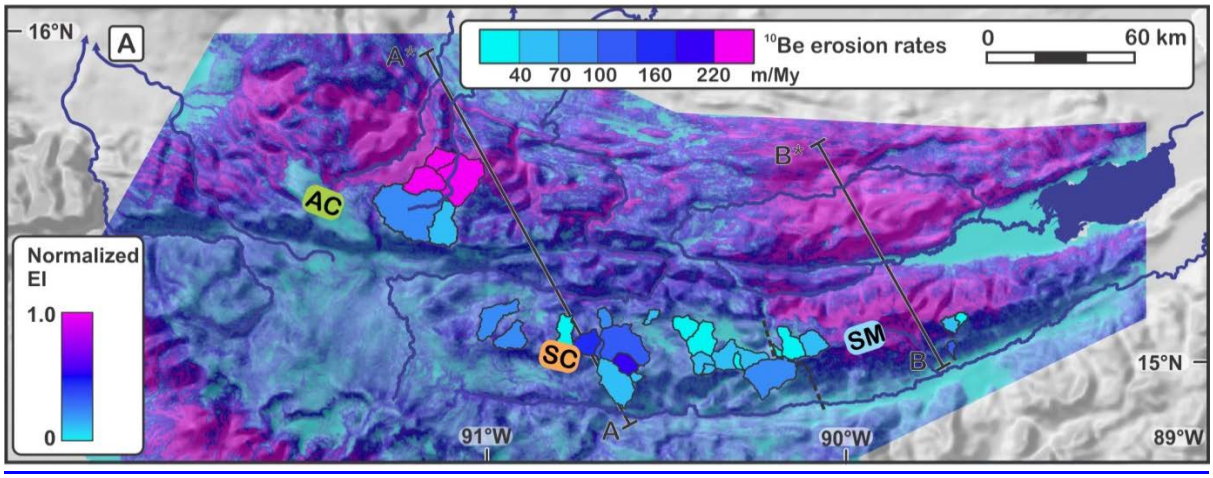

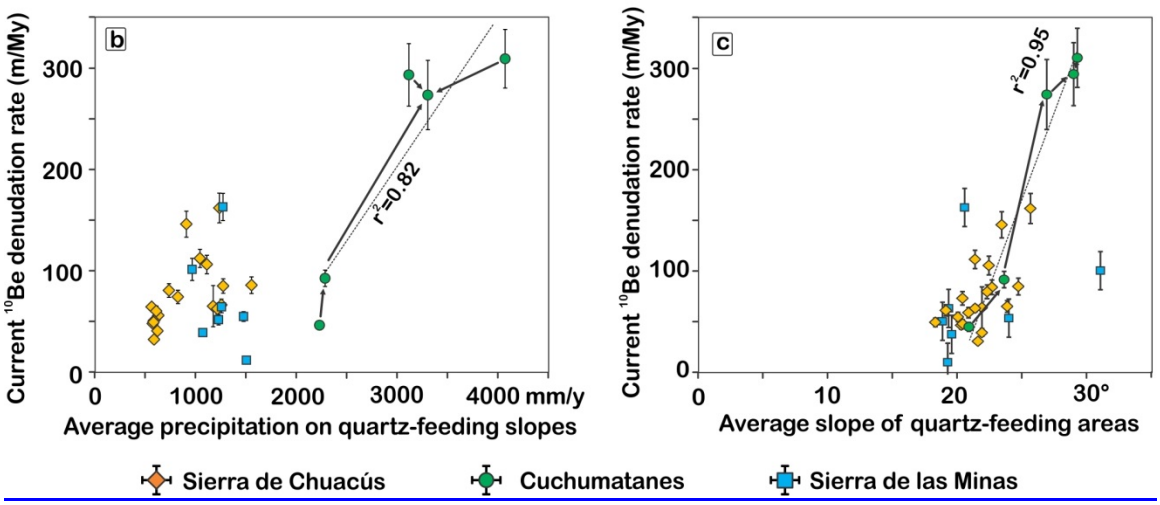

Figure 13. (a) Map showing the spatial distribution of normalized catchment-wide ^{10}Be erosion rates superposed to the predicted spatial distribution of erosion according to the normalized erosion index. ~~(~~(b) ~~and (c)~~ ~~^{10}Be~~ catchment-wide ^{10}Be erosion rates ~~vs.~~as a function of catchment-averaged precipitation. (c) catchment-wide ^{10}Be erosion rates as a function of catchment-averaged slope (from quartz-contributing slopes) Arrows: downstream connections between nested catchment within the AC range. Dashed line: linear correlation within AC range data, with correlation coefficient (r^2) reported next to the line.

5.~~dissection depth~~1.2. Evolution of climate driven by the rise of the AC range, and expected consequences on the erosion of the SC range

The distribution of precipitation (Fig.2) shows that the AC range currently prevents the ingress of Caribbean moisture tracking from the Yucatán and Petén lowlands. It can be expected, therefore, that moisture was able to reach the SC range before the AC range started to rise. Such a deeper inland penetration of the moisture is confirmed by paleo-precipitation estimates obtained from the study of tree species and paleosols in the 7.4 Ma forest of Sicaché (Fig. 2). The subtropical forest grew on the floor of one of the abandoned late Miocene paleovalleys. The characteristics of the paleosols preserved below the forest suggest mean annual precipitation in the 950-1,300 mm·yr^{-1} range (Brocard et al., 2011). The area where the fossil forest crops out is drier today and covered by xerophytic vegetation. The fossil forest is located on the southern side of the AC range; it documents therefore a deeper penetration of Caribbean moisture toward the SC range at 7 Ma. It therefore suggests that precipitation was higher on the SC range between 12 and 7 Ma, and that it decreased with the

rise of the AC range. Drying of the SC range, in turn, can be expected to have contributed to the decrease in hillslope erosion rates over the SC range. Aridification may have changed the balance between water and sediment discharge (Sklar and Dietrich, 2006; Beaumont et al., 1992; Whipple and Tucker, 1999), but if, in the process, streams were left not exceedingly overfed nor underfed with sediment, one can expect river incision to have scaled with stream discharge (Sklar and Dietrich, 2006). ~~Maya surface (b) and vs. catchment-averaged erosion index (b), for two models of erosion index: slope-rainfall and slope-runoff (shear stress model). Arrows indicate nested catchment links (p-p: PAS to PAE, sm: SMS to SMM to SMI; s-s: SALS to SALI, x-a: XOL to ACA; xc: XEU to CUB).~~In that case the decrease in river incision rates observed at the base of the SC range (see section 4.1) could be, in part, due to the aridification of the SC range. The rise of the AC range could have affected hillslope erosion and river incision over the SC range by such a top-down process, from precipitation to hillslopes to streambeds. However, the AC range also altered the routing of water away from the SC range. In doing so, it sparked a massive adaptation of the drainage to the new tectonic field, to such extend that it also contributed to the decrease in incision rates. This aspect is explored in the following section.

5.2.

~~The downstream increase in erosion rate along the southern flank of the SM range (from FRI to RAN, Fig. 13b) scales with both the increase in EI and with the depth of erosion below the low-relief uplands (Fig. 13b). Because climate is drier down the Motagua valley, this increase in erosion rates is mostly contributed to by the increase in slope. In the SC range, the downstream increase in slope in the nested catchments (p-p) produces a smaller increase in erosion rate despite the same increase is EI. Farther down the range, pediments combine with the dry climate to decrease the average EI of the catchments (x-a, x-c, s-s, and sm, Fig. 13b). Yet, in 3 out of 4 instances, this decrease is not reflected by a decrease in measured hillslope erosion rates. Therefore, it seems that at such low erosion rates, the changes in slope and/or annual precipitation are poor proxies of the processes that drive erosion.~~

~~A comparison of current hillslope erosion rates and of long-term hillslope erosion rates (approximated by the amount of dissection below the low-relief uplands averaged over each catchment) provides some insight into the evolution of these erosion rates over the past millions of years: in the fast eroding catchments of the AC range, current hillslope erosion is much faster than dissection below the 12-My-old low-relief upland (line 1:1 on Fig. 13b). It is likely that most of their incision has taken place over the past 7 My (line 1:1.7, Fig. 13 b), because the upper Miocene paleovalleys of the AC range are only slightly incised into its low-relief uplands (e.g. Fig. 12b1). Over the past 7 My, AC range erosion rates are similar to its present-day hillslope erosion rates, at 200-350 m/My (Fig. 9). The overall increase since the upper Miocene is compatible with the interception of precipitation on the windward flanks of the AC range, and also with the rapid lowering of river base levels along the northern side of the range, which also promoted valley incision. In the SM and SC ranges, the current rates of hillslope erosion are comparable to dissection rates below the low-relief uplands integrated over the past 12 Ma. The four steepest catchments of these ranges do not include low-relief uplands or pediments. In these catchments, present-day rates are 2-3 times higher than long-term dissection rates. Considering that a most of the dissection occurred before 7 My ago, it is~~

~~likely that these modern erosion rates are significantly higher (> 50 m/My) than the <30 m/My base level fall of the streams that drain the SC range over the past 7 My. Having higher hillslope erosion rates than valley incision rates means that the SC range and the southern flank of the SM range have entered a stage of long term topographic decay. While the increase in hillslope erosion rate in the AC range may combine an increase in precipitation with an increase in base level lowering rate, the topographic decay of the SM range seems to combine a decrease in base lowering rate to a decrease in precipitation. Both act as to lower hillslope erosion rates, but they also decrease the rapidity of the topographic decay of the SM range. The origin of the decrease in valley incision rates is analyzed in the following section.~~ **Effect of the rise of the AC range on tectonically-driven**

~~**5.2. Bottom-up control on river incision**~~

~~5.2.1. Tectonic control of~~ river incision ~~rate~~

~~5.2.~~ The rise of the AC range results sparked widespread reorganization of the range-transverse drainage (Brocard et al., 2011), leading to the tectonic defeat of many rivers that used to cross the range. The rivers that maintained a course transverse to the rising structure adapted their gradient to the new crustal strain field. We review first the evidence for faster uplift in the AC range than in the SC range, then analyse the consequences of this faster uplift on incision rates long the rivers that cross the AC range, upstream of the AC range, within the SC range. We also analyse the contribution of the rise of the AC range to river course lengthening along the Polochic fault, analyse how this affected river incision in the SC range.

5.2.1.~~1.~~ Fast, ongoing rise of the AC range from river channel steepness

The deformation of paleovalleys abandoned during the uplift of the AC range documents >1-2 km of rock uplift in the AC range relative to the SC range since the late Miocene (Brocard et al., 2011). Such deformation implies faster rock uplift rates in the AC range over the past 7 My. Whether such difference remains today is important for analysing river profile dynamics. Glacial and fluvial landforms of the AC range do suggest that that the AC range still rises faster than the SC range. Glacial landforms provide some indirect clues. A 20 x 30 km ice cap spread over the summit plateau of the AC range (Fig. 1) during the last glaciation (Anderson et al., 1973; Lachniet and Vazquez-Selem, 2005). On other neotropical mountains the moraines of the last glaciation are set in older tracts of moraines, left by previous, more extensive ice-caps and glaciers (Lachniet and Vazquez-Selem, 2005). In the AC range, however, they are not observed. Their absence implies that earlier ice caps were smaller than the one that developed during the last glaciation, and that their deposits have been eroded away by the most recent ice cap. Considering that there is no particular reason why climatic forcing would have affected Central Guatemala in a different manner, the most straightforward explanation is that the part of the range above the

equilibrium line of accumulation (ELA), has increased steadily from one glacial cycle to the next as a result of surface uplift, and that this uplift has been significant enough to overcome differences in the intensity between glacial cycles. The effect of surface uplift is made easier by the fact that the top of the range is a plateau, such that small increments of uplift bring large areas of the range above the ELA. The current driver of surface uplift is still contraction (Guzmán-Speziale, 2010; Authemayou et al., 2011b), just as in the early stages of mountain growth, to which erosional unloading may now contribute more than in the early stages, driven by the deep dissection of the northern flank of the AC range.

The steepness of river profiles in the AC range further support the hypothesis that the range still lifts up faster than the SC range. The projection of river profiles in χ space (Figs. S4-2 to S4-7) shows that, in each ~~range,~~of the analysed areas (AC, SC, and SM ranges), linearized segments ~~with~~that share similar streambed conditions (alluvial, boulder-armoured, bedrock) tend form share similar θ_n-normalized steepness ~~values~~ (Fig. 14a). Rivers ~~flowing~~that flow over bedrock are~~, in most cases,~~ steeper than rivers ~~flowing~~that flow over immobile boulders, which in turn are steeper than ~~streambeds displaying~~ rivers that flow over alternations of gravel bars, or bedrock and boulder, which~~,~~ in turn~~,~~ are steeper than ~~entirely~~ alluvial ~~reaches. Among~~rivers. Each category, however, ~~differences are observed~~exhibit steepness values that change from one range to the next (Fig. ~~14b~~14 b,c,d).

~~Bedrock reaches are detachment-limited; their gradient are therefore expected to~~It is expected that the bedrock rivers conform to the predictions of the stream power law, because their incision is detachment-limited. At dynamic equilibrium, their steepness should therefore scale with rock uplift, bedrock erodibility and precipitation (Whipple and Tucker, 1999). ~~At dynamic equilibrium, the steepness of such~~ The progressive increase in steepness from the SC range to the the AC range does not result from an increase in bedrock erodibility, because erodibility is higher in the AC range than in the SC and SM ranges. It does not result either from the observed increase in precipitation from the SC to the AC range, as the increase would instead decrease river gradient. The steeper reaches of the AC range are therefore best explained by faster incision in the AC range, driven by faster rock uplift. This is consistent with the higher ^{10}Be hillslope erosion rates measured in the AC range, assuming that slopes and channels ~~is a function of streambed erodibility, stream discharge, and rock uplift. The progressive increase in steepness from the SC range to the southern side of the SM range, to the northern side of the SM range, and finally to the AC range, does not result from an increase in bedrock erodibility, as erodibility is roughly similar along the strike SC-SM range, and higher in the AC range. Therefore, the steeper reaches of the AC range and of the northern SM range are better explained by faster river incision. This is consistent with higher ^{10}Be hillslope erosion rates in the AC range. Higher precipitation along the N and NW flank of the AC range, and along the N flank of the SM range does not modify the intrinsic concavity of river profiles enough to prevent linearization for θ_n=0.5.~~ are well coupled there (Callahan et al., 2019).

Boulder-armoured and alluvial channels are also steeper in the AC range (Fig. 14b,c). Boulders act as bedrock, and boulder-armoured reaches could therefore be expected to evolve like other detachment-limited channels. However, alluvial channels are likely transport-limited, and the slope of transport-limited reaches is less sensitive to rock uplift (Whipple and Tucker, 2002; Cowie et al., 2008). The increase most likely reflects an increase in bedload grain size with increasing erosion

rate, resulting from shorter residence times and more limited comminution of bedrock blocks in hillslope soils (Riebe et al., 2015; Neely and DiBiase, 2020).

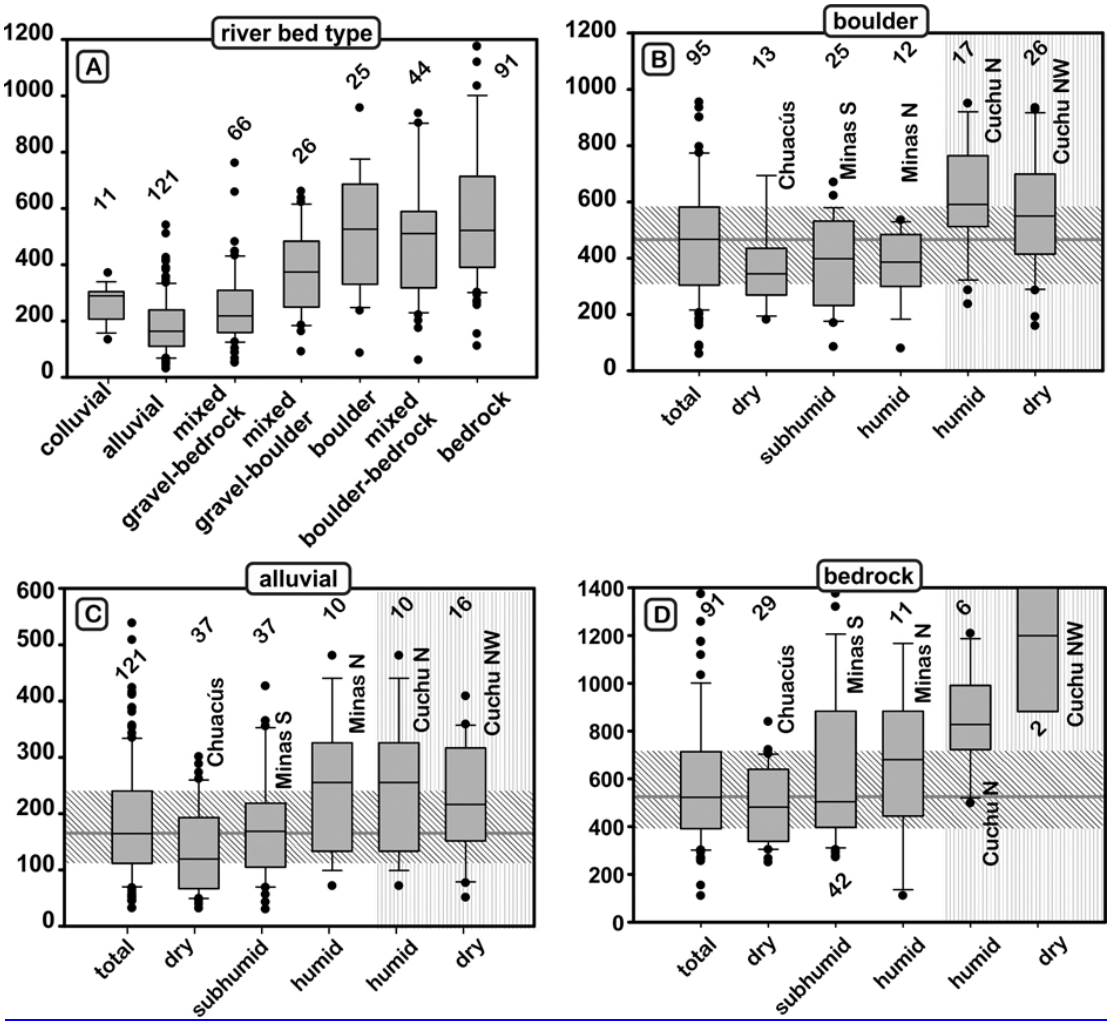

Figure 14. Box plots of stream segment normalized steepness as a function of streambed type and location.
(a) Comparison of steepness by streambed environment; (b), (c), and (c): spatial variations in channel steepness across the study area, according to the regions defined on Fig.7, for the three main types of streambed environment: (b): boulder, (c): alluvial, (d): bedrock. Numbers above box plots: number of segments. Oblique hatches: mean defined by the total number of segments. Vertical hatches: actively uplifting AC range.

5.2. The changes in the steepness of bedrock channels is mimicked by the changes in steepness of boulder armoured channels and by those of bedload dominated channels (Fig. 14b,c). While boulders may behave like bedrock, bedload channels are likely transport limited. In both cases, however, the increase most likely reflects an increase in boulder and bedload grain size. The increase in grain size with increasing incision rate would result from a more limited comminution of bedrock blocks in hillslope soils, reflecting their shorter residence time in saprolites and soils. The effect is stronger among boulder reaches, and may result from two processes. First, higher intensity rainfall events in the SM range (Bucknam et al., 2001) and in the AC range relative to the SC range may allow them to straddle the transition from diffusive-driven hillslope erosion to landslide-driven erosion. The abundance of debris flows in the SM range supports this possibility: in Panama, the transition to landslide-driven erosion occurs at mean annual rainfall values of 800-1,000 mm (Stallard and Kinner, 2005), which is the threshold crossed when moving from the SC to SM range. Second, in the AC range, where fewer debris flow deposits are observed, coarsening may be result from the delivery of large blocks from the resistant formations that cap the upper slopes, rather than from the increase in incision rate alone. The specific contribution of tectonic uplift to river steepening in the AC range is further explored in the following section.

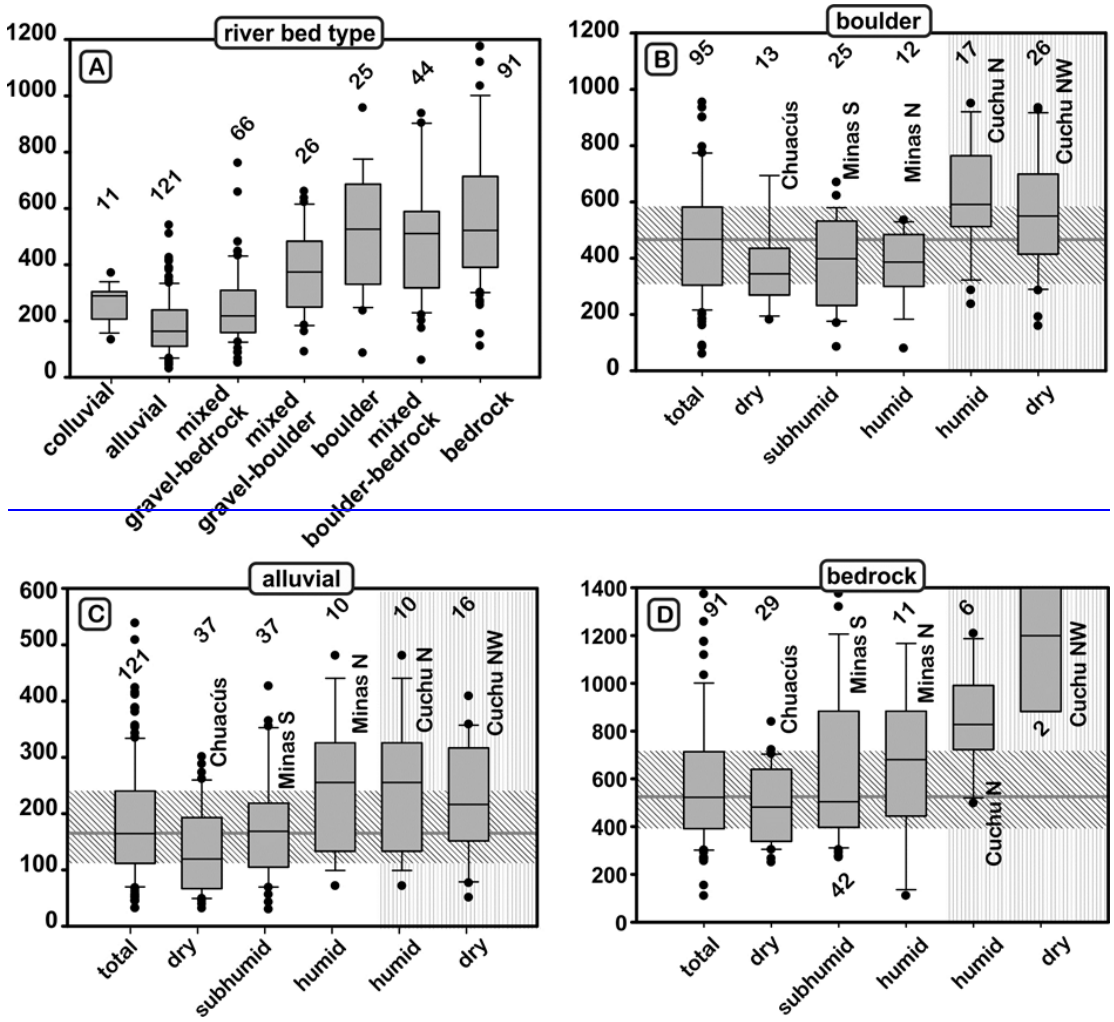

~~Figure 14. Box plots of stream segment normalized steepness as a function of streambed type and location. (a): Comparison of steepness by streambed environment; (b), (c), and (c): spatial variations in channel steepness across the study area, according to the regions defined on Fig.7, for the three main types of streambed environment: (b): boulder, (c): alluvial, (d): bedrock. Numbers above box plots: number of segments. Oblique hatches: mean defined by the total number of segments. Vertical hatches: actively uplifting AC range.~~

~~5.2.1.~~2. Tectonic steepening of rivers transverse the AC range

The four rivers that still cross the AC range are the Cuilco, Selegua, Chixóy, and Cahabón Rivers (Fig. 7). The Cahabón River is the smallest these. It is affected by an ongoing pulse of drainage rearrangement that started at ~1 Ma that led to the

shrinking of its headwaters, south of the Polochic fault, a process that will soon lead to its complete beheading south of the fault (Brocard et al., 2012). ~~across~~To analyse the effect of the AC range

~~Uplift in~~on the ~~AC range led to the diversion of many rivers. Among~~transverse river we therefore focus on the three ~~rivers were able to maintain their course across the range, Two (the Chixóy and Selegua rivers)~~other rivers. Of these, two, exhibit ~~significantly~~ steeper profiles as they cross the AC range, namely the Chixóy and Selegua Rivers (Fig. 15). ~~The lithologies incised by these rivers across~~As they cross the AC range ~~are also crosses by the same rivers~~these rivers incise rock formations that they already incise farther upstream, ~~where they do not generate~~without displaying any similar ~~(drainage area normalized)~~ steepening. ~~Considering that increased discharge would decrease river gradient, rather than increase~~, from which it~~, we conclude~~ can be concluded that the ~~increase observed across the AC~~steepening is ~~a response to~~ not caused by the present for more resistant rocks, but instead by faster ~~tectonic~~ uplift of the AC range (Leland et al., 1998; Kirby, 2003)~~.~~, consistent with the interpretation of the steepening of shorter rivers draining only the AC range (see previous section). The lack of substantial steepening along the ~~third river (the~~ Cuilco River~~) may~~ could imply that there, the AC range ~~is~~ no longer ~~uplifting in the west.~~rises faster than the areas located farther upstream. This ~~is at odds~~interpretation, however, is at odds with documented ongoing contractional deformation ~~documented~~ nearby~~, at the western end of the Polochic fault~~ (Authemayou et al., 2012). ~~Alternately, it may reflect the fact that the Cuilco River is alluviated over its entire length, and therefore transport limited. Transport limited conditions generate less steepening than detachment limited reaches in response to enhanced rock uplift (Cowie et al., 2008). Transport-limited conditions along the Cuilco River, in turn, result from the large bedload production of the Central American volcanic arc, located nearby in the headwaters of the Cuilco River. Similarly, the Chixóy River collects gravel in its headwaters within the volcanic arc. This bedload, however, is delivered to the river farther upstream. By the time the Chixóy River reaches the AC range, most gravel is contributed by the AC and SC ranges~~Instead, the lack of steepening may rather stem from the Cuilco River being a transport-limited river over its entire length, as evidenced by its continuous cover of alluvium, in contrast to the Selegua and Chixóy that display an alternation of bedrock and alluvial reaches, typical of detachment-limited rivers. Transport-limited conditions indeed generate less steepening than detachment-limited conditions in response to enhanced rock uplift (Cowie et al., 2008; Whipple and Tucker, 2002). A profuse delivery of volcanic gravel in the headwaters of the Cuilco River, where the river drains the Central American volcanic arc, probably explains this behaviour. The Chixóy River also drains the volcanic arc in its headwaters, but volcanic gravel sources are located farther from the AC range, such that, by the time the Chixóy River reaches the AC range, the petrological composition of its bedload reflect that of the most proximal gravel sources (Deaton and Burkart, 1984), ~~implying that headwater-derived gravel has been trapped and/or comminuted before reaching the AC range. The Selegua River displays the steepest steepening as it crosses the AC range. Likewise, it reflects the fact that its headwaters are located in an area characterized by shallower slopes and underlain by a basement rocks, with make the river comparatively gravel-starved. Such limited access to erosion tools are compensated by a larger increase in gradient~~the gravel

produced in the arc being comminuted or/and trapped upstream. ~~(Sklar and Dietrich, 2006). The small drainage area of the~~
~~Selegua River overall also makes it prone to detachment-limited behaviour (Brocard and Van der Beek, 2006).~~

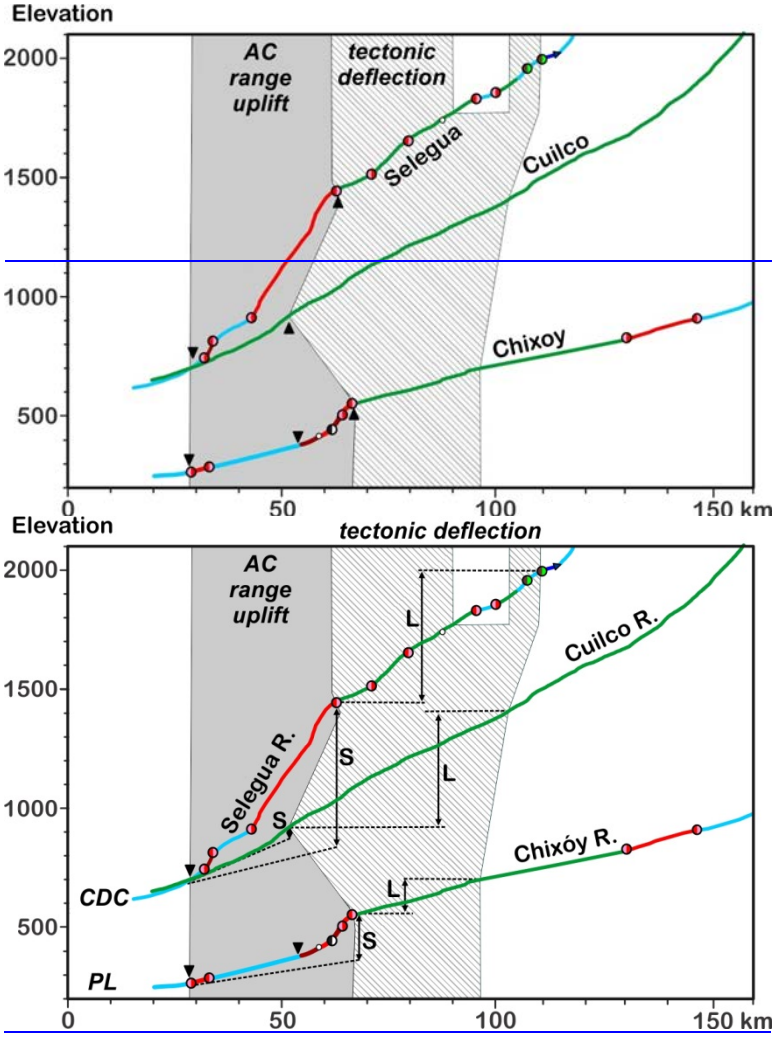

Figure 15. Long profiles of rivers transverse to the AC range: Chixóy, Selegua, and Cuilco, with indications of reaches affected by vertical rock uplift (grey area), and those affected by horizontal lengthening along the Polochic fault (hatched area). S and L: contributions of steepening and lengthening to the uplift of river profiles, upstream of the AC range. River knickpoint nomenclature: see Fig. 12.

5.2.~~2. Stalling~~ 3. Transient slowing of incision ~~at the base of~~in the SC range

~~Inception of uplift along~~**in response to river steepening in the AC range** ~~modified the dynamics of the rivers that crossed the range, initiating accelerated incision across the AC range, and a slowing down of incision farther upstream. This was followed, along many of these rivers, by a phase of river aggradation before their abandonment, consecutive to the reorganization of their drainage (Brocard et al., 2011). In Plio-Quaternary times a similar evolution affected the rivers flowing across the northern side of the SM range. Normal faulting spurred valley infilling, upstream of the rising structures, followed by drainage reorganization (Brocard et al., 2012). Aggradation upstream of a rising structure can be viewed as a transient, adaptive response of rivers to a changing uplift pattern along detachment-limited rivers (Brocard et al., 2012; van der Beek et al., 2002; Attal et al., 2008), or as an equilibrium response, under a stable uplift field, along transport limited rivers (Humphrey and Konrad, 2000). The steepening of river profiles in response to accelerated rock uplift across the AC range generates a transient phase of surface uplift, during which incision does not counterbalances rock uplift upstream of the steepened reaches. If the rock uplift rate of the SC range does not increases at the pace of the uplift of the AC range, such uplift of river profiles requires a decrease in river incision rate upstream of the AC range. In effect, river incision slowed down considerably before drainage reorganization, but has remained extremely slow ever since (Brocard et al., 2011). This stalling of incision has allowed potentially up to 1,000 m of surface uplift, which is the current average elevation of valley floors, along the northern base of the SC range (Fig. 16a,b). The resumption of river incision, expected to mark the return to dynamic equilibrium, has not occurred along the SC range. This implies either that river steepening is still under way across the AC range, and that dynamic equilibrium between river incision and rock uplift has not been reached yet, or that other processes prevent the resumption of erosion rates. Of two potential causes, the first one is climatic: it results from the aridification of the SC range. The second possible cause is tectonic, and results from the fact that the Cuilco, Selegua, and Chixóy River are deflected by the Polochic fault (Fig.15). Cumulative slip along the Polochic fault has generated a left-lateral deflection of these rivers, lengthening of their courses by 25 km. The maintenance of a downstream gradient sufficiently steep to along at least the downstream dispersal of river bedload, if not incision, along the lengthened reaches, requires additional surface uplift, upstream of the tectonic deflections, which may contributes, in part or in whole, to the current passive surface uplift of the SC range.~~

The ~~similar stalling of~~ steepening of rivers across the AC range represents the response of rivers to the rise of the AC range, in an area previously characterized by a foreland, crossed by shallow-gradient rivers. The phase of steepening, from shallow-gradient rivers to steep-gradient ones, should end with the achievement of an equilibrium state whereby the gradient of the transverse rivers is steep enough for river incision to counterbalance rock uplift in the AC range. For such steepening to occur, the headwaters must rise with respect to the foreland. This results in surface uplift in the SC range. Surface uplift requires a transient imbalance, upstream of the AC range, with incision rates lower than rock uplift rates. The sharp drop in incision rates in the SC range from 145-205 $m \cdot My^{-1}$ to <30 $m \cdot My^{-1}$ after ~7 Ma (see section 4.1) can be

viewed, therefore, as driven by the steepening of the Chixóy River in response to the rise of the AC range, because the Chixóy River is the post-7 Ma outlet of most SC range rivers.

Using the river profiles of the Chixóy River (Fig.15), it can be assessed that, ~190 m of surface uplift along the ~~Motagua valley~~Chixóy can be ascribed to river steepening resulting from the rise of the AC range, at ~27 m·My^{-1}. If, before 7 Ma, rock uplift rates in the SC range matched its incision rates of 145-205 m·My^{-1} (Fig.9), then, if such uplift rates were sustained in the SC range after 7 Ma, then 1.5 to 2 My would be necessary to lift up the Chixóy River and its tributaries to their current elevation, upstream of the AC range. Incision would resume afterwards. Such estimates have various limitations, in particular because both the Chixóy and Selegua Rivers experienced large changes in drainage area upstream of the AC range during the 7 Ma reorganization event, which affected their gradient across the AC range (Brocard et al., 2011). The Chixóy River was initially smaller, and therefore probably steeper, before receiving water and sediment contributions from of all surrounding streams at 7 Ma. Conversely, the Río Selegua lost some of its headwaters, and such loss may have contributed to its steepening. The calculation, however, suggest that the timescale of equilibration should be much shorter than the 7 My that have elapsed since the AC range started to rise. Ever increasing rock uplift rate in the AC range would promote continuous steepening, and therefore could prevent the return of incision, upstream of the AC range. Although plausible, such evolution remains speculative, because available data lack the resolution necessary to test it. We identified, however, other processes that delay the resumption of incision along the northern flank of the SC range.

5.2.4. Slowing of incision in the SC range in response to river lengthening along the Polochic fault

One such process is the lengthening of rivers as they cross the Polochic fault, before flowing across the AC range. Their course is progressively set off by slip on the Polochic fault, leading to the development left-lateral deflections that lengthen their course. Rivers maintain a gradient sufficiently steep along these deflections such as to allow at least the bypass of their bedload. This results in the uplift of the streambeds, commensurate to the amount of river lengthening. Before the rise of the AC range, such deflections where located in the foothills of SC range, at the entrance of the northern foreland. Streambed uplift, at a place where streambeds are shallowly incised, allowed for repeated avulsions toward the foreland, periodically annealing deflections (Sieh and Jahns, 1984). The rise of the AC range led to deeper entrenchment of tectonic deflections along the Polochic fault, preventing the annealing of deflections, and ensuring that all slip on the Polochic fault results in permanent river lengthening and uplift. The courses of the Chixóy, Selegua, and Chilco Rivers have thus been lengthened by 25-40 km (Fig.7), and the westward increase the length of deflection, in a context of westward decrease of total slip on the Polochic fault (Authemayou et al., 2011b), was interpreted as the result of earlier entrenchment of the rivers in the west (Brocard et al., 2011). River lengthening drove 500, 600 m, and 150 m of surface uplift along the Cuilco, Selegua, and Chixóy Rivers, respectively (Fig.15). Because left-lateral slip rate of the Polochic fault has been fairly steady

over the past 7 ~~My cannot be ascribed to the rise of a tectonic structure across its course.~~Ma, at 2.9 ± 0.4 mm·y^{-1} along the tectonic deflection of the Chixóy River (Authemayou et al., 2012; Bartole et al., 2019), river lengthening and uplift, likewise, must have steadily uplifted the upstream parts of the Cuilco, Selegua, and Chixóy River, at 15 ± 2 m·My^{-1} along the Chixóy River. In contrast to river steepening, the effect of such uplift on incision rates, upstream of the AC range, is permanent.

5.2.5. Respective contributions of tectonics and climate to the stalling of river incision in the SC range

With estimated rates of ~27 m·My^{-1} and 15 ± 2 m·My^{-1}, tectonic steepening and river lengthening are the two bottom-up processes that we could identify that contributed the rise of the AC range, and to some decrease in river incision rates. Still, they only represent a fraction of the drop in river incision rates from 145-205 m·My^{-1} before 7 Ma, to <30 m·My^{-1} after ~7 Ma. Such evolution implies therefore either a substantial decrease in rock uplift rates in the SC range after 7 Ma, or/and a strong effect of the aridification of the SC range on river incision rates.

A decrease in rock uplift rates in the SC range is supported by the difference in elevation between paleovalleys located in the AC range, such as V3 (Fig. 2, Fig.8a), which underwent 2.8 km of uplift since ~7 Ma (assuming an initial foreland elevation of 0.3 km), and the Chixóy River, which only underwent 0.35 km of uplift in the meantime. If the Chixóy River had lifted up since 7 Ma at the rate at which river incision occurred in the SC range before 7 Ma (145-205 m·My^{-1}), then the difference in elevation between V3 and the Chixóy River (0.9 km) would be only 1/3rd of its present-day value. Their difference in elevation is even slightly smaller than the 1 km back-tilting of paleovalleys V4-V5, south of the Polochic fault (Fig.2 (Brocard et al., 2011)).

Fluvial and volcanoclastic aggradation in the range of 50-300 m occurred along the rivers that drain the northern flank of the SC range prior to 7 Ma, as documented by the sedimentary fills of the paleovalleys, upstream of the AC range. They support the view of a strong imbalance in uplift rates between the two ranges from the start. Such aggradation can be viewed as the transient response of these rivers to increased uplift farther downstream (van der Beek et al., 2002; Attal et al., 2008), due in these case, to the rise of AC range (Brocard et al., 2011). A similar aggradation is observed along the northern drainage in Plio-Quaternary times, along the northern flank of the SM range, in response to the rise of transtensional horsts and tilted blocks (Brocard et al., 2012). The return to pre-aggradation levels would mark the return to equilibrium, characterized by a lack of rock uplift, of the SC range with respect to the foreland, hence the lack of river incision. In this view, the few 10s of meter of incision since 7 Ma would represent a fine balance between river incision and rock uplift in the SC range, with rock uplift providing quite precisely the 350 m of surface uplift needed to counterbalance river steepening in the AC range and river lengthening above the Polochic fault. There is, however, no obvious process whereby such fine balance of rock uplift rates would be achieved.

Alternately, instead of an equilibrium response, the absence of incision could be viewed as an absence of response to tectonic processes, in a landscape subjected to aridification after 7 Ma. By decreasing water discharge, aridification would reduce stream power. This would initially reduce incision in the SC range, while promoting river steepening in both the SC and AC ranges (along rivers which mostly drain the AC range), furthering surface uplift. Second, it may have altered the balance between water and sediment discharge in such a way as to reduce sediment transport capacity and river incision (Beaumont et al., 1992), or limited the availability of tools for eroding the bedrock (Sklar and Dietrich, 2006). A contribution of climate to the slowing of incision is also suggested by the evolution of the southern flank of the SC and SM ranges, which, although exposed to a different tectonic forcing than the northern side of the SC range, underwent a similar evolution of incision rates as the northern flank of the range. There, the only possible contribution of the Motagua River to the stalling of incision would be through a considerable lengthening of its course at its downstream end, into the Caribbean Sea, requiring surface uplift farther upstream in order to maintain the downstream dispersal of sediments. Some lengthening probably occurred as a result of the emergence, at the its downstream end, of a transtensional basin filled with terrigenous sediments that marine middle Miocene sediments (Carballo-Hernandez et al., 1988). This lengthening of >180 km currently involves <75 m of surface uplift. A stalling of incision along the southern flank of the range, would, at equilibrium, involve southward tilting of the range, such as to accommodate the difference in surface uplift. It ~~can result, too, from the establishment of aridity along the central part of the valley~~seems highly unlikely that independent tectonic phenomena, such as the uplift of the AC range in the north, the lengthening of rivers on the Polochic fault, the decrease in rock uplift rates, and the lengthening of the Motagua River in the west, would converge such as to produce the similar stalling of incision on either side of the SC range. The aridification of the range, which is well documented on either side (Machorro, 2014), appears therefore as an import factor, slowing down river incision.

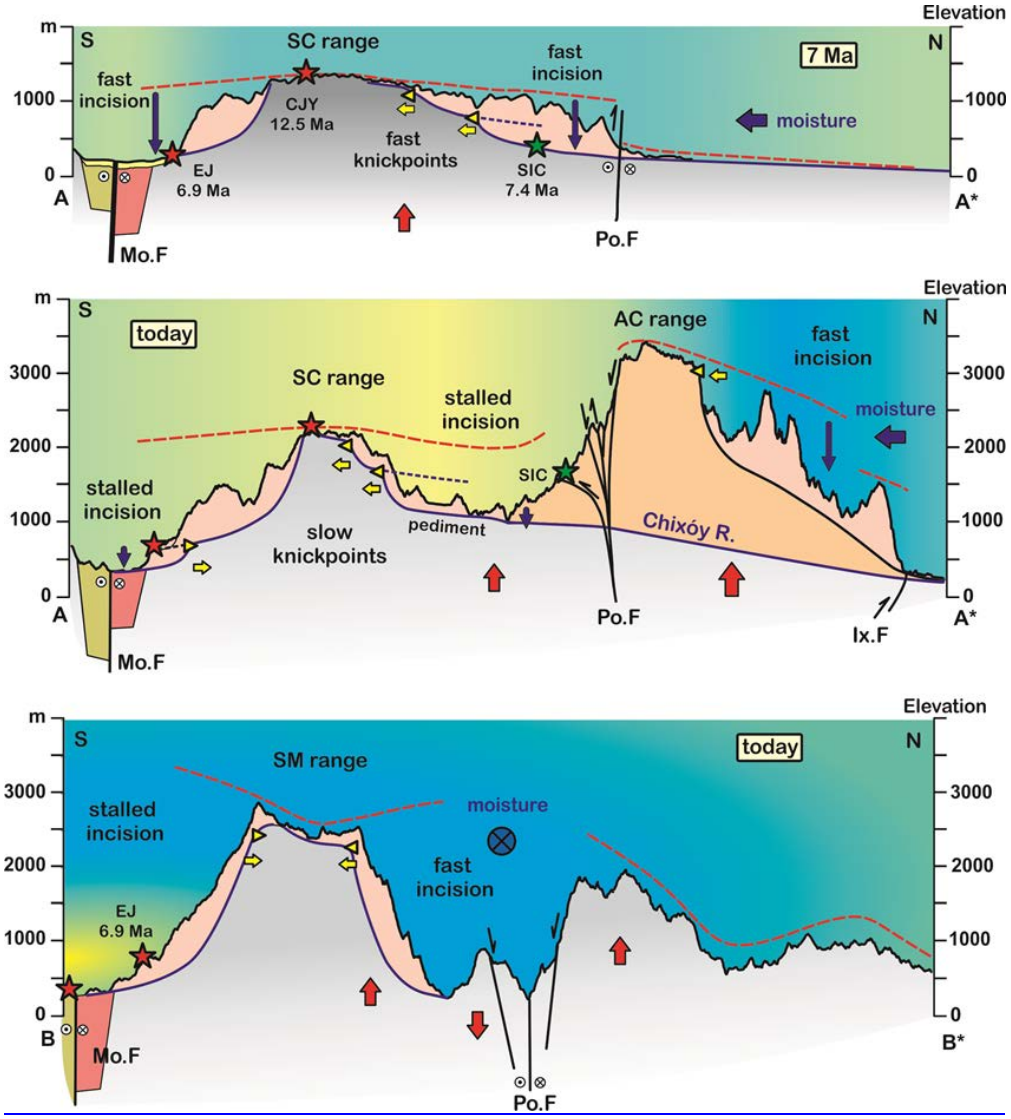

Figure 16. Development of the central ranges of Guatemala. Along profiles A-A* and B-B* (see Fig. 13a for location).

~~but it also may be driven by bottom-up processes. In this case, the floor of the Motagua valley may have risen by lengthening of the Motagua River course, driven by the progressive emergence, at its downstream termination, of transtensional basins in the Caribbean Sea (Carballo-Hernandez et al., 1988). The present-day difference in elevation (200-600m) between the floor of the Motagua valley, south of the SC range, and the floor of the Chixóy basin, north of the SC range, could be inherited~~

from before 7 Ma ago, or could have been acquired,**5.3. Topographic evolution of the SC range in response to the uplift of the AC range**

5.3.1. Slowing down of hillslope erosion, topographic decay, and backwearing

Modern ^{10}Be-derived hillslope erosion rates SC are higher (> 50 m·My^{-1}) than the <30 m·My^{-1} long-term river incision rates around the SC range (Fig.10). This suggest that the relief of the SC range has been slowing decaying over the past 7 My, by 5° southward tilting of the SC range.. Hillslope degradation during decay could possibly account the lower average steepness of quartz-feeding slopes in the SC range (22±3°) compared the AC range (26 ± 4°). Hillslope steepness degradation should be associated with a decrease in the local relief of the SC range. The preservation of the Maya surface on many summits, combined with the absence of substantial incision around the base of the range however imply that the height of the SC range has not been been significantly reduced over the past 7 My. Instead, decay appears to have proceeded through the backwearing of the slopes, from the base of the range towards its divide. This is manifested by the development of pediments that expand towards the range interior, and by the presence of upstream-migrating river knickpoints within these backwearing slopes.

5.3. Effects2. Origin of climate and tectonics onmigrating river knickpoints within the celeritySC range

Three clusters of migrating knickpoints are found at different elevations along the northern flank of the SC range (Fig. 8b and 12a2). The uppermost cluster consists of convex knickpoints that dissect the middle Miocene Maya surface. They represent the front of an erosion wave that formed in response to the initial uplift of the SC range at 12 Ma. These knickpoints may have nucleated near the base of the range, along the Polochic fault, which represented the boundary between the SC range and the foreland from 12 to 7 Ma (Fig. 16a). The second cluster consists of convex knickpoints located 500 m farther down the northern flank of the SC range (Fig. 8b and 12a2). These knickpoints have heights of 200-300 m (Fig. S4-3). Assuming that this represents the amount of stream incision associated to their passage, the this passage must predate 7 Ma, because rivers have only incised 20-90 m over the past 7 My between these knickpoints and the northern front of the SC range (Brocard et al., 2011).

Hillslope erosion is expected to increase in the downstream direction across upstream migrating knickpoints. A larger increase in hillslope erosion is expected to reflect faster upstream knickpoint migrationLike the upper knickpoints, therefore, they could have nucleated on the Polochic fault. ^{10}Be hillslope erosion rates however suggest that these two generations of knickpoints migrate very slowly today. Indeed, hillslope erosion rates should increase across upstream-migrating knickpoints in the downstream direction. Faster migrating knickpoints should geometrically promote larger differences in hillslope erosion between upstream and downstream areas (Brocard et al., 2016b). In the study area, the knickpoints that dissect the low-relief uplands do affect hillslope erosion rates, but this increase is much larger in the AC and

SM ranges than in the SC range (Fig.10 and 13c). The lack of substantial increase in the SC range suggests that knickpoints are almost immobile there. Given that these knickpoints are not located near any obvious site where they could have nucleated, it is likely that they formed some distance downstream. Alternately, they could have formed in situ, by some yet unidentified process. If these knickpoints formed farther downstream, they necessarily migrated faster in the past, before stalling at their current location. Knickpoint celerityEither marginal (e.g. catchments XEU to Cub) to negligible (e.g. SMS to SMM) increase in erosion rate is documented across these knickpoints (see section 4.2), suggesting that they have stalled. Knickpoint celerity is influenced by top-down processes, such as the amount of water runoff and sediment discharge delivered from upslope (Crosby and Whipple, 2006; Brocard et al., 2016b)., and under certain circumstances, it can be influenced by bottom-up processes, such as the rate of base level fall (Whittaker and Boulton, 2012). Therefore, both the stability of the base level around the SC range over the past 7 My, and the reduction in rainfall resulting from the rise of the AC range may have contributed, together with decreasing upstream drainage area, to the slowing down of migrating knickpoints within the SC range (Fig. 16a,b). Their migration considerably slowed down over time, through a combination of (Crosby and Whipple, 2006), and Base levels has been stable over the past 7 My along the northern flank of the SC range, and along the southern flanks of the SC and SM. By contrast, base levels have fallen rapidly along the northern flanks of the AC and SM ranges, due to tectonic separation between the Petén lowlands/Central Depression of Chiapas and the AC range, and between the Izabal releasing bend and the SM range. Such differences may have driven, in part or in whole, the differences in celerity from a range to the other. Nonetheless, knickpoint celerity is also controlled by top-down processes such as the amount of water runoff and sediment discharge delivered from upslope (Crosby and Whipple, 2006; Brocard et al., 2016b; Whittaker and Boulton, 2012). The reduction in rainfall over the SC range, resulting from the >3,000 m surface rise of the AC range, can therefore be expected to have also contributed to the slowing down of erosion waves along the SC range (Fig.of aridification in the SC range (Fig.16b). 16a,b). No [10]Be measurements are available along the northern side of the SM range, but the abundance of precipitation implies that knickpoints are expected to migrate faster there. Most of the surface uplift the SM range occurred in concert with that of the SC range (as documented by the El Jute basalt). However the evolution of the northern flank of the SM range differs from that of the SC range in that it likely became wetter with time, in response to the channeling of moisture along the Lake Izabal releasing bend. The releasing bend nucleated in the east, in middle Miocene time, steadily growing westward ever since (Bartole et al., 2019). Tectonic subsidence in the bend opened a topographic gap between the SM range and the mountains located farther to the north. Fluxes of Caribbean moisture are channeled along the gap, from which they rise along the northern flank of the SM range (Fig. 4, (Brocard et al., 2012)). The channeling of moisture along the northern side of range may have contributed to the growth of the rain shadow along its southern flank (Fig. 16c). The prominent knickpoints of the northern flank are therefore likely migrating faster than their southern counterparts, under the influence of this relief-controlled precipitation regime.

The third cluster of knickpoints is located along the base of the mountain. It consists of concave-up knickpoints located at the apex of the pediments that have developed along the range (Fig. 8b and 12a2). These pediments are currently extensively buried under pumice deposited during a large, late Pleistocene eruption (Brocard and Morán, 2014; Rose et al., 1987). Pediments usually form under semi-arid climates, along drainages with stable base levels; they grow by their apex, in the upstream direction (Pelletier, 2010; Strudley et al., 2006; Thomas, 1989). The pediment of the SC range have developed in an area that has been incising slowly over the past 7 My (<30 m·My-1) in an area where climate is among the driest in Guatemala (Machorro, 2014), over slate, schists, gneisses, and granite. The concave-up migrating knickpoint located at the apexes of these pediments can be regarded as knickpoints that spearhead a wave of decreased incision (Baldwin, 2003).

~~The rise of the SM, SC, and AC ranges, and thereby for the spatial distribution of precipitation, has been driven by a tectonic displacements transverse to the strike of the plate boundary, during phases of enhanced transpression and transtension. The dominant, left lateral component of the plate motion does not generate surface uplift. Still, it may alter the distribution of precipitation by laterally displacing topographic obstructions over time. The Polochic fault moves the AC range westward relative to the SC range. By removing this topographic obstruction, the Polochic fault will ultimately re-expose the SC range to the Caribbean moisture. The velocity of the sliding (25 km in 7 My, (Authemayou et al., 2012)), however, is small compared to the length of range. Besides, the AC range may keep growing vertically and lengthwise such as to keep pace with its lateral offset. Left lateral tectonics has therefore a limited impact in this specific case, on the evolution of erosion rates by top-down processes.~~

~~Finally, it must be noticed that the aridification of the SC range also requires an efficient containment of the Pacific moisture by the Central American volcanic arc. The arc today supports stratovolcanoes more than 4,000 m high that rest on a crystalline Palaeozoic basement up to 3,500 m high. The arc currently efficiently contains the Pacific moisture. Its topographic evolution and uplift chronology are unfortunately fully unconstrained, and do not allow us to assess their influence on the climate of central Guatemala over time.~~

~~5.4. Origin of the migrating knickpoints~~

~~Clusters of headward migrating knickpoints are observed at mid-elevation along most of the studied mountain flanks, downstream of the clusters of knickpoints that dissect the low relief uplands (Fig.12). These mid-elevation knickpoints likely migrate at different celerities and have been generated by different processes.~~

~~Some scattered headward migrating knickpoints dot the northern, southern, and northwest flanks of the AC range (Fig. 12b1,2). Along its northern flank, these knickpoints lie upstream of a broad area of stream steepening, over the hanging wall of the Ixcóy fault. They could mark the front of a wave of accelerate incision, triggered by an acceleration of differential tectonic uplift (Whittaker et al., 2007) across the Ixcóy fault, while the overall steepening may reflect increasing uplift rate in the downstream direction, at dynamic equilibrium (Kirby and Whipple, 2001). The NW flanks of the AC range differs in that no tectonic separation of the Maya surface occurs at the base of the NW flank, where the Maya surface is affected by a kink fold (Fig.2 and 4). Mid-elevation migrating knickpoints there could have been produced by river steepening, without nucleating over a specific tectonic dislocation (Willenbring et al., 2013). Similarly, river steepening could account for the two imbricated waves of erosion observed along the paleovalley of Quilén-Novillo-Chancol, on the southern side of the range (Fig.8a).~~

~~Knickpoints are also observed at the base of the SC range, near the Chixóy River, at the downstream end of rivers that drain the N side of the range. These knickpoints, which are located downstream of the pediments, are restricted to the Chixóy Basin and are not observed along the northern flank of the SM range (Fig. 12b2). They could therefore result from the recent propagation of a wave of incision along the Chixóy River, which hosts a potentially migrating knickpoint slightly farther upstream (downstream of Sacapulas). The Chixóy River knickpoint, however, could also be lithogenic, or could result from uplift in the footwall of a normal fault near Sacapulas. This later fault is probably no longer active, as its scarp shows no indication of recent slip. The Chixóy River has established its range-parallel course between the AC and SC range ~7 My ago, during the reorganization of the drainage, as a collector at the lowest point in the saddle between the two ranges (Brocard et al., 2011). Today, however, the axis of this saddle is located 6-8 km farther south, suggesting that the saddle has migrated as a result of the enlargement of the AC range. The knickpoints located very near the Chixóy River could therefore~~

~~have a tectonic origin, is a result of renewed uplift resulting from this enlargement, rather than spearheading a recent wave of incision.~~

~~A prominent cluster of headward migrating knickpoints is located 500 m farther up the northern flank of the AC range (Fig.~~Streambed analysis further shows that these knickpoints are located at the transition between detachment-limited and transport-limited reaches downstream (Fig. S4-3) as predicted by theory (Whipple and Tucker, 2002). Lateral planation tend to dominate over vertical incision, downstream of that transition (Brocard and Van der Beek, 2006), which is also consistent with pediment development downstream. The fact that these concave-up knickpoints are located downstream of the steepest river reaches, downstream of the cluster of convex-up knickpoint located halfway the mountain side may not be coincidental, and could in fact imply that the second cluster of knickpoints did not nucleate, as hypothesized above at the front of the range. Rather, they has formed and grown in height and steepness progressively inside the range, ahead of the pediment apexes, rather than through nucleation along the Polochic fault. They would grow due to faster backwearing of the lower slopes than downwearing of the upper slopes, thus generating the steepest river reaches immediately upstream of the pediments. From a conceptual point of view, the river reaches located between the mid-flank convex knickpoints and the basal concave knickpoints can be viewed as the lips and toes of large knickzones (or knickpoint faces (Gardner, 1983)). Models predict that, if water discharge has larger influence than river gradient on stream incision, such knickpoint faces steepen and amplify over time during backwearing ~~8b and 12a2). If this wave of erosion was initiated by a distal tectonic event, they likely initiated over the first major tectonic dislocation encountered in the downstream direction, namely the Polochic fault. If so, the event that generated them would predate the uplift of the AC range. Indeed, only 20-90 m of incision has occurred over the past 7 My at the downstream end of these rivers (Brocard et al., 2011), and the knickpoints have typical amplitudes of 200-300m (Fig. S4-3). They could have been generated by accelerated differential uplift across the Polochic fault (Fig.16a), and their migration up the Chuacús range would have considerably slowed down over time, through a combination of decreasing upstream drainage area (Crosby and Whipple, 2006), and aridification of the SC range, and would subsist today, almost frozen, along the northern side of the SC range (Fig.16b). That the base of the knickzones lies in close association with the pediments that formed along the northern base of the SC (Fig. 8b and 12a2) further suggests that the knickpoints and pediments may be genetically related. If the process of upstream-directed growth of pediments (Pelletier, 2010; Strudley et al., 2006) proceeds faster than slope lowering farther upstream, they could generate the formation of knickpoints at the base of the range. The steepening of these knickpoints would occur by faster migration of their concave-up base (corresponding to the pediment apex) than their convex-up upper lip. Such evolution of headward-migrating knickpoint profiles is expected when river incision is controlled more by river discharge than river gradient~~ (Weissel and Seidl, 1998; Tucker and Whipple, 2002). This intermediate cluster is not found farther east, along the wet flank of the SM range, where no pediments have formed at the base of the range (Fig. 12d, 16c). There, only one cluster of large migrating knickpoints separates the very flat uplands of the SM range from its deeply incised, wet lower flank (Fig. 8d). The aridification, therefore, appears to be responsible to the development of stepped topography.

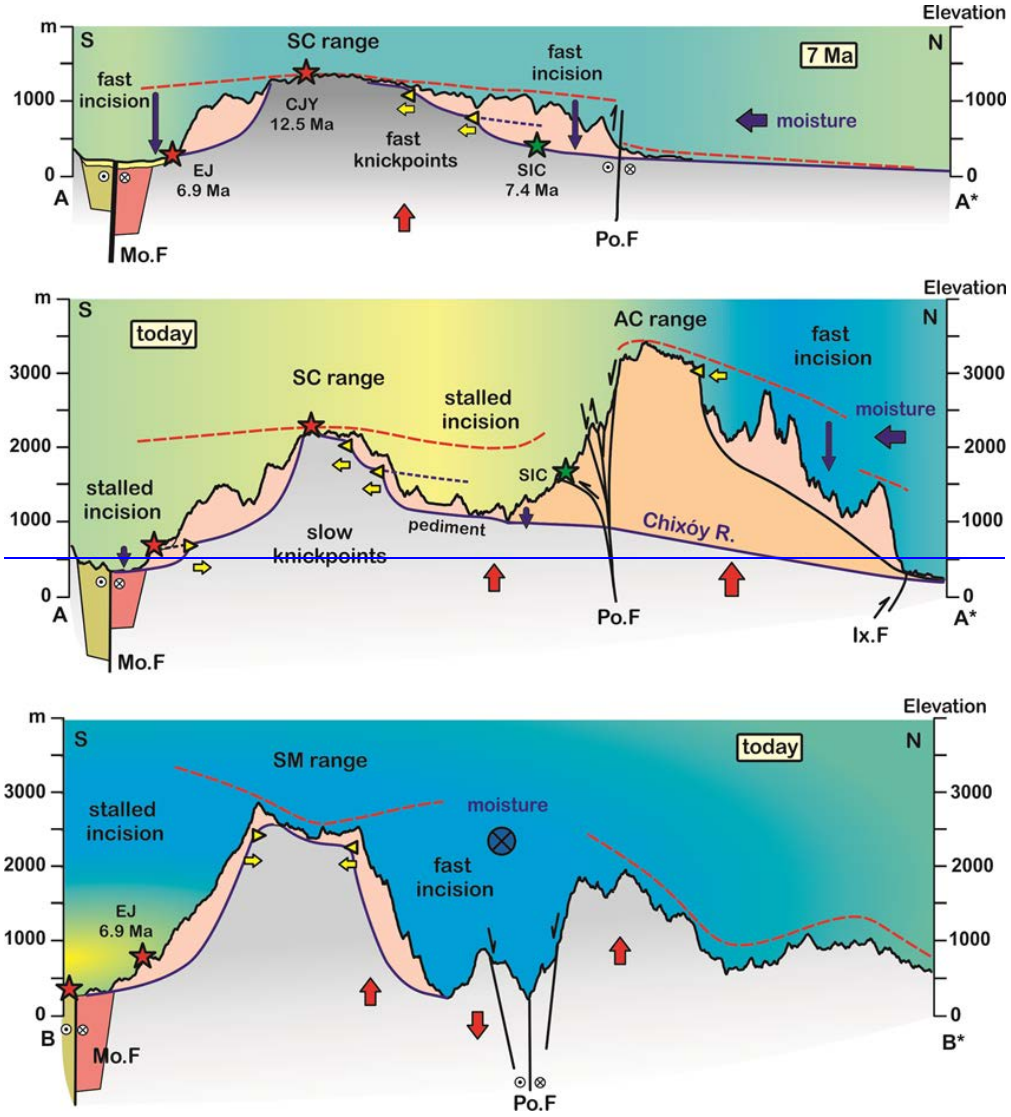

Figure 16. Development of the central ranges of Guatemala. Along profiles A-A* and B-B* (see Fig. 13a for location).

Mid elevation headward migrating knickpoints along the southern flank of the SM-SC range are mostly found south of the SC range, along the upper reaches of the Motagua River. These migrating knickpoints lie at the head of valleys incised into degraded low relief pediments that are, at places, covered by ignimbrites (Fig. 12a1). These ignimbrites are not dated, but considering that they hang above the Motagua River about the same elevation as the El Jute basalt, they could be late Miocene in age, an age consistent with the age of other ignimbrites farther north (Brocard et al., 2011) and farther south in Central America (Jordan et al., 2007). Downstream convergence of these ignimbrite with the Motagua River, and coeval steepening of the Motagua River upstream of the convergence point suggest that renewed incision is taking place in the

~~headwaters of the Motagua River. It is probably driven by uplift in the Central American Volcanic Arc, which forcing is difficult to track farther upstream, because the Motagua River course becomes increasingly chocked by the recurrent deposition of pyroclastic aprons, emplaced during caldera forming eruptions along the volcanic arc (Wunderman and Rose, 1984). The last such eruption disrupted the course of the Motagua River 84 ka ago. Primary pumice flows deposited 100-200 m of pumice along the base of the SC range (Fig.12a), and several tens of meters of reworked pumice all along the base of the SM range, (Tobisch, 1986). This short lived event did not generate knickpoints along the tributaries of the Motagua River, become most streams quickly incised the pumiceous deposits down to their pre eruption level. The pumice, however, altered the upper course of the Motagua River, such that the river has epigenetically incised its upper reaches in harder volcanic substrates, generating knickpoints. At the other, downstream end of the Motagua River, sea level variations had no noticeable impact on the studied reaches of the Motagua River, upstream of Los Amates (LA, Fig. 12a)., such that the Motagua River remains a stable base level for the streams that drain the southern flank of the SM SC range.~~

~~The northern flank of the SM range stands out for its absence of mid elevation knickpoints. They may have never existed, or could have migrated faster upstream, as a result of the high precipitation along this flank of the range, merging with the high elevation knickpoints that incise the ledge of the low relief uplands. The stacking of erosion waves has been proposed to account for the presence of some prominent knickpoints elsewhere (Crosby and Whipple, 2006).~~

~~**5.5. Pediment formation**~~

~~A series of pediments has formed between the AC and the SC range, where incision rates have been the slowest over the past 7 My (<30 m/My, Fig. 9), and where climate is the driest (Machorro, 2014). They have developed on granite and slate of the Santa Rosas Fm., as well as on schists and gneisses of the Chuacús Fm. They are currently extensively covered by the Los Chocoyos pumice, a volcanoclastic unit deposited during an eruption of the Atitlán caldera 84 ka ago (Brocard and Morán, 2014; Rose et al., 1987). This recent depositional event gives the impression that the pedimented areas are sedimentary basins, overlain by thick sedimentary fills. Actually the pedimented surfaces are exposed by erosion at shallow depth, below the pumice (e.g. Fig. 8b). Pediments tend to form in semi arid landscapes, and require a stable base level (Pelletier, 2010). Along the northern side of the SC range, their apex are located immediately downstream of the detachment to transport limited transition, marked by concave up knickpoints in the river profiles (Fig. S4 3, (Whipple and Tucker, 2002)), where lateral planation starts to dominates over vertical incision (Brocard and Van der Beek, 2006). In this context, the apex of these pediments can be seen as transient, upstream migrating knickpoints marking a decrease in incision rate~~

5.3.3. Range-hopping erosion and the development of dry orogen interiors

The evolution of the study area can be summarized as follows. Orogenesis started with the rise and coeval incision of the SC-SM range, from 12 to 7 Ma (Fig.16a). After 7 Ma, rock uplift decreased in the SC range while the AC range

started to rise in its northern foreland. Fast uplift in the SC range led to the tectonic defeat of many rivers which, upon exiting the SC range, flowed across the foreland. Most of the defeated rivers were rerouted into the drainage of the Chixóy River, one the four rivers that maintained a course across the AC range. Transient steepening of these range-transverse rivers in response to the fast rise of the AC range and lengthening of these same rivers along the Polochic fault promoted surface uplift within the SC range. The complete cessation of river incision along the northern side of the range may therefore result from a combination of river steepening, river lengthening, and from the decrease in rock uplift rates with the SC range. However, the fact the stalling of incision is as complete along the southern side of the range as along the northern side suggest that tectonics was not the only cause, but that the aridification of the SC range, resulting from the rise of the AC range, was also instrumental in the stalling of river incision. The decrease in precipitation over the SC range reduced erosion on its hillslopes, decreased river discharge, and therefore contributed to the stalling of river incision on both sides of the range. Precipitation and erosion concentrated on the northern flanks of the AC and SM ranges, while the SC range was becoming almost passively uplifted.

The high erosion rates and wet slopes that characterize the AC range today are therefore reminiscent of the SC range from 12 to 7 Ma. The AC range has become the range that intercepts the moisture rising from foreland, while the SC has become a range located upstream, in its rain shadow. As such, it displays traits of dry orogen interior ranges and orogenic plateaus: it erodes slowly and undergoes a progressive topographic decay, marked here by the development of pediments along its base. Pediment development is promoted by a combination of aridity and of very low incision rates. Low incision rates that result from a combination of aridification in the rain shadow of frontal ranges, and of tectonic steepening of river gradients across the front ranges, is expected to characterized the growth of orogenic plateaus forming by lateral accretion (Sobel et al., 2003; Garcia-Castellanos, 2007). In the case of orogenic plateaus, however, the combination of decreased precipitation and rise of new frontal ranges achieve the disintegration of drainages, isolating dry interior drainages from the drainage of front ranges. River incision along interior drainage is reduced by the high-elevation base level maintained in the endohreic catchments. The reduction in local relief over then combines a continuation of pre-existing trends in topographic decay and pedimentation, and an added contribution of progressive sediment infilling of the now closed catchments (Sobel et al., 2003). The drying of the SC range could evolve –or not- toward full drainage disintegration.

Continued extension of the pediment and their coalescence could lead to the formation of an intramontane pediplain (Baulig, 1957), at elevations of 0.9-1.2 km, halfway between the high-standing remnants of the middle Miocene Maya surface, and the Petén-Yucatán lowlands. The Central American Dry Corridor, which straddle the SC range, continues to the NW over the Central Depression of Chiapas (Fig.1a), where more extensive pediments have developed over the basement of the Sierra Madre de Chiapas (Authemayou et al., 2011a), in an area isolated from the Pacific moisture by the Sierra Madre de Chiapas to the SE, and from Caribbean moisture by the Sierra de Chiapas in the NW (Fig.1a). These pediments are in a more advanced process of coalescence and pediplain. The formation of such pediplains, in a context of active orogenesis

may explain the great abundance of low-relief perched surfaces that appear to have form in many orogens, without significant pauses in mountain building (Calvet et al., 2015; Pain and Ollier, 1995; Babault et al., 2005).

~~(Baldwin, 2003).~~

~~Other pediments have formed in a similar setting, 200 km to the NW over the crystalline basement of the Sierra Madre de Chiapas (Authemayou et al., 2011a), in a dry area, isolated from the Pacific moisture by the Sierra Madre de Chiapas to the SE, and from Caribbean moisture by the Sierra de Chiapas in the NW. The Central Depression of Chiapas act as a stable base level for these pediments, and therefore appears to be passively uplifting, upstream of the Sierra de Chiapas, with respect to the Yucatán lowlands, much like the Chixóy Basin, upstream of the AC range, while the still uplift Sierra de Chiapas undergoes topographic decay along its NW flank.~~

~~The tectonic defeat and drying of ranges located on the leeside of newly uplifting ranges is expected to mark the nucleation and lateral growth of orogenic plateaus above crustal accretionary wedges (Sobel et al., 2003; Garcia Castellanos, 2007). The decrease of topographic relief over the plateau interior combines a weakening of the crust, which does not allow the lithosphere to support tall reliefs, and the filling of intramontane basins with alluvium. We show here that pedimentation is an important contributing process, especially during the initial stages of topographic lowering, when the rivers draining the drier parts of the orogen are still connected with the foreland, allowing the dispersal of the sediments. In the case of fully-developing orogenic plateaus, increasing arid conditions during later stage eventually promote the disintegration of the river drainages, the disconnection of their base level from surrounding lowlands, and the full retention of erosional products within the intramontane basins (Sobel et al., 2003; Garcia Castellanos, 2007) .~~

6. Conclusions

- ~~The~~ Radiometric ^{39}Ar-^{40}Ar dating on volcanic rocks confirms our earlier ~~studies suggesting~~finding that the mountains ~~of Central Guatemala located~~range the closest to the plate boundary (~~Sierra de las Minas and Sierra de Chuacús) rose and were~~the SM-SC range) was mostly incised during the ~~middle~~ late Miocene ~~(12-7 My ago). Since then, the SM and SC ranges have stopped rising relative to the surrounding valleys (Motagua valley and Chixóy Basin), while~~ , from 12 to 7 Ma. Incision almost completely stalled afterwards, during the formation of the Altos de Cuchumatanes ~~range, located~~(AC range), farther north~~, has been uplifting and eroding~~.

- ~~Strong uplift~~The deformation of paleovalleys indicates that the AC range ~~over the past 7 My~~ experienced > 1,000 m of uplift relative to the SC range ~~results from oblique contraction combined to erosional unloading. The northern flank of~~ over the past 7 My. Today the ~~SM range has been gain some relief from the continued and westward propagation of the Lake Izabal releasing bend.~~ range is highly dissected. High river profile steepness and ever-expanding ice-caps indicate that the AC range still undergo fast rock and surface uplift.

- The concentration of detrital terrestrial ^{10}Be ~~concentration~~ in the ~~bedload~~sediments of rivers ~~draining catchments distributed throughout~~that drain these ranges show that ~~current hillslope erosion rates mimic the current patterns of stream incision: they~~hillslope y reach 300 m~~/~~·My^{-1} in the AC range, but are commonly ~~lower than~~ <100 ~~m/~~·My^{-1} in the SC-SM ~~ranges. In the AC~~ range~~, hillslope erosion equals stream incision. In the SC range and along the southern flank~~. The patterns of ~~the SM range, hillslope erosion outpaces base level lowering, implying an overall trend of topographic decay.~~

~~Current~~ hillslope erosion rates ~~coincide with~~therefore mimic the ~~current distributions~~spatial patterns of precipitation~~.~~ and stream incision.

~~-~~ Precipitation is strongly controlled by topographic obstructions resulting from the rise of the ~~SM and SA ranges~~AC range, which ~~intercept the~~intercepts Caribbean moisture. Precipitation is high along the northern flanks of the AC ~~and SM ranges, while the southern flank of the SM range and both sides of the SC~~ range ~~lie~~, but low over the SC range, which lies within rain shadows. Fossil vegetation preserved ~~in~~at the ~~Chixóy River basin documents~~base of the SC range indicates a wetter climate at 7 ~~My ago~~Ma, when the ~~rain shadow was less pronounced or absent~~AC range started to grow.

- In this context, the slow current hillslope erosion rates in the SC range ~~appears~~appear to ~~result from~~ be contributed in part by the rise of the ~~SM~~AC and ~~AC range and~~by the development of ~~these~~ rain shadows. It can be hypothesized, therefore, that hillslope erosion rates in the SC range were higher before the uplift of the AC ~~and northern SM range started. The slowing of river incision at the base of the SC range and on the southern side of the SM range, because they occurred as the uplift of the AC range started, can be interpreted as the shutting down of erosion as a result of the growing rain shadow.~~

~~The defeat of many rivers draining the SC range across the AC range, during the early stages of its growth, and the temporal coincidence between this defeat and the overall cessation of stream incision in the SC range further suggests that tectonic uplift along the AC~~ range ~~has switched off~~. Aridification may have also contributed to the decrease in river incision ~~upstream of the AC range, allowing the SC range to passively rise by up to 1,000 m, without undergoing significant erosion.~~ rates over the SC range.

- The ~~slowing of erosion~~rise of the AC range led to the steepening of river profiles along the rivers that maintained a course across the rising range. The steepening of river profiles triggered a transient decrease in river incision rates upstream of the AC range. The lack of resumption of river incision upstream of the AC range implies either that these rivers have not re-established equilibrium profiles, or that other factors prevent the return of incision. Aridification and river lengthening are the most likely contributors.

- The rise of the AC range indeed led to the entrenchment of range-transverse rivers along the Polochic strike-slip fault. Fault slip has driven continuous lengthening of river courses on top of the fault over the past 7 My. Lengthening contributes to the rise of river profiles upstream of the Polochic fault, and therefore to the slowing down of river incision in the SC range.

- In the SC range hillslope erosion slightly outpaces base level lowering, implying an overall trend to slow topographic decay, despite continuing surface uplift. The persistence of Middle Miocene low-relief surfaces on mountain tops in the SC range however implies no net reduction in the range height, and a decay that proceeds by ~~top~~ backwearing rather than downwearing.

- The slowing down ~~(precipitation), and by~~or erosion rates over the ~~bottom-up transmission of incision along streams crossing the AC~~SC range~~,~~ has resulted in ~~the~~a slowing down and stacking of upstream-migrating ~~waves of~~

~~dissection. Some of the headward migrating~~ knickpoints ~~dotting the northern flank of~~and erosion waves over the SC range ~~may predate~~and of the ~~rise~~development of ~~the AC range~~pediments at its base.

~~Such shutting down of stream incision and hillslope erosion by top-down (precipitation) and bottom-up (tectonic steepening) processes provides a field illustration of mechanisms involved in the lateral growth of orogenic plateaus.~~

Author contributions

Gilles Brocard: project design, river ^{10}Be sampling (~~Cuchumatanes, Sierra de las Minas~~AC and SM ranges), ^{10}Be sample processing (~~Cuchumatanes, Sierra de las Minas~~AC and SM ranges), river segment analysis~~.~~, manuscript preparation, with contributions from all authors. Jane Willenbring: ^{10}Be sample processing (~~Sierra de las Minas, Sierra de Chuacús).~~SM-SC range). Tristan Salles: river profile segmentation. Mickael Cosca: ^{40}Ar/^{39}Ar dating. Axel ~~Guttierez~~Guttiérez- and ~~Noe~~ Noé Cacao-Chiquín: ^{10}Be stream sampling (~~Sierra de las Minas, Sierra de Chuacús~~SM-SC range). Sergio Morán-Ical: field work coordination. Christian Teyssier: project design and coordination.

Competing interest: The authors declare that they have no conflict of interest.

Aknowledgments

This work was supported by the Department of Geology and Geophysics at the University of Minnesota, Minneapolis, UMN grant-in-aid 1003-524-5983, and by the Swiss National Science Foundation grant 200020-120117/1.

References

~~Abdullin, F., Solé, J., Solari, L., Shchepetilnikova, V., Meneses-Rocha, J. J., Pavlinova, N., and Rodríguez-Trejo, A.: Single-grain apatite geochemistry of Permian–Triassic granitoids and Mesozoic and Eocene sandstones from Chiapas, southeast Mexico: implications for sediment provenance, International Geology Review, 58, 1132–1157, 2016.~~

Anderson, T. H., Burkart, B., Clemons, R. E., Bohnenbe.Oh, and Blount, D. N.: Geology of the Western Altos de Cuchumatanes, Northwestern Guatemala Geological Society of America Bulletin, 84, 805-826, 10.1130/0016-7606(1973)84<805:gotwac>2.0.co;2, 1973.

Attal, M., Tucker, G. E., Whittaker, A. C., Cowie, P. A., and Roberts, G. P.: Modeling fluvial incision and transient landscape evolution: Influence of dynamic channel adjustment, Journal of Geophysical Research, 113, 10.1029/2007jf000893, 2008.

Authemayou, C., Brocard, G., Teyssier, C., Simon-Labric, T., Guttierrez, A., Chiquin, E. N., and Moran, S.: The Caribbean-North America-Cocos Triple Junction and the dynamics of the Polochic-Motagua fault systems: Pull-up and zipper models, Tectonics, 30, 10.1029/2010tc002814, 2011a.

Authemayou, C., Brocard, G., Teyssier, C., Simon-Labric, T., Guttiérrez, A., Chiquín, E., and Morán, S.: The Caribbean–North America–Cocos Triple Junction and the dynamics of the Polochic–Motagua fault systems: Pull-up and zipper models, Tectonics, 30, 2011b.

Authemayou, C., Brocard, G., Teyssier, C., Suski, B., Cosenza, B., Moran-Ical, S., Gonzalez-Veliz, C. W., Aguilar-Hengstenberg, M. A., and Holliger, K.: Quaternary seismo-tectonic activity of the Polochic Fault, Guatemala, Journal of Geophysical Research-Solid Earth, 117, 10.1029/2012jb009444, 2012.

Babault, J., Van Den Driessche, J., Bonnet, S., Castelltort, S., and Crave, A.: Origin of the highly elevated Pyrenean peneplain, Tectonics, 24, 2005.

Baldwin, J. A.: Implications of the shear stress river incision model for the timescale of postorogenic decay of topography, Journal of Geophysical Research, 108, 10.1029/2001jb000550, 2003.

Bartole, R., Lodolo, E., Obrist-Farner, J., and Morelli, D.: Sedimentary architecture, structural setting, and Late Cenozoic depocentre migration of an asymmetric transtensional basin: Lake Izabal, eastern Guatemala, Tectonophysics, 750, 419-433, 2019.

Baulig, H.: Peneplains and pediplains, Geological Society of America Bulletin, 68, 913-930, 1957.

Beaumont, C., Fullsack, P., and Hamilton, J.: Erosional control of active compressional orogens, in: Thrust tectonics, Springer, 1-18, 1992.

Bosc, E.: Geology of the San Agustin Acasaguastlan Quadrangle and Northeastern part of El Progresso Quadrangle, Guatemala, PhD thesis, Rice Univ., Houston, 1971a.

Bosc, E. A.: Geology of the San Agustin Acasaguastlan quadrangle and northeastern part of El Progreso quadrangle Rice University, 131 pp., 1971b.

Brocard, G., and Van der Beek, P.: Influence of incision rate, rock strength, and bedload supply on bedrock river gradients and valley-flat widths: Field-based evidence and calibrations from western Alpine rivers (southeast France), S. D. Willett et al., Spec. Pap. Geol. Soc. Am, 398, 101-126, 2006.

Brocard, G., Teyssier, C., Dunlap, W. J., Authemayou, C., Simon-Labric, T., Cacao-Chiquin, E. N., Gutierrez-Orrego, A., and Moran-Ical, S.: Reorganization of a deeply incised drainage: role of deformation, sedimentation and groundwater flow, Basin Research, 23, 631-651, 10.1111/j.1365-2117.2011.00510.x, 2011.

Brocard, G., Willenbring, J., Suski, B., Audra, P., Authemayou, C., Cosenza-Muralles, B., Moran-Ical, S., Demory, F., Rochette, P., Vennemann, T., Holliger, K., and Teyssier, C.: Rate and processes of river network rearrangement during incipient faulting: The case of the cahabon river, guatemala, American Journal of Science, 312, 449-507, 10.2475/05.2012.01, 2012.

Brocard, G., and Morán, S.: Phreatic clastic dikes and other degasing structures in the Los Chocoyos pumice formation, Guatemala, Revista Guatemalteca de Ciencias de la Tierra, 1, 55-65, 2014.

Brocard, G., Morán, S., Dura, T., and Vásquez, O.: The Plio-Pleistocene lacustrine Jolom Naj Formation of Cobán, Alta Verapaz: implications for the growth and demise of the Cahabón River network, Guatemala, Revista Guatemalteca de Ciencias de la Tierra, 2, 45-56, 2015a.

Brocard, G., Morán, S., Jared Vasquez, O., and Fernandez, M.: Natural hazard associated with the genesis of Lake Chichoy, Alta Verapaz, Guatemala, Revista Guatemalteca de Ciencias de la Tierra, 3, 5-19, 2016a.

Brocard, G. Y., Willenbring, J. K., Scatena, F. N., and Johnson, A. H.: Effects of a tectonically-triggered wave of incision on riverine exports and soil mineralogy in the Luquillo Mountains of Puerto Rico, Applied Geochemistry, 63, 586-598, 2015b.

Brocard, G. Y., Willenbring, J. K., Miller, T. E., and Scatena, F. N.: Relict landscape resistance to dissection by upstream migrating knickpoints, Journal of Geophysical Research: Earth Surface, 121, 1182-1203, 2016b.

Brown, E., Stallard, R. F., Larsen, M. C., Raisbeck, G. M., and Yiou, F.: Denudation rates determined from the accumulation of in-situ produced Be-10 in the Luquillo experimental forest, Puerto Rico.
, Earth and Planetary Science Letters, 129, 193-202, 10.1016/0012-821x(94)00249-x, 1995.

Bucknam, R. C., Coe, J. A., Chavarría, M. M., Godt, J. W., Tarr, A. C., Bradley, L.-A., Rafferty, S., Hancock, D., Dart, R. L., and Johnson, M. L.: Landslides triggered by Hurricane Mitch in Guatemala–inventory and discussion, US Geological Survey Open File Report, 1, 2001.

Burkart, B.: Offset across the Polochic fault of Guatemela and Chiapas, Mexico Geology, 6, 328-332, 10.1130/0091-7613(1978)6<328:oatpfo>2.0.co;2, 1978.

Callahan, R. P., Ferrier, K. L., Dixon, J., Dosseto, A., Hahm, W. J., Jessup, B. S., Miller, S. N., Hunsaker, C. T., Johnson, D. W., and Sklar, L. S.: Arrested development: Erosional equilibrium in the southern Sierra Nevada, California, maintained by feedbacks between channel incision and hillslope sediment production, GSA Bulletin, 131, 1179-1202, 2019.

Calvet, M., Gunnell, Y., and Farines, B.: Flat-topped mountain ranges: Their global distribution and value for understanding the evolution of mountain topography, Geomorphology, 241, 255-291, 2015.

Carballo-Hernandez, M., Banks, N., Franco-Austin, J., and Lopez-Aguilar, L.: Cuenca Amatique, Guatemala: Una Cuenca Transtencional al Sur del Limite de Placas NorteAmericana–Caribe, Paper Presented at Congreso Geologico Chileno, 1988,

Champel, B., van der Beek, P., Mugnier, J. L., and Leturmy, P.: Growth and lateral propagation of fault-related folds in the Siwaliks of western Nepal: Rates, mechanisms, and geomorphic signature, Journal of Geophysical Research-Solid Earth, 107, 10.1029/2001jb000578, 2002.

Clarke, B. A., and Burbank, D. W.: Bedrock fracturing, threshold hillslopes, and limits to the magnitude of bedrock landslides, Earth and Planetary Science Letters, 297, 577-586, 10.1016/j.epsl.2010.07.011, 2010.

Cowie, P. A., Whittaker, A. C., Attal, M., Roberts, G., Tucker, G. E., and Ganas, A.: New constraints on sediment-flux-dependent river incision: Implications for extracting tectonic signals from river profiles, Geology, 36, 535-538, 10.1130/g24681a.1, 2008.

Crosby, B. T., and Whipple, K. X.: Knickpoint initiation and distribution within fluvial networks: 236 waterfalls in the Waipaoa River, North Island, New Zealand, Geomorphology, 82, 16-38, 10.1016/j.geomorph.2005.08.023, 2006.

Deaton, B. C., and Burkart, B.: Time of sinistral slip along the Polochic fault of Guatemala Tectonophysics, 102, 297-&, 10.1016/0040-1951(84)90018-0, 1984.

~~Duvall, A., Kirby, E., and Burbank, D.: Tectonic and lithologic controls on bedrock channel profiles and processes in coastal California, Journal of Geophysical Research: Earth Surface, 109, 2004.~~

Ferrier, K. L., Kirchner, J. W., Riebe, C. S., and Finkel, R. C.: Mineral-specific chemical weathering rates over millennial timescales: Measurements at Rio Icacos, Puerto Rico, Chemical Geology, 277, 101-114, 10.1016/j.chemgeo.2010.07.013, 2010.

~~Finnegan, N. J., Roe, G., Montgomery, D. R., and Hallet, B.: Controls on the channel width of rivers: Implications for modeling fluvial incision of bedrock, Geology, 33, 229-232, 10.1130/g21171.1, 2005.~~

Ferrier, K. L., Perron, J. T., Mukhopadhyay, S., Rosener, M., Stock, J. D., Huppert, K. L., and Slosberg, M.: Covariation of climate and long-term erosion rates across a steep rainfall gradient on the Hawaiian island of Kaua ‘i, Geological Society of America Bulletin, 125, 1146-1163, 2013.

Finnegan, N. J., Hallet, B., Montgomery, D. R., Zeitler, P. K., Stone, J. O., Anders, A. M., and Yuping, L.: Coupling of rock uplift and river incision in the Namche Barwa-Gyala Peri massif, Tibet, Geological Society of America Bulletin, 120, 142-155, 10.1130/b26224.1, 2008.

Flores, K. E., Martens, U. C., Harlow, G. E., Brueckner, H. K., and Pearson, N. J.: Jadeitite formed during subduction: In situ zircon geochronology constraints from two different tectonic events within the Guatemala Suture Zone, Earth and Planetary Science Letters, 371-372, 67-81, 10.1016/j.epsl.2013.04.015, 2013.

Galewsky, J.: Rain shadow development during the growth of mountain ranges: An atmospheric dynamics perspective, Journal of Geophysical Research: Earth Surface, 114, 2009.

Garcia-Castellanos, D.: The role of climate during high plateau formation. Insights from numerical experiments, Earth and Planetary Science Letters, 257, 372-390, 2007.

Gardner, T. W.: Experimental study of knickpoint and longitudinal profile evolution in cohesive, homogeneous material, Geological Society of America Bulletin, 94, 664, 10.1130/0016-7606(1983)94<664:esokal>2.0.co;2, 1983.

Goldrick, G., and Bishop, P.: Differentiating the roles of lithology and uplift in the steepening of bedrock river long profiles: an example from southeastern Australia, The Journal of Geology, 103, 227-231, 1995.

Gould, W. A., Alarcón, C., Fevold, B., Jiménez, M. E., Martinuzzi, S., Potts, G., Quiñones, M., Solórzano, M., and Ventosa, E.: The Puerto Rico Gap Analysis Project volume 1: land cover, vertebrate species distributions, and land stewardship, Gen. Tech. Rep. IITF-39, 1, 2008.

Guttiérrez, A.: Caracterización de conglomerados y areniscas en la formación Subinal, en el suroriente del país, University San Carlos de Guatemala, 90, 2008.

Guzmán-Speziale, M.: Beyond the Motagua and Polochic faults: Active strike-slip faulting along the Western North America–Caribbean plate boundary zone, Tectonophysics, 496, 17-27, 10.1016/j.tecto.2010.10.002, 2010.

Harp, E. L., Wilson, R. C., and Wieczorek, G. F.: Landslides from the February 4, 1976, Guatemala earthquake, US Government Printing Office Washington, DC, 1981.

Harvey, A. M.: Effective timescales of coupling within fluvial systems, Geomorphology, 44, 175-201, 2002.

Hirschman, T.: Reconnaissance geology of part of the Department of El Progreso, Guatemala: Unpub, Master's thesis, Univ. Indiana, 1962.

Holder, C. D.: Rainfall interception and fog precipitation in a tropical montane cloud forest of Guatemala, Forest Ecology and Management, 190, 373-384, 10.1016/j.foreco.2003.11.004, 2004.

Howard, A. D.: A detachment-limited model of drainage basin evolution, Water resources research, 30, 2261-2285, 1994.

Howard, A. D.: Badland morphology and evolution: Interpretation using a simulation model, Earth Surface Processes and Landforms: The Journal of the British Geomorphological Group, 22, 211-227, 1997.

Humphrey, N. F., and Heller, P. L.: Natural oscillations in coupled geomorphic systems: An alternative origin for cyclic sedimentation, Geology, 23, 499, 10.1130/0091-7613(1995)023<0499:noicgs>2.3.co;2, 1995.

~~Humphrey, N. F., and Konrad, S. K.: River incision or diversion in response to bedrock uplift, Geology, 28, 43-46, 10.1130/0091-7613(2000)28<43:riodir>2.0.co;2, 2000.~~

Johnson, K.: Geology of the Gualan and southern Sierra de las Minas Quadrangles, Guatemala [Ph. D. thesis]: Binghamton, State University of New York, 1984.
Jordan, B., Sigurdsson, H., Carey, S., Lundin, S., Rogers, R., Singer, B., and Barquero-Molina, M.: Petrogenesis of Central American Tertiary ignimbrites and associated Caribbean Sea tephra, Geological Society of America Special Papers, 428, 151-179, 2007.
Kirby, E., and Whipple, K.: Quantifying differential rock-uplift rates via stream profile analysis, Geology, 29, 415, 10.1130/0091-7613(2001)029<0415:qdrurv>2.0.co;2, 2001.
Jackson, J., Ritz, J. F., Siame, L., Raisbeck, G., Yiou, F., Norris, R., Youngson, J., and Bennett, E.: Fault growth and landscape development rates in Otago, New Zealand, using in situ cosmogenic Be-10, Earth and Planetary Science Letters, 195, 185-193, 10.1016/s0012-821x(01)00583-0, 2002.
Kirby, E.: Distribution of active rock uplift along the eastern margin of the Tibetan Plateau: Inferences from bedrock channel longitudinal profiles, Journal of Geophysical Research, 108, 10.1029/2001jb000861, 2003.
Lachniet, M. S., and Vazquez-Selem, L.: Last Glacial Maximum equilibrium line altitudes in the circum-Caribbean (Mexico, Guatemala, Costa Rica, Colombia, and Venezuela), Quaternary International, 138-139, 129-144, 10.1016/j.quaint.2005.02.010, 2005.
Leland, J., Reid, M. R., Burbank, D. W., Finkel, R., and Caffee, M.: Incision and differential bedrock uplift along the Indus River near Nanga Parbat, Pakistan Himalaya, from Be-10 and Al-26 exposure age dating of bedrock straths, Earth and Planetary Science Letters, 154, 93-107, 10.1016/s0012-821x(97)00171-4, 1998.
Liang, Z., Liu, H., Zhao, Y., Wang, Q., Wu, Z., Deng, L., and Gao, H.: Effects of rainfall intensity, slope angle, and vegetation coverage on the erosion characteristics of Pisha sandstone slopes under simulated rainfall conditions, Environmental Science and Pollution Research, 1-10, 2019.
Machorro, R. C., S.: Drought assessment in the Dry Corridor of Guatemala, Earth Science Review of Guatemala, 1, 11, 2014.
McAdams, B. C., Trierweiler, A. M., Welch, S. A., Restrepo, C., and Carey, A. E.: Two sides to every range: orographic influences on CO 2 consumption by silicate weathering, Applied Geochemistry, 63, 472-483, 2015.
Meijers, M., Brocard, G., Lüdecke, T., Cosca, M., Teyssier, C., Whitney, D., and Mulch, A.: Rapid Late Miocene Surface Uplift of the Central Anatolian Plateau Margin., Earth and Planetary Research Letters, 2018.
Merritts, D. J., Vincent, K. R., and Wohl, E. E.: LONG RIVER PROFILES, TECTONISM, AND EUSTASY - A GUIDE TO INTERPRETING FLUXIAL TERRACES, Journal of Geophysical Research-Solid Earth, 99, 14031-14050, 10.1029/94jb00857, 1994.
Montgomery, D. R., and Stolar, D. B.: Reconsidering Himalayan river anticlines, Geomorphology, 82, 4-15, 10.1016/j.geomorph.2005.08.021, 2006.
Mudd, S. M., and Furbish, D. J.: Responses of soil-mantled hillslopes to transient channel incision rates, Journal of Geophysical Research: Earth Surface, 112, 2007.
Mudd, S. M., Attal, M., Milodowski, D. T., Grieve, S. W., and Valters, D. A.: A statistical framework to quantify spatial variation in channel gradients using the integral method of channel profile analysis, Journal of Geophysical Research: Earth Surface, 119, 138-152, 2014.
Muller, P. D.: Geology of the Los Amates quadrangle and vicinity, Guatemala, Central America, State University of NY, 1979.
Murphy, B. P., Johnson, J. P., Gasparini, N. M., and Sklar, L. S.: Chemical weathering as a mechanism for the climatic control of bedrock river incision, Nature, 532, 223, 2016.

Neely, A. B., and DiBiase, R. A.: Drainage Area, Bedrock Fracture Spacing, and Weathering Controls on Landscape-Scale Patterns in Surface Sediment Grain Size, Journal of Geophysical Research: Earth Surface, 125, e2020JF005560, 2020.

Newcomb, W. E.: Geology, Structure and Metamorphism of the Chuacus Group, Rio Hondo Quadrangle and Vicinity, Guatemala, State University of New York at Binghamton, 1975.

Ortega-Gutierrez, F., Solari, L. A., Sole, J., Martens, U., Gomez-Tuena, A., Moran-Ical, S., Reyes-Salas, M., and Ortega-Obregon, C.: Polyphase, high-temperature eclogite-facies metamorphism in the Chuacus Complex, Central Guatemala: Petrology, geochronology, and tectonic implications, International Geology Review, 46, 445-470, 10.2747/0020-6814.46.5.445, 2004.

Ortega-Obregón, C., Solari, L., Keppie, J., Ortega-Gutiérrez, F., Solé, J., and Morán-Ical, S.: Middle-Late Ordovician magmatism and Late Cretaceous collision in the southern Maya block, Rabinal-Salamá area, central Guatemala: implications for North America–Caribbean plate tectonics, Geological Society of America Bulletin, 120, 556-570, 2008.

Pain, C., and Ollier, C.: Inversion of relief—a component of landscape evolution, Geomorphology, 12, 151-165, 1995.

Pelletier, J. D.: How do pediments form?: A numerical modeling investigation with comparison to pediments in southern Arizona, USA, Geological Society of America Bulletin, 122, 1815-1829, 10.1130/b30128.1, 2010.

Perron, J. T., and Royden, L.: An integral approach to bedrock river profile analysis, Earth Surface Processes and Landforms, 38, 570-576, 10.1002/esp.3302, 2013.

Ramos Scharrón, C. E., Castellanos, E. J., and Restrepo, C.: The transfer of modern organic carbon by landslide activity in tropical montane ecosystems, Journal of Geophysical Research, 117, 10.1029/2011jg001838, 2012.

Ratschbacher, L., Franz, L., Min, M., Bachmann, R., Martens, U., Stanek, K., Stubner, K., Nelson, B. K., Herrmann, U., Weber, B., Lopez-Martinez, M., Jonckheere, R., Sperner, B., Tichomirowa, M., McWilliams, M. O., Gordon, M., Meschede, M., and Bock, P.: The North American-Caribbean Plate boundary in Mexico-Guatemala-Honduras, Geological Society, London, Special Publications, 328, 219-293, 10.1144/sp328.11, 2009.

~~Rogers, R. D., Karason, H., and van der Hilst, R. D.: Epeirogenic uplift above a detached slab in northern Central America, Geology, 30, 1031-1034, 10.1130/0091-7613(2002)030<1031:euaads>2.0.co;2, 2002.~~

Riebe, C. S., Sklar, L. S., Lukens, C. E., and Shuster, D. L.: Climate and topography control the size and flux of sediment produced on steep mountain slopes, Proceedings of the National Academy of Sciences, 112, 15574-15579, 2015.

Rogers, R. D., and Mann, P.: Transtensional deformation of the western Caribbean–North America plate boundary zone, Geological Society of America Special Papers, 428, 37-64, 2007.

Roper, P.: Stratigraphy of the Chuacu¤ s Group on the south side of the Sierra de las Minas range, Guatemala, Geol. Mijn, 57, 309-313, 1978.

Rose, W. I., Newhall, C. G., Bornhorst, T. J., and Self, S.: Quaternary silicic pyroclastic deposits of atitlan caldera, Guatemala, Journal of Volcanology and Geothermal Research, 33, 57-80, 10.1016/0377-0273(87)90054-0, 1987.

~~Rose, W. I., Conway, F. M., Pullinger, C. R., Deino, A., and McIntosh, W. C.: An improved age framework for late Quaternary silicic eruptions in northern Central America, Bulletin of Volcanology, 61, 106-120, 1999.~~

Rosenbloom, N. A., and Anderson, R. S.: Hillslope and channel evolution in a marine terraced landscape, Santa Cruz, California, Journal of Geophysical Research: Solid Earth, 99, 14013-14029, 1994.

Royden, L., and Taylor Perron, J.: Solutions of the stream power equation and application to the evolution of river longitudinal profiles, Journal of Geophysical Research: Earth Surface, 118, 497-518, 2013.

Sieh, K. E., and Jahns, R. H.: Holocene activity of the San Andreas fault at Wallace Creek, California, Geological Society of America Bulletin, 95, 883, 10.1130/0016-7606(1984)95<883:haotsa>2.0.co;2, 1984.

Simon-Labric, T., Brocard, G. Y., Teyssier, C., van der Beek, P. A., Fellin, M. G., Reiners, P. W., and Authemayou, C.: Preservation of contrasting geothermal gradients across the Caribbean-North America plate boundary (Motagua Fault, Guatemala), Tectonics, n/a-n/a, 10.1002/tect.20060, 2013.

Sklar, L. S., and Dietrich, W. E.: The role of sediment in controlling steady-state bedrock channel slope: Implications of the saltation–abrasion incision model, Geomorphology, 82, 58-83, 10.1016/j.geomorph.2005.08.019, 2006.

Sobel, E. R., Hilley, G. E., and Strecker, M. R.: Formation of internally drained contractional basins by aridity-limited bedrock incision, Journal of Geophysical Research: Solid Earth, 108, 2003.

Strudley, M. W., Murray, A. B., and Haff, P. K.: Emergence of pediments, tors, and piedmont junctions from a bedrock weathering–regolith thickness feedback, Geology, 34, 805, 10.1130/g22482.1, 2006.

Thattai, D., Kjerfve, B., and Heyman, W.: Hydrometeorology and variability of water discharge and sediment load in the inner Gulf of Honduras, western Caribbean, Journal of Hydrometeorology, 4, 985-995, 2003.

Thomas, M. F.: The role of etch processes in landform development. I. Etching concepts and their applications, Zeitschrift für Geomorphologie, 33, 129-142, 1989.

Tobisch, M. K.: Part I, late Cenozoic geology of the central Motagua Valley, Guatemala: part II, uplift rates, deformation and neotectonics of Holocene marine terraces from Point Delgado to Cape Mendocino, California, 1986.

Tucker, G. E., and Whipple, K.: Topographic outcomes predicted by stream erosion models: Sensitivity analysis and intermodel comparison, Journal of Geophysical Research, 107, 10.1029/2001jb000162, 2002.

van der Beek, P., Champel, B., and Mugnier, J. L.: Control of detachment dip on drainage development in regions of active fault-propagation folding, Geology, 30, 471-474, 10.1130/0091-7613(2002)030<0471:coddod>2.0.co;2, 2002.

~~Walker, J. A., Singer, B. S., Jicha, B. R., Cameron, B. I., Carr, M. J., and Olney, J. L.: Monogenetic, behind-the-front volcanism in southeastern Guatemala and western El Salvador: 40 Ar/39 Ar ages and tectonic implications, Lithos, 123, 243-253, 2011.~~

Weissel, J. K., and Seidl, M. A.: Inland propagation of erosional escarpments and river profile evolution across the southeast Australian passive continental margin, Rivers over rock: fluvial processes in bedrock channels, 189-206, 1998.

Whipple, K., and Meade, B.: Orogen response to changes in climatic and tectonic forcing, Earth and Planetary Science Letters, 243, 218-228, 10.1016/j.epsl.2005.12.022, 2006.

Whipple, K. X., and Tucker, G. E.: Dynamics of the stream-power river incision model: Implications for height limits of mountain ranges, landscape response timescales, and research needs, Journal of Geophysical Research, 104, 17661, 10.1029/1999jb900120, 1999.

Whipple, K. X., and Tucker, G. E.: Implications of sediment-flux-dependent river incision models for landscape evolution, Journal of Geophysical Research-Solid Earth, 107, 10.1029/2000jb000044, 2002.

Whipple, K. X.: Bedrock rivers and the geomorphology of active orogens, Annu. Rev. Earth Planet. Sci., 32, 151-185, 2004.

Whittaker, A. C., ~~Cowie, P. A., Attal, M., Tucker, G. E., and Roberts, G. P.: Contrasting transient and steady-state rivers crossing active normal faults: new field observations from the Central Apennines, Italy, Basin Research, 19, 529-556, 10.1111/j.1365-2117.2007.00337.x, 2007.~~

~~Whittaker, A. C.,~~ and Boulton, S. J.: Tectonic and climatic controls on knickpoint retreat rates and landscape response times, Journal of Geophysical Research, 117, 10.1029/2011jf002157, 2012.

Willenbring, J. K., Codilean, A. T., and McElroy, B.: Earth is (mostly) flat: Apportionment of the flux of continental sediment over millennial time scales, Geology, 41, 343-346, 10.1130/g33918.1, 2013a.

Willenbring, J. K., Gasparini, N. M., Crosby, B. T., and Brocard, G.: What does a mean mean? The temporal evolution of detrital cosmogenic denudation rates in a transient landscape, Geology, 41, 1215-1218, ~~2013~~2013b.

Willett, S. D., and Brandon, M. T.: On steady states in mountain belts, Geology, 30, 175, 10.1130/0091-7613(2002)030<0175:ossimb>2.0.co;2, 2002.

Williams, E. A., and McBirney, A. R.: Volcanic history of Honduras, University of California publications in Geological Sciences, 85, 1-65, 1969.

~~Wunderman, R. L., and Rose, W. I.: Amatitlán, an actively resurging cauldron 10 km south of Guatemala City Journal of Geophysical Research, 89, 8525-8539, 10.1029/JB089iB10p08525, 1984.~~

~~Yanites, B. J., Ehlers, T. A., Becker, J. K., Schnellmann, M., and Heuberger, S.: High magnitude and rapid incision from river capture: Rhine River, Switzerland, Journal of Geophysical Research: Earth Surface, 118, 1060-1084, 10.1002/jgrf.20056, 2013.~~